Lecture Notes in Electrical Engineering 534

Axaykumar Mehta
Brijesh Naik

Sliding Mode Controllers for Power Electronic Converters

Springer

Lecture Notes in Electrical Engineering

Volume 534

Lecture Notes in Electrical Engineering (LNEE) is a book series which reports the latest research and developments in Electrical Engineering, namely:

- Communication, Networks, and Information Theory
- Computer Engineering
- Signal, Image, Speech and Information Processing
- Circuits and Systems
- Engineering.

The audience for the books in LNEE consists of advanced level students, researchers, and industry professionals working at the forefront of their fields. Much like Springer's other Lecture Notes series, LNEE will be distributed through Springer's print and electronic publishing channels.

More information about this series at http://www.springer.com/series/7818

Axaykumar Mehta · Brijesh Naik

Sliding Mode Controllers for Power Electronic Converters

Springer

Axaykumar Mehta
Department of Electrical Engineering
Institute of Infrastructure Technology
Research and Management
Ahmedabad, Gujarat, India

Brijesh Naik
Instrumentation and Control
Engineering Department
Sarvajanik College of Engineering
and Technology
Athwalines, Surat, Gujarat, India

ISSN 1876-1100 ISSN 1876-1119 (electronic)
Lecture Notes in Electrical Engineering
ISBN 978-981-13-3151-0 ISBN 978-981-13-3152-7 (eBook)
https://doi.org/10.1007/978-981-13-3152-7

Library of Congress Control Number: 2018960217

This Springer imprint is published by the registered company Springer Nature Singapore Pte Ltd.
The registered company address is: 152 Beach Road, #21-01/04 Gateway East, Singapore 189721, Singapore

Dedicated to our parents

Preface

The power electronic converter (PEC) is the most important part of various electrical and electronic systems. Various robotic systems,biomedical systems,modern computers and cell phone systems require accurately controlled power supplies or switching mode power supplies (SMPS). Although many of the power electronic devices are functioning in open-loop mode, i.e., without any control system, there are certain systems which require precise/robust control strategy to maintain voltage or current at desired levels in the presence of load disturbances or supply-side variations. The pulse-width modulation (PWM) has been the most preferred technique for feedback control implementation which involves the duty cycle variation to control the output voltage. Various control strategies are available in the literature. Among them, sliding mode control (SMC) technique has become more popular recently due to its inherent suitability for switching-type devices and also its robustness property against matched uncertainties.

The conventional SMC has been used for various power electronic converters, but it has certain drawbacks due to the practical limitation of switching. The imperfections in the switching device and also saturation nonlinearities result in steady-state error. Here, it is worth to mention that the tuning of controller parameter plays a very vital role for the steady-state and dynamic performance of the converter, particularly under load variations. Also, it has been observed that the power converters may become unstable due to the improper selection of tuning parameters. In case of classical SMC controller, there is only one tuning parameter that has to perform multiple tasks: (i) governing speed of response; (ii) compensating load variations. Hence, the choice for tuning parameter is restricted. Moreover, the tuning parameter is not adaptive under load variation condition in case of classical SMC which does not allow the Region Of Existence (ROE) where sliding mode exists to vary.

It is a well-known concept among sliding mode fraternities that the integral sliding function eliminates the steady-state error. In this monograph, firstly proportional–integral type of function is proposed for the DC–DC Buck converters to overcome the drawback of the steady-state error. A detailed analysis of the Region

Of Existence (RoE), stability, and controller design with the proposed sliding function is presented. Further, it is also observed that with proper tuning of parameters RoE becomes less sensitive to load variations, and hence, the adaptive mechanism is proposed to improve the robustness of the controller. The performance of the proposed controller scheme is checked with simulation and experimentally under the load variation disturbances. Both the results are also compared with the classical SMC technique which reveals that the proposed scheme outperforms the conventional SMC techniques.

It is noted that the proposed SMC with proportional–integral-type sliding function does not facilitate the finite reaching and hence the responses of the load voltage result in steady state exponentially. Hence, to facilitate finite-time reaching, the above strategy is modified a little bit with new integral sliding mode control with finite-time reaching (ISMCFTR). The control technique is further applied to DC–DC Boost converter where the controller parameters are tuned adaptively. It is observed from the responses that the load disturbance rejection is faster with ISMCFTR as compared to conventional SMC.

Further, this monograph proposes SMC controller with PI-type sliding surface for the Zeta converter which is noninverting-type Buck–Boost converter. Here, the limitation is in the choice of sliding surface, and hence, type control law is proposed to improve the steady-state performance.

Until now, only the DC–DC converters have been discussed. However, the DC–AC converters are of interest in this age of battery-operated systems. From domestic low-power to luxurious high-power/medical/industrial applications, the Boost DC–AC converters or very well known as inverters are the heart of many types of equipment and need careful technical design. Control of voltage and/or frequency of the AC signal is of major interest, and such inverters are well known as variable-voltage variable-frequency (VVVF) inverters. The inverters may or may not require precise controllers depending upon the requirements of the systems. It is preferable to use a well-designed control strategy to avoid disturbance effects due to supply-side or load-side variations. Here, an attempt is made to design SMC controller for the inverter to improve the performance under load variation condition.

For the applications involving use of DC–AC or AC–DC converters, it is desirable that the input power factor must be controlled to an optimum value, i.e. close to unity. For many DC power supplies, the input power factor is of interest as it is the direct measure of the overall efficiency. It is possible to control the power factor at the supply side so that the supply current and voltage may remain in phase and one can assure unity or optimum power factor. Of course, this requires extra efforts and sometimes may cause switching losses. The converter suitable for power factor control is Boost power factor controller (Boost PFC). In this monograph, a design methodology using SMC technique for PFC is presented. The simulation results show the efficacy of the algorithm.

It may be noted that various SMC techniques are available in the wide variety of the literature for PECs. However, the main drawback of SMC is chattering which is unavoidable phenomena, and it deteriorates the performance of the switching

PECs. Among all the available chattering attenuation techniques, the higher-order sliding mode technique has become more popular. In this monograph, a design methodology of second-order sliding mode control for DC–DC Buck converter is explored. The bounds for the controller tuning parameters are obtained, and stability conditions are inferred. Moreover, the implementation guidelines are also presented for practical implementation. Finally, the simulation and experimental results are presented to show the efficacy of the converter.

Ahmedabad, India
June, 2018

Axaykumar Mehta
Brijesh Naik

Acknowledgements

It is a pleasure to acknowledge our indebtedness to teachers, colleagues, and students. It would have been almost impossible to publish this monograph without the support from our family members. We would like to express our sincere gratitude to all the researchers and contributors in the field of sliding mode control. We thank all those who have helped directly or indirectly to publish this monograph. Finally, we also acknowledge the publisher and reviewers for helping to prepare the penultimate draft of this edition.

Contents

About the Authors

Axaykumar Mehta received his Bachelor of Engineering in electrical engineering (1996), Master of Technology (2002), and Ph.D. (2009) from Gujarat University, Ahmedabad; Indian Institute of Technology Kharagpur; and Indian Institute of Technology Bombay, respectively. He is currently acting as Associate Professor in the Department of Electrical Engineering, Institute of Infrastructure Technology Research and Management (IITRAM), Ahmedabad, Gujarat, India. He has more than 21 years of teaching experience at UG and PG levels at various premier institutions of the state. He has presented and published 60 research papers in national/international reputed conferences and refereed journals and 3 monographs/books with Springer. He has also published three patents at Indian Patent Office, Mumbai. He is the recipient of Pedagogical Innovation Award 2014 from Gujarat Technological University (GTU). His research interests are sliding mode control and observer, networked control systems, multi-agent systems, and control of smart grids/micro-grids. He is Senior Member of IEEE, Member of IEEE Industrial Electronics Society (IES) and Control Systems Society (CSS), Life Member of Indian Society for Technical Education (ISTE), Institution of Engineers India (IEI), Systems Society of India (SSI), and Society of Power Engineers (SPE).

Brijesh Naik has an M.Tech. from Indian Institute of Technology Bombay, India, and received his Ph.D. from Gujarat Technological University, Ahmedabad, India. Currently, he is Associate Professor in the Instrumentation & Control Dept., Sarvajanik College of Engineering and Technology, Surat, India. He has 16 years of teaching and research experience. He has taught courses on various subjects, including process instrumentation, modern digital control systems, measurement and instrumentation, biomedical instrumentation, industrial control systems, and power electronics. He has also published a number of research papers in reputed journals and conferences. He is a member of Institution of Engineers, India.

Acronyms

DSC	Digital Signal Controller
GPIO	General-Purpose Input–Output
HOSM	Higher-Order Sliding Modes
HOSMC	Higher-Order Sliding Mode Control
ISMCFTR	Integral SMC with Finite-Time Reaching
LTI	Linear Time-Invariant (system)
LTV	Linear Time-Variant (system)
PCL	Prescribed Convergence Law
PEC	Power Electronic Converters
PFC	Power Factor Controller
PI	Proportional–Integral
PID	Proportional–Integral–Derivative
ROE	Region Of Existence
SMC	Sliding Mode Control
SMPS	Switching-Mode Power Supply
SOSMC	Second-Order Sliding Mode Control
THD	Total Harmonic Distortion
VSC	Variable Structure Control
VSS	Variable Structure Systems

Nomenclature

r_L	Load resistance, Ω
α	Tuning parameter of sliding mode controller
β	Voltage divider ratio
T	Modified sliding function
E	Pure DC input voltage
V_i	DC input voltage from regulator
γ	Tuning parameter of sliding mode controller
C	Capacitor in F
L	Inductor in H
D	Diode
SW	Switch
V_{ref}	Reference voltage V
I_{ref}	Reference current A
V_d	Desired voltage
V_μ	Scaled reference voltage
κ	Tuning parameter for SOSMC
ψ	Tuning parameter for SOSMC
S	Sliding surface
u	Controller output
ε	Dead zone in switching elements
x_i	ith state
i_r	Load current in ampere
i_L	Inductor current in ampere
i_C	Capacitor current in ampere
t	Time
f	Supply frequency in Hz
f_s	Switching frequency in Hz
χ, ρ	Nominal duty ratio and duty ratio
ρ	Duty cycle or duty ratio
W	Time period for PWM signal

K	State feedback controller gain
A	State-space system matrix
B	Actuator gain matrix
V	Lyapunov function
δx_{ie}	Deviation of state x_i from equilibrium point x_{ie}
V_{con}	Control voltage for PWM signal
τ	$\frac{t}{LC}$
Q	$R\sqrt{\frac{C}{L}}$
g, f, h	Function of state vector and time
σ	Sliding surface in case of SOSMC
K_m	Lower bound
K_M	Upper bound
Γ	Function of σ in case of SOSMC
κ	Tuning parameter for SOSMC
Z	Bound on a parameter

Chapter 1
Introduction

1.1 Background

The sliding mode control (SMC) technique also known as variable structure system (VSS) has its roots in Soviet Union. However, it was not revealed to the world until Itkis [10] published a book and a research article by Utkin [30] in IEEE transactions. Many researchers [3, 4, 6, 7, 21] in Soviet Union and France [9] have worked enough and provided the strong background for the evolvement of the SMC technique. The SMC was derived from the relay feedback control technique. The most significant factors of SMC technique are reaching mode (RM), sliding mode (SM), and steady-state mode (SS). The terms have very specific meanings. Starting from the initial condition, the phase trajectory is attracted to the sliding manifold during the RM. Once the phase trajectory hits the manifold, it slides toward the origin of the phase plane called SM. Then the phase trajectory stays at the origin and steady state is achieved. The whole exercise of designing SMC law requires a fairly good mathematical model of the system. The switching component in SMC law is desired in most of the cases to ensure the phase trajectory does not leave the sliding manifold and thus it reaches origin. Once the trajectory reaches to sliding phase, the system dynamics are governed by the surface dynamics and hence the system is immune to matched uncertainties. However, the switching component in the control law induces high-frequency chattering and hence its application to the real system is a bit challenging.

The SMC technique is applied to a wide class of systems like linear time-invariant, linear time-variant, nonlinear, delayed systems, in the domain of electrical system, mechanical system, etc. Power electronics being a specific domain in power engineering also make use of SMC technique. In the literature, majority of power electronic converters (PEC) are controlled with PWM-based PI or PID controllers. However, SMC for many PEC like Buck, Boost converters and rectifiers proposed by Utkin [31, 32] in his book in 1999. Since then many researchers have contributed in the field.

A. Mehta and B. Naik, *Sliding Mode Controllers for Power Electronic Converters*, Lecture Notes in Electrical Engineering 534,
https://doi.org/10.1007/978-981-13-3152-7_1

Being discontinuous in nature, SMC is inherently suitable to switching PEC due to the involvement switching action in converter circuit. The increasing usage of robotic and other mobile electrical-electronic systems imposed the great demand for stable and well-controlled PEC. These type of systems frequently exposed to changes in electrical load, supply-side variations, and parameter variations. The SMC can be the choice as it can provide robustness against the same. As stated earlier, the SMC can provide robustness for the matched uncertainties or disturbances in the input channel of the system. The increasing usage of robotic and other mobile electrical-electronic systems imposed the great demand for stable and well-controlled PEC. These type of systems frequently exposed to changes in electrical load, supply-side variations, and parameter variations. Hence, the choice of SMC is justified for the control of various switching PEC.

Although it is not always easy to design a good control systems with classical techniques [1, 22], some tools are available for design and those are some professional software tools [14, 34]. There are many types of analog compensators available named as Type I, II, and III compensators [1, 8, 23].

The modeling of PEC and control techniques is discussed in the wide variety of books and research articles [1, 24, 31]. In [16], they proposed a general unified approach to modeling for PECs. The modeling, control, and detailed analysis of various PECs can be also be found in [24]. With various methodologies, variety of control algorithms have been implemented. One of the main tasks of the controller is to control the load voltage of converter. In [25], they have presented a large-signal nonlinear control technique (One Cycle Control) which dynamically controls the duty ratio of a switch such that in each cycle the average value of controlled variable is proportional to the reference. The technique is good at rejecting source power perturbations, but effects of load disturbances are excluded. With the frequency domain controller design approach, the voltage regulation of pulse-width modulation (PWM)-based DC–DC switching converter is discussed [13]. The small signal model of the converter is used. The SMC turned out to be a popular control technique in the field of power electronics after Utkin [32] discussed about its applications to various PECs. In many cases, SMC is applied to the various power electronic and electromechanical systems [5, 32]. The fundamentals of SMC can be found in [15]. The design, analysis, and experimentation of DC–AC Boost with SMC is presented in Caceres and Barbi [2]. A good graphical and analytical explanation for DC–DC PEC under SMC is available in [26]. In the article [12], they proposed fixed-frequency hysteresis controller (FFHC). This controller uses SMC and FFHC with hysteresis band. In [20, 33], they have described SMC-based technique for control of PECs. In 2012, Hasan [11] suggested the adaptive terminal SMC for DC–DC Buck converter with nonlinear sliding surface. This control law assures finite-time reaching. The effect of load variation is examined for the converter under the proposed control strategy.

Tan [27–29] proposed a sliding mode control with hybrid modeling for different PECs. The existence conditions for sliding modes are also derived, and the term Region of Existence (ROE) is coined. It is also identified that the higher values of controller parameters can lead to sustained oscillations especially for PEC with

high-power applications [17]. Moreover, the conventional SMC for PEC results in steady-state error in load voltage for a given reference. Also, the ROE is not fixed on the phase plane and in fact varies according to the load disturbances. For that Tan [29] suggested adaptive tuning but it required the measurement of load current. For steady-state error elimination, a double-integral sliding surface is suggested. In [18], they proposed modified SMC controller for improving steady-state performance. However, chattering alleviation is still a challenge. In general, steady-state error and chattering attenuation need more attention from the research fraternity.

With this background, this monograph focuses on minimizing the steady-state error in controlled variable and improving robustness of PEC with modified sliding function. Some PECs like Buck, Boost, and Buck Boost (Zeta converter) are tested with the proposed SMC law with PI-type sliding function. The proposed SMC proved to be better in elimination of steady-state error. The ROE and robustness against load disturbances are also examined. The need for adaptive tuning due to load requirement no longer exists with this proposed SMC, and hence, no additional measurement of load current is required. It is also proved that the proposed SMC leads to minimization of steady-state error. The detailed analysis for stability and switching frequency is presented. Moreover, some efforts are also put to use latest techniques like HOSMC-second-order SMC (2-sliding mode control) to attenuate chattering in controlled variable of PEC [19]. The overall research effort is to improve the tracking response of various PECs like Buck, Boost, Zeta, DC–AC inverters, and power factor controller (PFC) with the SMC. The main contributions of this monograph are summarized as below:

1.2 Contributions of the Monograph

The main contributions of this monograph are indicated as below:

1.2.1 Introduction to Sliding Mode Control and Review of Classical Control of Power Electronic Converters

A literature review of classical state feedback and sliding mode control theory and power electronic converters is presented. The basics of sliding mode control strategy are discussed with suitable example. The state feedback control for DC–DC Buck converter is designed, and its efficacy is examined for load disturbances variations.

1.2.2 Sliding Mode Controller with PI-Type Sliding Function for DC–DC Buck Converter

The SMC with a proportional–integral-type sliding function for Buck converter is proposed. The proofs of stability and zero steady-state error is presented. The simulation and experimental results are presented. It is shown that the proposed SMC law for Buck converter results in better steady-state response of load voltage than conventional SMC for a given reference. The efficacy of the proposed SMC law is evaluated with load disturbances variations. The proposed SMC law provides robustness against load disturbances. Effects of variations in controller parameters explored. The discussion of stability, frequency limits of the switching device, and steady-state performance of the load voltage is presented. Moreover, to facilitate finite-time reaching the integral SMC with finite-time reaching (ISMCFTR) is proposed. With ISMCFTR, the load voltage is forced to be equal to reference voltage within finite time. The guidelines for tuning parameters of the ISMCFTR are given. Simulation results demonstrate the efficacy of the system under ISMCFTR.

1.2.3 Sliding Mode Controller with PI-Type Sliding Function for DC–DC Boost Converter

The proposed SMC with PI-type sliding function is applied to DC–DC Boost or step-up converter. Here the adaptive mechanism is used to improve the performance of the converter in terms of load voltage quality in presence of load disturbances. The ROE is also defined for a proposed algorithm. It is shown with simulation results that the load disturbance rejection is quite faster with the proposed adaptive SMC law.

1.2.4 Sliding Mode Controller with PI-Type Sliding Function for Zeta Converter

The Zeta converter is a type of Buck Boost converter with noninverting output. It is complex fourth-order nonlinear (bilinear) system. The limitations here in designing the SMC are the choice of sliding manifold which is overcome by the proposed algorithm. The proposed SMC reduces the steady-state error in load voltage for a given reference.

1.2.5 Application of Sliding Mode Controller with PI-Type Sliding Function for Inverter and Power Factor Controller

The idea of designing sine wave inverter with Zeta converter as a pre-stage is proposed. The performance is evaluated with proposed and compared with conventional SMC law. Further, power factor controller using DC–DC Boost converter with proposed SMC law is designed and the performance is compared with PWM/PI controller

1.2.6 Output Feedback Second-Order Sliding Mode Control for DC–DC Buck Converter

The main drawback of implementing classical SMC law is chattering which can be attenuated by second-order sliding mode control strategy. Here a design methodology for DC–DC Buck converter using SOSMC is presented which further extended to output feedback SOSMC law. The performance of Buck converter with SOSMC is evaluated and also compared with that of conventional SMC. For designing SOSMC for Buck converter, it is required to evaluate the bounds on the uncertainty. Further, the effects of the tuning parameters on load voltage are analyzed. It is proved through simulation and experimentally that the performance of Buck converter is superior with SOSMC as compared to the conventional SMC.

1.2.7 Organization of the Monograph

The monograph examines DC–DC Buck, Boost, and Zeta converters with the proposed modified SMC controller, and the performance is compared with conventional SMC law. The monograph also provides implementation guidelines for real applications. Further, the monograph includes the modern SMC techniques known as higher-order SMC or 2-sliding mode control for the Buck converter which attenuates the chattering effects.

The monograph is organized as under:

This chapter provides the background and literature survey on sliding mode control technique and controller design methodologies DC–DC converters.

In Chap. 2, the review of continuous-time SMC with its robustness property against the matched uncertainties is discussed. The model of DC–DC Buck converter and its AC equivalent model which is to be used for design purpose is discussed at length. To begin with controller design, first the classical approaches of designing compensator for the PEC are presented and also extended to state feedback controller.

Further, to elaborate the design principals, the guidelines for designing compensator are also presented.

Chap. 3 discusses the design of SMC controller with proportional plus integral-type sliding function for DC–DC Buck converter. The simulation and experimental results are presented to show the efficacy of the controller.

In Chap. 4, the proposed methodology of SMC with PI sliding function is extended for DC–DC Boost converter. Also the adaptive gain mechanism for tuning controller gain is proposed to make the algorithm adaptive to load variations. The efficacy of the control strategy is evaluated with simulation results.

Chapters 5 and 6 present the design of Zeta converter with proposed SMC algorithm and its application to design sine wave inverter for low-power AC applications. Further, the performance of power factor controller using Zeta converter is also tested in simulation with PWM+PI and SMC law.

Chapter 7 presents the design of DC–DC Buck converter using 2-sliding mode controller. The comparison of load voltage responses with conventional SMC law and 2-sliding mode control law is presented. The implementation guidelines are also provided. The stability bounds of controller parameters are obtained. The simulation and experiment results are presented to show the efficacy of the controller.

Finally, the conclusions of the entire research work are presented in Chap. 8 followed by the scope for future work.

References

1. Ang, S., Oliva, A.: Power Switching Converters. CRC Press, Taylor and Francis Group, Boca Raton (2005)
2. Caceres, R., Barbi, I.: A boost DC-AC converter analysis, design and experimentation. IEEE Trans. Power Electron. **14**(1), 134–141 (1999)
3. Dolgolenko, Yu.V.: Sliding modes in relay indirect control systems. In: Proceeding of 2nd All-Union Conference on Control (1955)
4. Drazenovic, B.: The invariance conditions in variable structure systems. Automatica, Pergamon Press **5**(3) (1969)
5. Edwards, C., Spurgeon, S.: Sliding Mode Control Theory and Applications. Taylor & Francis, London (1998)
6. Emelyanov, S.V.: Method of designing complex control algorithms using an error and its first time-derivative only. Autom. Remote Control **18**(10) (1957)
7. Emelyanov, S.V.: Theory of Variable Structure Systems. Nauka, Moscow (1970)
8. Fan, H.: Design tips for an efficient non-inverting buck-boost converter. Analog Applications Journal, Texas Instruments, pp. 20–25 (2014)
9. Hamel, B.: *àl' étude mathématique des systèms de réglage par tout ou rien* (1949). (in French)
10. Itkis, Yu.U.: Control Systems of Variable Structure. Wiley, New York (1976)
11. Komurcugil, H.: Adaptive terminal sliding-mode control strategy for DC-DC buck converters. ISA Trans. **51**, 673–681 (2012). (Elsevier)
12. Maity, S., Suraj, Y.: Analysis and modeling of an FFHC-controlled DC-DC buck converter suitable for wide range of operating conditions. IEEE Trans. Power Electron. **27**(12), 4914–4924 (2012)

13. Martinez-Salamero, L., Cid-Pastor, A., Aroudi, A.E., Giral, R., Calvente, J., Ruiz-Magaz, G.: Sliding-mode control of DC-DC switching converter, pp. 1910–1916. Preprints of the 18th IFAC World Congress, Milano, Italy (2011)
14. Mattingly, D.: Designing stable compensation networks for single phase voltage mode buck regulators. Technical Brief, Intersil (TB417.1) (2003)
15. Mehta, A., Bandyopadhyay, B.: Frequency-Shaped and Observer-Based Discrete-Time Sliding Mode Control. Springer, Berlin (2015)
16. Middlebrook, R., Cuk, S.: A general unified approach to modelling switching converter power stages. IEEE Power Electron. Spec. Conf. 73–86 (1976)
17. Naik, B., Mehta, A.: Sliding mode controller with modified sliding function for buck type converters. In: 22nd IEEE International Symposium on Industrial Electronics. Taipei (2013)
18. Naik, B., Mehta, A.: Sliding mode controller with modified sliding function for DC-DC buck converter. ISA Trans. **70**, 279–287 (2017). (Elsevier)
19. Naik, B., Mehta, A.: DC-DC buck converter with second order sliding mode control: analysis design and implementation. Int. J. Power Electron. Inderscience (Accepted for publication) **xx**, xxx–xxx (2018)
20. Perry, A.G., Fen, G., Liu, Y.F., Sen, P.: A new sliding mode like control method for buck converter. In: 35th Annual IEEE Power Electronics Specialists Conference, pp. 3688–3693. Aachen, Germany (2004)
21. Popovski, A.M.: Linearization of sliding operation mode for a constant speed controller. Autom. Remote Control **2**(3) (1950)
22. Pressman, A.I.: Switching Power Supply Design. Mc-Graw Hill, New York (1991)
23. Rahimi, A., Parto, P., Asadi, P.: Compensator design procedure for buck converter with voltage mode error-amplifier. Application Note, International Rectifier (AN-1162) (2011)
24. Sira-Remirez, H., Silva-Ortigoza, R.: Control Design Techniques in Power Electronics Devices. Springer, London (2006)
25. Smedley, K.M., Cuk, S.: One-cycle contol of switching converters. IEEE Trans. Power Electron. **10**(6), 625–633 (1995)
26. Spiazzi, G., Mattavelli, P., Rossetto, L.: Sliding mode control of DC-DC converters, University of Padova, Italy
27. Tan, S.C., Lai, Y.M., Tse, C.K.: On the practical design of sliding mode voltage controlled buck converter. IEEE Trans. Power Electron. **20**(2), 425–436 (2005)
28. Tan, S.C., Lai, Y.M., Tse, C.K.: Indirect sliding mode control of power converters via double integral sliding surface. IEEE Trans. Power Electron. **23**(2), 600–611 (2008)
29. Tan, S.C., Lai, Y.M., Tse, C.K.: Sliding Mode Control of Switching Power Converters. CRC Press, Boca Raton (2012)
30. Utkin, V.: Variable structure systems with sliding mode. IEEE Trans. Autom. Control **22**(2), 212–222 (1977)
31. Utkin, V.I.: Sliding Modes and Their Applications in Variable Structure Systems. Mir, Moscow (1978)
32. Utkin, V., Guldner, J., Shi, J.: Sliding Mode Control in Electromechanical Systems. Taylor & Francis, London (1999)
33. Wang, Q., Li, T., Feng, J.: Discrete time synergetic control for DC-DC converter. In: PIERS Proceedings, pp. 1086–1091. Xi'an, China (2010)
34. Zhang, H.: Modeling and loop compensation design of switch mode power supplies. Application Note 149, Linear Technology (149-1) (2015)

Chapter 2
Introduction to Sliding Mode Control of Power Electronic Converters

2.1 Introduction

Sliding mode control (SMC) has been of interest among research scientists and engineers since long. Its applicability to the wide variety of systems and its inherent robustness to input disturbances are the major causes to make it one of the most powerful control strategies. The SMC is a consequence of discontinuous control which was the subject of interest for many engineers of France [10] and USSR [11, 19]. Basically, they were analyzing the problem of oscillations in bang–bang control systems. The first studies concerned with the analysis of oscillations in bang–bang control; later on, it turned rapidly to the synthesis problem in different ways. One of the ways was time optimal control, and the other deals with robustness and linearization. The objective of both the approaches was quite different. However, they resulted to have much in common.

In the beginning of 1960s, the first fundamental SMC law was discovered. Before that, many control engineers were looking for the control law which could provide robustness to variations in system parameters for military and aeronautical applications. In 1962, B. Hamel's idea was the first due to which the studies of nonlinear controllers were initiated.

In the mid of the twentieth century, some Russian scientists [6, 7, 16] have come up with a new dimension in the field of control systems engineering popularly known as sliding mode control or variable structure control. Many researchers have contributed in the field [3, 20] and carried out experiments using sliding mode control for real-world complex applications. The SMC laws presented two different aspects:

- Astute combinations of linear and nonlinear signals which provide pseudo-linear control.
- They generate sliding motion through switching actions or commutations.

Consider the case of double integrator. The transfer function of the system is given by,

A. Mehta and B. Naik, *Sliding Mode Controllers for Power Electronic Converters*, Lecture Notes in Electrical Engineering 534,
https://doi.org/10.1007/978-981-13-3152-7_2

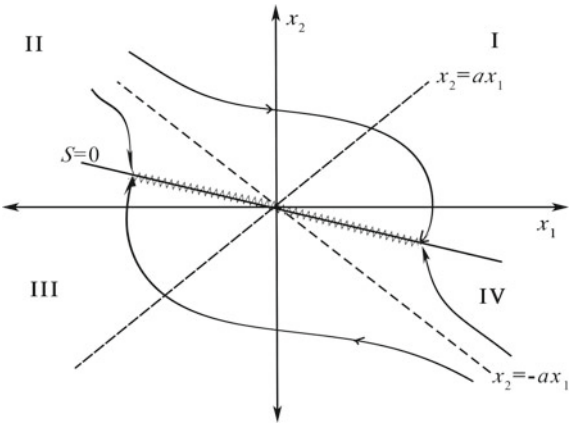

Fig. 2.1 Trajectories in the phase plane

$$\frac{y(s)}{u(s)} = \frac{a^2}{s^2}. \tag{2.1}$$

Where y denotes the output and u is the control effort or input to the system. Let the states be defined as

$$\dot{x_1} = x_2 \tag{2.2}$$

$$\dot{x_2} = a^2 u. \tag{2.3}$$

Also, note that $y = x_1$. Let the control law u be defined by the following equation.

$$u = -|x_1| sgn(x_1 + \alpha x_2) \tag{2.4}$$

In Eq. (2.4), the term $x_1 + \alpha x_2 = S$ is the switching function or sliding function or sliding surface. The control law commutes while crossing the line $S = 0$. In Fig. 2.1, the phase trajectories are shown under the SMC law. There are four regions in the phase plane named as I, II, III, and IV.

In the regions II and IV, the condition $x_1 sgn(S) < 0$ is satisfied and the phase trajectories are hyperbolas with asymptotes $x_2 = \pm a x_1$. While in the regions I and II, the condition $x_1 sgn(S) > 0$ is satisfied and the phase trajectories are ellipses with the equation,

$$a^2 {x_1}^2 + {x_2}^2 = constant. \tag{2.5}$$

With $\alpha > 0$, it can be assured that the phase trajectories will hit the sliding function and thereby the sliding motion over the sliding hyperplane will occur leading the trajectories toward the origin of the phase plane. This fact can be visualized in Fig. 2.1. Basically, during the ideal sliding motion where $S = 0$, the relation between

the states is $\dot{x_1} = -\frac{x_1}{\alpha}$ and hence the condition $x_1\dot{x_1} < 0$ is established. This states that the positive-definite function $L = \frac{{x_1}^2}{2}$ is minimized which leads to the state regulation. However, it cannot be always the case that the sliding motion occurs at the first hit of the phase trajectory to the sliding surface. As, for example, it can be easily seen that if the control law is defined as

$$u = -sgn(S) \tag{2.6}$$

then the sliding motion occurs if the condition $|x_2| < \alpha a^2$ is satisfied. This fact can be derived by observing the time derivative of the energy function of the sliding hyperplane $\left(\frac{S^2}{2}\right)$ to be negative; i.e., $S\dot{S} < 0$ is satisfied. This condition is known as reaching condition.

It is interesting to note that the system of Eqs. (2.4) and (2.5) has solution if u is Lipschitz [2] and so continuous. Hence, the classical theory of ordinary differential equations is no longer useful. The SMC in a broader view deals with the differential equations with the discontinuous right-hand side [2, 8]. In the following section, the design of continuous-time SMC for linear time-invariant system is presented.

2.2 Sliding Mode Control Technique

Vadim Utkin in 1978 [20] and in 1999 [21] published their popular work in which SMC for PECs is the main focus. In 1999, Sarah et al. [5] also published their popular book. Recent work in SMC may be found in [9, 12, 18].

Let a linear time-invariant (LTI) continuous-time system be defined as,

$$\dot{x} = Ax + Bu, \tag{2.7}$$

$$y = Cx + Du, \tag{2.8}$$

where matrices $A \in R^{n\times n}$, $B \in R^{n\times m}$, $C \in R^{l\times n}$, $D \in R^{l\times m}$, and $x \in R^n$ is the state vector, $y \in R^l$ is the system output, and $u \in R^m$ is the input to the system. The system in Eq. (2.2) can be rewritten as,

$$\begin{bmatrix} \dot{x}_1 \\ \dot{x}_2 \end{bmatrix} = \begin{bmatrix} a_{11} & a_{12} \\ a_{21} & a_{22} \end{bmatrix} \begin{bmatrix} x_1 \\ x_2 \end{bmatrix} + \begin{bmatrix} B_1 \\ B_2 \end{bmatrix} u. \tag{2.9}$$

The above equation can be converted to a regular form [5, 11, 21] by linear transformation matrix M such that,

$$\dot{q} = Qq + Hu. \tag{2.10}$$

Where $q = Mx, x = [x_1 \;\; x_2]^T, q = [q_1 \;\; q_2]^T, Q = \begin{bmatrix} q_{11} & q_{12} \\ q_{21} & q_{22} \end{bmatrix}, H = \begin{bmatrix} 0 \\ H_2 \end{bmatrix}$. Now, let us assume that there exist sliding mode control law u which forces the phase trajectory to slide on the hyperplane S on a phase plane for $\alpha > 0, \alpha \in R$ given by,

$$S = \alpha q_1 + q_2 = Pq \tag{2.11}$$

where $P = [\alpha \;\; 1], \alpha > 0, \alpha \in R$.

Now, setting $S = 0$ in Eq. (2.11) and considering Eq. (2.10) the following result is achieved.

$$\dot{q_1} = (q_{11} - q_{12}\alpha)q_1 \tag{2.12}$$

There exists α for which Eq. (2.12) can have the stable dynamics. As explained in Chap. 1, there are three modes in the sliding mode control namely reaching mode (RM), sliding mode (SM), and steady-state mode (SS) [15]. In RM, the phase trajectory is attracted to the sliding hyperplane S. During the SM, the phase trajectory *slides* on the sliding surface toward the origin of the phase plane. And the states are forced to remain at the origin during SSM [17, 18]. Let the Lyapunov Function [14] V to be,

$$\begin{aligned} V &= \frac{1}{2}S^2 \\ \dot{V} &= S\dot{S} \end{aligned} \tag{2.13}$$

Naturally, the minimization of V is possible if the following condition,

$$S\dot{S} < 0 \tag{2.14}$$

is satisfied. Equation (2.14) is known as reachability condition which guarantees the RM. It can be achieved if there is a definite relationship between S and its time derivative $\dot{S}$. One way to achieve it is to use a signum function [15, 21]. The following relationship

$$\dot{S} = -\eta sgn(S) \tag{2.15}$$

can be the choice. Here, in the above equation η is a positive scalar.

With this background and setting $\dot{S} = 0$, one can now derive the control law using Eqs. (2.10), (2.11), and (2.15) as,

$$\begin{aligned} \dot{S} &= -\eta sgn(S) = PQq + PHu, \\ u &= -(PH)^{-1}[PQq + \eta sgn(S)], \end{aligned} \tag{2.16}$$

provided that matrix (PH) is invertible. Note that the SMC involves the switching function and may cause chattering in the controlled variable. However, this may be considered as the drawback of the control technique, the system under SMC is insensitive to the matched uncertainties, i.e., disturbances in the input channel. In

the following section, the invariance of SMC technique for matched uncertainty is proved.

2.2.1 *Invariance Property of Sliding Mode Control for Matched Uncertainties*

It is interesting to prove that the performance of a system under SMC remains insensitive to matched uncertainties [4, 21]. Consider the system of Eq. (2.2) to be in regular form and the sliding surface to be,

$$S = Px. \tag{2.17}$$

Now, the expression for the equivalent control effort u can be found by setting $\dot{S} = 0$, and considering Eq. (2.2),

$$\begin{aligned} P\dot{x} &= 0, \\ u &= -(PB)^{-1}PAx. \end{aligned} \tag{2.18}$$

If there exists some matched disturbance to the system of and in the presence of disturbance h, the system equation can be rewritten as,

$$\dot{x} = Ax + Bu + h. \tag{2.19}$$

Due to the presence of h and setting $\dot{S} = 0$, the controller effort u of Eq. (2.18) now becomes,

$$u = -(PB)^{-1}P[Ax + h]. \tag{2.20}$$

Substituting the u of Eq. (2.20), the closed-loop dynamics of the system can now be written as,

$$\dot{x} = Ax - B\left[(PB)^{-1}P(Ax + h)\right] + h. \tag{2.21}$$

By arranging the terms in Eq. (2.21), one can get,

$$\dot{x} = (Ax - B(PB)^{-1}PAx) + (I - B(PB)^{-1}P)h \tag{2.22}$$

It is clear form Eq. (2.22) that the term $(I - B(PB)^{-1}P)h$ becomes zero if h is a matched uncertainty or matched disturbance; i.e., there exists a δ such that $h = B\delta$. This proves the invariance of SMC for matched uncertainties.

2.2.2 *Review of Conventional Control for Power Electronic Converters*

There are many control strategies available in the wide variety of literature. Among them the pulse width modulation (PWM)-based control strategy is quite common. However, the analysis is quite complex. As proved in previous sections, the sliding mode control (SMC) is robust for matched disturbances. Moreover, SMC is a switching control and hence inherently suitable for switching power converters. The analog implementation of PWM may be sensitive to noise. Digital implementation is preferred in many cases but they too require programming. The PWM-based control can be affected due to overmodulation and undermodulation. Implementation of SMC is quite straightforward compared to PID/PWM-based control strategy. However, many researchers have carried theoretical and experimental research works for the domain; few of them have preferred SMC technique for power converters. As the SMC is now tested for many switching power converters, the challenging issues are the elimination of steady-state error and chattering alleviation. For that, higher-order SMC may be the choice. With this background, one can imagine the importance of SMC for the power converters. The next sections discuss about modeling and state feedback control for DC-DC Buck converter.

2.3 Conventional State Feedback Control for Power Electronic Converters

This section focuses on the modeling and control of DC–DC Buck converter. The state feedback control is used. First, let us now discuss the state-space average modeling [13] for a DC–DC Buck converter.

Figure 2.2 shows the Buck converter with state feedback controller [14] with the convenient notations where dynamical equations are defined as,

$$x_1 = i_L \tag{2.23}$$

$$x_2 = V_o. \tag{2.24}$$

The state-space model of the Buck converter when switch is opened, i.e., SW is 1 or 'ON', can be described as [1],

$$\begin{bmatrix} \dot{x}_1 \\ \dot{x}_2 \end{bmatrix} = \begin{bmatrix} 0 & -\frac{1}{L} \\ \frac{1}{C} & -\frac{1}{RC} \end{bmatrix} \begin{bmatrix} x_1 \\ x_2 \end{bmatrix} + \begin{bmatrix} \frac{1}{L} \\ 0 \end{bmatrix} E. \tag{2.25}$$

For the period of time when the switch is closed, i.e., SW is 0 or 'OFF', the model can be described as,

$$\begin{bmatrix} \dot{x}_1 \\ \dot{x}_2 \end{bmatrix} = \begin{bmatrix} 0 & -\frac{1}{L} \\ \frac{1}{C} & -\frac{1}{RC} \end{bmatrix} \begin{bmatrix} x_1 \\ x_2 \end{bmatrix} + \begin{bmatrix} 0 \\ 0 \end{bmatrix} E. \tag{2.26}$$

If the duty cycle of the pulse width modulated (PWM) signal is ρ and if W is the cycle time, the switch *on* and *off* time are to be represented as ρW and $(1-\rho)W$, respectively. In such a case, the state-space averaged model can be represented as [1],

$$\begin{bmatrix} \dot{x}_1 \\ \dot{x}_2 \end{bmatrix} = \begin{bmatrix} 0 & -\frac{1}{L} \\ \frac{1}{C} & -\frac{1}{RC} \end{bmatrix} \begin{bmatrix} x_1 \\ x_2 \end{bmatrix} + \begin{bmatrix} \frac{\rho}{L} \\ 0 \end{bmatrix} E. \tag{2.27}$$

If $\hat{}$ denotes a perturbation in a variable, the small signal or AC model for the state-space averaged model of Eq. (2.27) can be obtained as,

$$\begin{bmatrix} \dot{\hat{x}}_1 \\ \dot{\hat{x}}_2 \end{bmatrix} = \begin{bmatrix} 0 & -\frac{1}{L} \\ \frac{1}{C} & -\frac{1}{RC} \end{bmatrix} \begin{bmatrix} \hat{x}_1 \\ \hat{x}_2 \end{bmatrix} + \begin{bmatrix} \frac{\chi}{L} \\ 0 \end{bmatrix} \hat{E} + \begin{bmatrix} \frac{E}{L} \\ 0 \end{bmatrix} \hat{\rho}. \tag{2.28}$$

Here, χ represents the duty cycle of the converter in open loop, i.e., the nominal value of the duty cycle and $\hat{\rho}$ is the perturbation in the duty cycle. This can be interpreted as the relation $\rho = \chi + \hat{\rho}$. It is reasonable to assume that the E is fairly smooth and hence perturbation in E, i.e., $\hat{E} = 0$. Then, Eq. (2.28) can be written as,

$$\dot{\hat{x}} = \bar{A}\hat{x} + B\hat{\rho}, \tag{2.29}$$

where

$$B = \begin{bmatrix} \frac{E}{L}. \\ 0 \end{bmatrix}. \tag{2.30}$$

Now perturbation in χ, i.e., $\hat{\rho} = \frac{\chi}{V_{con}} \hat{V}_{con}$. If we use state feedback as shown in Fig. 2.2,

$$\hat{V}_{con} = -K\hat{x}. \tag{2.31}$$

So,

$$\dot{\hat{x}} = \bar{A} + B\left(-\frac{\chi}{V_{con}} K\hat{x}\right) \tag{2.32}$$

$$\dot{\hat{x}} = \left(\bar{A} - B\frac{\chi}{V_{con}} K\right)\hat{x} \tag{2.33}$$

The small signal ac equivalent model of the Buck converter or any converter describes the dynamics around the operating point. The state feedback in this case provides improved stability for the operating point conditions. The feedback can provide considerably better response of the system (which is output voltage in this case) for small variations in the parameters of the system when compared to the system

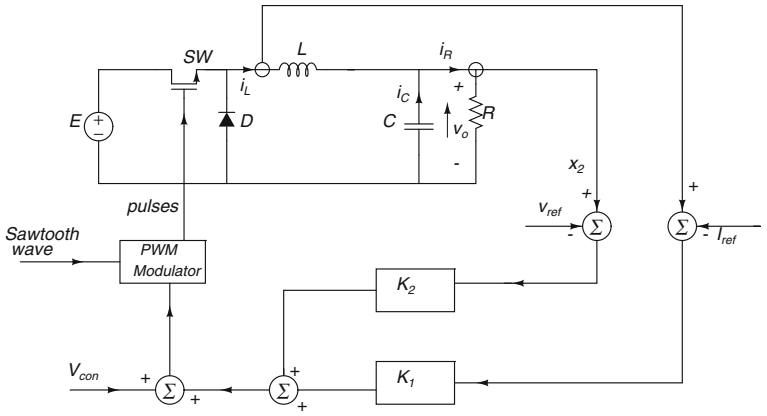

Fig. 2.2 State feedback control scheme for Buck converter

Table 2.1 Parameters for state feedback control for DC–DC Buck Converter

Symbol	Description	Value
L	Inductance	1.33 mH
C	Capacitance	94 μF
E	DC supply voltage	24 V
R	Load resistance	4 or 2.8 Ω
	Initial capacitor voltage	0 V
χ	Nominal duty cycle	0.3
W	Time cycle (PWM)	0.000005
V_{ref}	Reference for x_2	6.8 V
I_{ref}	Reference for x_1	$\frac{V_{ref}}{R}$ A
Load disturbance	at 0.5 s	4 to 2.8 Ω
K_1	Feedback gain	−0.36558
K_2	Feedback gain	−0.2020
V_{con}	Control voltage for PWM	3 V

without feedback. The state feedback gain $K = [K_1 \;\; K_2]$ can be obtained by pole placement method [14]. However, the desired closed-loop poles are required which are to be set. The simulation parameters are set as per Table 2.1. The simulation results are shown in Figs. 2.3 and 2.4.

During the simulation, the load disturbance in the load resistance is introduced at 0.5 s. The load varies from 4 to 2.8 Ω. The output voltage and inductor current are shown in Fig. 2.3. The set voltage is 6.8 V in case of closed-loop mode. The open-loop responses are quite noisy and less smooth than those with feedback. Also,

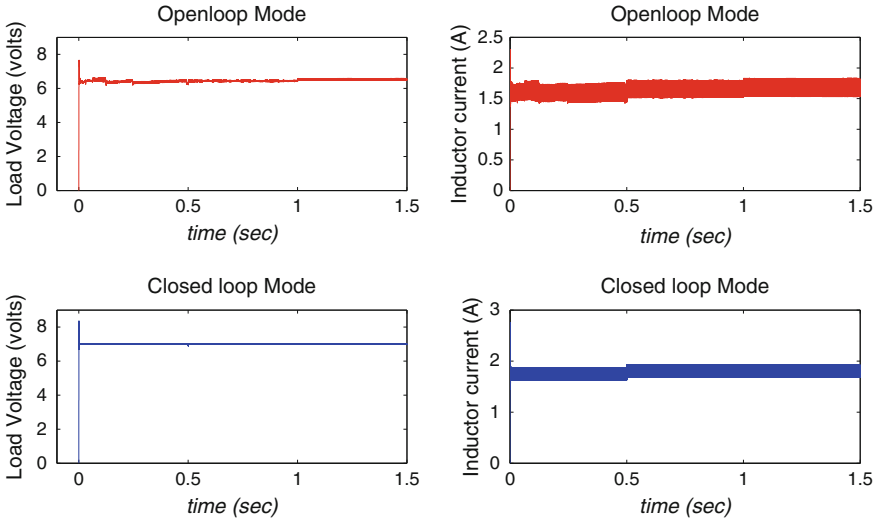

Fig. 2.3 Load voltage and inductor current in open loop and closed loop

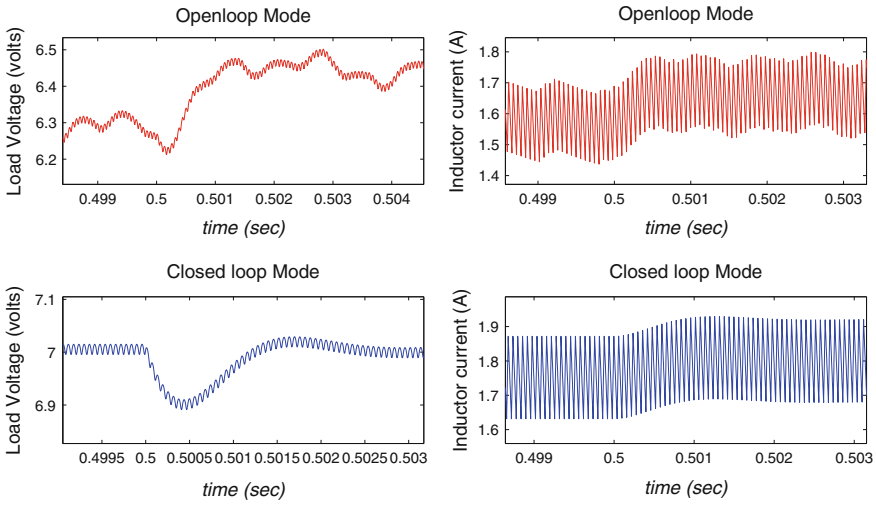

Fig. 2.4 Load voltage and inductor current in open loop and closed loop (scaled view of Fig. 2.3)

it is observed that the voltage and current follow the references quite satisfactory. The load disturbance at 0.5 s is apparently visible in the responses. Figure 2.4 is the scale magnified view; Fig. 2.3 facilitates the better view of the responses during the load disturbance.

2.4 Summary

In this chapter, the basics of SMC is discussed. Also, it is shown that the technique provides robustness against the matched or input disturbances. Along with that, the modeling of a DC-DC Buck converter with model averaging technique is presented. The AC analysis or small signal AC model of the converter is presented. Also, the guidelines for designing the controller to achieve the desired responses with PWM are outlined with suitable examples and with simulation results. The next chapter introduces the proposed modified SMC technique for DC–DC Buck converters which may be preferable over conventional SMC as it provides good steady-state responses of load voltage and better performance in the presence of load disturbances.

References

1. Ang, S., Oliva, A.: Power Switching Converters. CRC Press, Taylor & Francis Group, Boca Raton (2005)
2. Barbot, J.P., Perruquetti, W.: Sliding Mode Control in Engineering. Marcel Dekker Inc., New York (2002)
3. Dolgolenko, Yu.V.: Sliding modes in relay indirect control systems. In: Proceeding of 2nd All-Union Conference on Control (1955)
4. Drazenovic, B.: The invariance conditions in variable structure systems. Automatica, Pergamon Press **5**(3) (1969)
5. Edwards, C., Spurgeon, S.: Sliding Mode Control Theory and Applications. Taylor & Francis, London (1998)
6. Emelyanov, S.V.: Method of designing complex control algorithms using an error and its first time-derivative only. Autom. Remote Control **18**(10) (1957)
7. Emelyanov, S.V.: Theory of Variable Structure Systems. Nauka, Moscow (1970)
8. Filippov, A.: Differential Equations with Discontinuous Right Hand Sides. Kluwer Ac. Pub., Boston (1983)
9. Fridman, L., Moreno, J., Iriarte, R.: Sliding Mode After the First Decade of the 21st Century. Springer, Berlin (2011)
10. Hamel, B.: *àl' étude mathématique des systèms de réglage par tout ou rien* (1949). (in French)
11. Lukyanov, A., Utkin, V.: Methods of reducing equations for dynamic systems to a regular form. Autom. Remote Control **42**(4) (1981)
12. Mehta, A., Bandyopadhyay, B.: Frequency-Shaped and Observer-Based Discrete-Time Sliding Mode Control. Springer, Berlin (2015)
13. Middlebrook, R., Cuk, S.: A general unified approach to modelling switching converter power stages. In: IEEE Power Electronics Specialists Conference, pp. 73–86 (1976)
14. Ogata, K.: Modern Control Engineering. Prentice Hall, New Jersey (1997)
15. Perry, A.G., Fen, G., Liu, Y.F., Sen, P.: A new sliding mode like control method for buck converter. In: 35th Annual IEEE Power Electronics Specialists Conference, pp. 3688–3693. Aachen, Germany (2004)
16. Popovski, A.M.: Linearization of sliding operation mode for a constant speed controller. Autom. Remote Control **2**(3) (1950)
17. Sabanovic, A., Fridman, L., Spurgeon, S.: Variable Structure Systems from Principles to Implementation. IET, London (2004)
18. Shtessel, Y., Edwards, C., Fridman, L., Levant, A.: Sliding Mode Control and Observation. Springer Science+Business Media, New York (2014)

19. Tzypkin, Y.: Theory of Relay Control Systems. Gostekhiz-dat, Moscow (1955)
20. Utkin, V.I.: Sliding Modes and Their Applications in Variable Structure Systems. Mir, Moscow (1978)
21. Utkin, V., Guldner, J., Shi, J.: Sliding Mode Control in Electromechanical Systems. Taylor & Francis, London (1999)

Chapter 3
Sliding Mode Controller with PI-Type Sliding Function for DC–DC Buck Converter

3.1 Introduction

The Buck converter is the most popular in industry due to its high efficiency and simplicity which emanates from its linear and minimum phase type by nature. Also known as step-down converter, a Buck converter finds its applications for majority of electronics devices including power supplies for computers. Buck converters and other power electronic converters (PECs) functioning in closed-loop control mode are the demand of many industrial and domestic applications like instrumentation systems, AC–DC drives, telecommunications, and renewable energy systems. Most of the electronic devices demand stable and controlled power supply for better dynamic and steady-state performance. Although pulse-width modulation (PWM) technique-based controllers are already in action since long, the sliding mode control (SMC) enters with a new dimension in the field of control systems for PEC. The modeling and control techniques for PEC are available in the wide variety of literature [1, 7].

In this chapter, the design of sliding mode controller with proportional–integral-type sliding function for DC–DC Buck converter is presented. The converter with conventional sliding mode controller results in a steady-state error in load voltage. The proposed modified sliding function improves the steady-state and dynamic performance of the converter and facilitates better choices of controller tuning parameters. The conditions for the existence of sliding modes for the control scheme are derived. The stability of the closed-loop system with proposed sliding mode control is proved, and the improvement in steady-state performance is exemplified. The idea of adaptive tuning for the proposed controller to compensate load variations is outlined. The comparative study of conventional and proposed control strategy is presented. The efficacy of the proposed strategy is endowed by the simulation and experimental results. Although the PID-type sliding surface is discussed in the literature [3], the proof of zero steady-state error and switching frequency analysis is not presented. Only simulation results were presented. Moreover, in the later sections of this chapter the integral SMC with finite-time reaching (ISMCFTR) is proposed.

A. Mehta and B. Naik, *Sliding Mode Controllers for Power Electronic Converters*, Lecture Notes in Electrical Engineering 534,
https://doi.org/10.1007/978-981-13-3152-7_3

With the ISMCFTR, the load voltage of the Buck converter approaches reference value in finite time. The conditions of existence of SM are obtained.

3.2 Mathematical Modeling

A sliding mode voltage controlled (SMVC) DC–DC Buck converter model is derived using state-space approach [6]. A mathematical model of DC-DC Buck converter in open loop can be derived using basic circuit analysis laws. The converter is with the pure resistive load and its output voltage is to be controlled with SMC as shown in the Fig. 3.1. The converter is assumed to be operated in continuous current conduction mode [4]. Let $\beta = \frac{R_2}{R_1+R_2}$ be the voltage divider ratio. The values or R_1 and R_2 are very high compared to the load resistor to avoid loading effect. If V_{ref} is a reference voltage, $V_\mu = \beta V_{ref}$ is the scaled down version of reference voltage. L is an inductor, C is a capacitor, D is the free-wheeling diode, V_o is the output or load voltage, V_i is the input voltage, and r_L is the load resistance. The SW is a n channel MOSFET switch turned ON or OFF with the output of SM controller which is in the form of pulses. Noting that $u = 1$ means SW is closed and $u = 0$ means SW is open, the state-space model of the electrical system can be derived by defining the states as follows:

$$x_1 = V_\mu - \beta V_o, \tag{3.1}$$

$$x_2 = \dot{x}_1. \tag{3.2}$$

From Eq. (3.2),

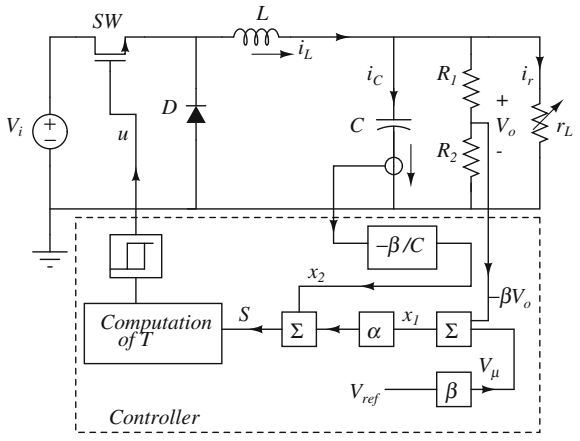

Fig. 3.1 DC–DC Buck converter with SMC

$$x_2 = -\beta \frac{dV_o}{dt} = -\frac{\beta}{C} i_C,$$

where i_C is the capacitor current which can be measured as shown in Fig. 3.1. Let i_L and i_r be the inductor current and load current, respectively. The equation for x_2 can be rewritten as,

$$x_2 = -\frac{\beta}{C}[i_L - i_r]. \tag{3.3}$$

Let the voltage drop across inductor v_L given by,

$$v_L = (uV_i - V_0) = L\frac{di_L}{dt}.$$

$$\implies i_L = \int \frac{uV_i - V_o}{L} dt.$$

So, Eq. (3.3) can be rewritten as,

$$x_2 = \dot{x}_1 = \frac{\beta}{C}\left(\frac{V_o}{r_L} - \int \frac{uV_i - V_o}{L} dt\right). \tag{3.4}$$

Hence,

$$\dot{x_2} = -\frac{1}{LC}x_1 - \frac{1}{r_L C}x_2 - \frac{\beta V_i}{LC}u + \frac{V_\mu}{LC}. \tag{3.5}$$

From Eqs. (3.2) and (3.5), the state-space model of Buck converter system is obtained as,

$$\begin{bmatrix} \dot{x}_1 \\ \dot{x}_2 \end{bmatrix} = \begin{bmatrix} 0 & 1 \\ -\frac{1}{LC} & -\frac{1}{r_L C} \end{bmatrix} \begin{bmatrix} x_1 \\ x_2 \end{bmatrix} + \begin{bmatrix} 0 \\ -\frac{\beta V_i}{LC} \end{bmatrix} u + \begin{bmatrix} 0 \\ \frac{V_\mu}{LC} \end{bmatrix}. \tag{3.6}$$

3.2.1 Sliding Mode Control for DC–DC Buck Converter

Let the sliding function S which establishes linear relationship among states be defined as,

$$S = \alpha x_1 + x_2 = Px, \tag{3.7}$$

where $P = [\alpha, 1]$, state vector $x = [x_1, x_2]^T$, α is a scalar, $\alpha > 0$, and it controls the first-order dynamics of Eq. (3.7). By reducing the value of α, one can slow down the reaching mode dynamics. It is known that sliding mode control occurs if the reaching condition

$$S\dot{S} < 0, \tag{3.8}$$

is satisfied [2, 7]. The sliding mode control law can be defined as per the following rule:

$$u = \begin{cases} 1 = ON, & S > 0 \\ 0 = OFF, & S < 0 \end{cases} \tag{3.9}$$

The control law in Eq. (3.9) will trigger the switching across the sliding manifold S. The switching device has operating frequency limitations, and hence, for practical implementation the following control law is preferred:

$$u = \begin{cases} 1 = ON, & S > \varepsilon \\ 0 = OFF, & S < -\varepsilon \end{cases} \tag{3.10}$$

where ε is a small positive number. Control law in Eq. (3.10) can reduce the severity of chattering by limiting chattering frequency, and hence, it is feasible for the implementation. The existence of sliding modes requires the following two conditions to be satisfied [1]. From Eqs. (3.6), (3.7), (3.8), and (3.9),

$$B_1 = \left(\alpha - \frac{1}{r_L C}\right) x_2 - \frac{1}{LC} x_1 + \frac{V_\mu - \beta V_i}{LC} < 0, \tag{3.11}$$

$$B_2 = \left(\alpha - \frac{1}{r_L C}\right) x_2 - \frac{1}{LC} x_1 + \frac{V_\mu}{LC} > 0. \tag{3.12}$$

Where $\begin{cases} G_1 = P\dot{x} & \text{for } 0 < S < \varepsilon \\ G_2 = P\dot{x} & \text{for } -\varepsilon < S < 0 \end{cases}$.

The region of existence (ROE) of sliding modes on the phase plane is the region where condition $S\dot{S} < 0$ is satisfied. From Eqs. (3.11) and (3.12), the ROE is determined by the three lines $G_1 = 0$, $G_2 = 0$, and $S = 0$ on the phase plane. It can be seen that there are two possibilities, $\alpha > \frac{1}{r_L C}$ and $\alpha < \frac{1}{r_L C}$. It may be observed that the slopes of lines $G_1 = 0$ and $G_2 = 0$ change due to variation in r_L. This imposes a limitation on the dynamic behavior of the system as α determines the speed of response. The choice of α is important due to the first-order dynamics which are given by,

$$x_1(t) = x_1(t_0) \exp^{-\alpha(t - t_0)}, \tag{3.13}$$

where $x_1(t_0)$ is the initial state at time t_0. The choice of α is important for the speed of response of states and allowing the maximum possible ROE on the phase plane. To meet the requirements, $\alpha = \frac{1}{r_L C}$ is chosen [6]. This restricts the selection of α as it governs the first-order dynamics of Eq. (3.13). If it may be possible to introduce one more tuning parameter that can compensate the load variation, the goal can be

achieved. The next section discusses the use of modified sliding function so that restriction in the selection of α is eliminated and better responses with load variation compensation is achieved through additional tuning parameter. The proposed sliding function in the next section not only eliminates the restriction in the choice of α but also gives better performance.

3.3 Proposed PI-Type Sliding Function

Let a proportional–integral-type function of sliding function be defined as,

$$T = S + \gamma \int_0^t S dt, \tag{3.14}$$

where $\gamma > 0$ is a scalar. Here, the integral term is used to achieve better steady-state performance of the load voltage under closed-loop control. This fact can be visualized from the following equations.

Taking Laplace transformation of Eq. (3.7),

$$\frac{S(s)}{x_1(s)} = s + \alpha \tag{3.15}$$

Similarly taking Laplace Transformation of Eq. (3.14) and from above equation,

$$\frac{T(s)}{x_1(s)} = \frac{T(s)}{S(s)} \frac{S(s)}{x_1(s)} = \frac{(s+\alpha)(s+\gamma)}{s} \tag{3.16}$$

Obviously, the above equation has proportional–integral–derivative (PID) controller type of characteristics. It is well known that increasing the order of the controller can lead to better performance. However, in this case smooth operation is not possible due to the presence of switch and hence we have to switch around $T = 0$ as per the following rule.

$$u = \begin{cases} 1 = ON, & T > 0 \\ 0 = OFF, & T < 0 \end{cases}. \tag{3.17}$$

Equation (3.17) can also be stated as,

$$u = \frac{1}{2}[1 + sgn(T)]. \tag{3.18}$$

Switching across $T = 0$ yields the following important result. Setting $T = 0$ in Eq. 3.14,

$$S = -\gamma \int_0^t S dt. \tag{3.19}$$

This is equivalent to,

$$\dot{S} = -\gamma S. \tag{3.20}$$

Which leads to minimization of S.

The existence of sliding modes is possible on the phase plane if the following two conditions are satisfied.

$$\lim_{T \to 0^+} \dot{T} < 0 \tag{3.21}$$

$$\lim_{T \to 0^-} \dot{T} > 0 \tag{3.22}$$

In the following theorem, it is proved that the reaching mode (RM) does occur by switching across $T = 0$. In RM, the phase trajectory hits the hyperplane $S = 0$ and then sliding mode (SM) occurs.

Theorem 3.1 *The switching across modified sliding function T leads the phase trajectory to reach to $T, S = 0$ manifold in finite time, and then to minimization of T, S; i.e., sliding mode occurs if the condition $T\dot{T} < 0$ is satisfied.*

Proof If γ is integral gain and $T > 0$, then $\dot{T} < 0$,
$\Rightarrow \dot{S} + \gamma S < 0$
$\Rightarrow \dot{S} < -\gamma S$
$\Rightarrow S\dot{S} < -\gamma S^2$
$\Rightarrow \frac{1}{2}\frac{d}{dt}(S^2) < -\gamma S^2$
$\Rightarrow S^2(t) < 2S^2(t_0)exp^{[-2\gamma(t-t_0)]}$,

where t_0 is the initial time and $\gamma > 0$. The above condition is important as it states that the S^2 must be decreasing any time if the sliding function T assumes positive value. Similarly, S^2 must be increasing if T assumes negative value. Once the phase trajectory hits the sliding manifold in the ROE, where $T\dot{T} < 0$ is satisfied, the sliding mode, SM [2], occurs and stability prevails.

The following subsection will be helpful to study the situation for which the reaching condition, $T\dot{T} < 0$, is satisfied and to find the ROE. The ROE is the region on the phase plane for which the reaching condition is valid.

3.3.1 Analysis of ROE and Stability

To evaluate ROE on the phase plane, consider $\dot{S} + \gamma S < 0$ which can be simplified as,

$\alpha\dot{x}_1 + \dot{x}_2 + \gamma\alpha x_1 + \gamma x_2 < 0.$

Now from the above equation and Eq. (3.6), with $u = 1$,

$$\begin{aligned} &\alpha x_2 + \left(-\frac{1}{LC}\right) x_1 + \left(-\frac{1}{r_L C}\right) x_2 \\ &+ \left(\frac{-\beta V_i + V_\mu}{LC}\right) + \gamma\alpha x_1 + \gamma x_2 < 0. \end{aligned}$$

$$\begin{aligned} \Rightarrow H_1 = &\left(\alpha - \frac{1}{r_L C} + \gamma\right) x_2 + \left(\alpha\gamma - \frac{1}{LC}\right) x_1 \\ &+ \left(-\frac{\beta V_i}{LC}\right) + \left(\frac{V_\mu}{LC}\right) < 0 \end{aligned} \tag{3.23}$$

Similarly, considering $u = 0$ for $T < 0$ we may write,

$$\begin{aligned} H_2 = &\left(\alpha - \frac{1}{r_L C} + \gamma\right) x_2 + \left(\alpha\gamma - \frac{1}{LC}\right) x_1 \\ &+ \left(\frac{V_\mu}{LC}\right) > 0. \end{aligned} \tag{3.24}$$

It can be seen from Eqs. (3.23) and (3.24) that the ROE is determined with lines $H_1 = 0$, $H_2 = 0$, and $S = 0$ on the phase plane [5]. It may be noticed that the dynamics of system states and the ROE on the phase plane can be determined with two independent parameters α and γ, respectively. By selecting $\gamma = \frac{1}{r_L C}$, the ROE on phase plane is insensitive to load variations. However, it should be noted that the higher values of α can lead to sustained oscillations or peak overshoots/undershoots in the load voltage [6]. Hence, the values of α and or γ must be low enough to prevent oscillations or overshoots in the load voltage. Selecting α as high as possible, faster dynamics can be achieved. The parameter γ can be adaptively tuned as per the changes in the load resistance. Practically, this is possible with the following relationship:

$$\gamma = \frac{1}{r_L C} = \frac{i_r}{V_o C}$$

where i_r is the load current. Hence, the setup for adaptive control requires the measurement of load current. Note that due to variations in the load resistance, the ROE on the phase plane does not vary.

The more practical way to fix the ROE on the phase plane, and which is independent on load variation, is to select α, γ very high compared to $\frac{1}{r_L C}$ in Eqs. (3.23) and (3.24).

3.3.2 The Switching Frequency and Steady-State Performance

3.3.2.1 Switching Frequency

It is obvious that the switching frequency is finite, and hence, the selection of the switching element should be carefully done. For that, firstly the permissible switching frequency should be determined. Let the dead zone in the switching element be represented by a small positive number ε. Then, the switching across T can be viewed as per Fig. 3.2.

Now, for the time period W_{ON}, we get,

$$W_{ON} = \frac{2\varepsilon}{\dot{T}^{-}} \tag{3.25}$$

and,

$$W_{OFF} = \frac{2\varepsilon}{\dot{T}^{+}}. \tag{3.26}$$

Here, $\dot{T}^{+}$ and $\dot{T}^{-}$ denotes $\dot{T} > 0$ and $\dot{T} < 0$, respectively.

Considering that the systems states variations as low amplitude AC signal during sliding modes, one can write the following set of equations during W_{ON} and W_{OFF}. Considering this fact and Eqs. (3.6), (3.17), from Eqs. (3.21) to (3.24) we get,

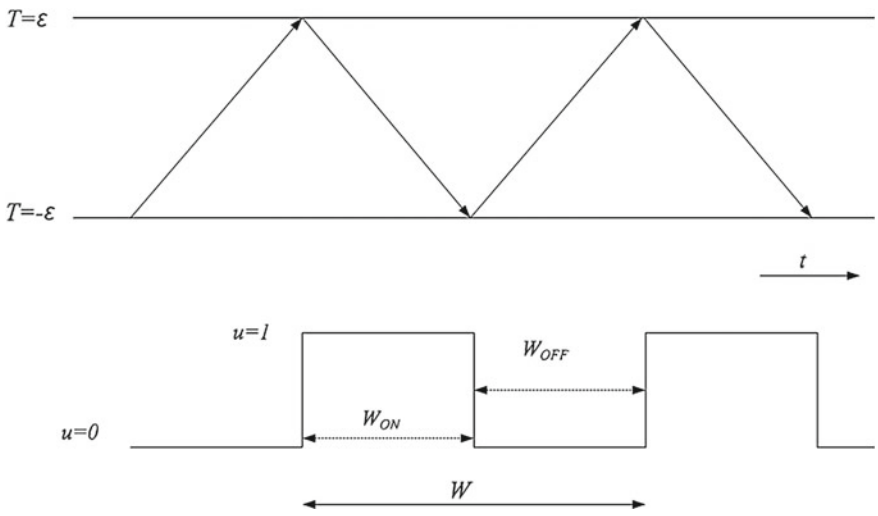

Fig. 3.2 Switching in sliding function with dead zone

$$\dot{T}^{-} = \left(-\frac{\beta V_i}{LC}\right) + \left(\frac{V_\mu}{LC}\right) \tag{3.27}$$

and,

$$\dot{T}^{+} = \left(\frac{V_\mu}{LC}\right). \tag{3.28}$$

From Eqs. (3.25), (3.26) to (3.27), (3.28), one can derive the expressions for W_{ON} and W_{OFF} as follows:

$$W_{ON} = \frac{2\varepsilon LC}{(-\beta V_i + V_\mu)} \tag{3.29}$$

$$W_{OFF} = \frac{2\varepsilon LC}{V_\mu} \tag{3.30}$$

Now, the switching frequency f_s is given by,

$$f_s = \frac{1}{W_{ON} + W_{OFF}} \tag{3.31}$$

From Eqs. (3.29) to (3.31), the switching frequency can be given by,

$$f_s = \frac{(V_\mu - \beta V_i)V_\mu}{2\varepsilon LC[2V_\mu - \beta V_i]} \tag{3.32}$$

Defining $w^2 = \frac{1}{LC}$ and considering the fact that $V_\mu = \beta V_{ref}$, Eq. (3.32) can be rewritten as,

$$f_s = V_{ref}\frac{(V_{ref} - V_i)\beta w^2}{2\varepsilon(2V_{ref} - V_i)} \tag{3.33}$$

Note that the switching frequency is inversely proportional to the size of the dead zone in the switching element ε and it depends on other systems parameters as mentioned in Eq. (3.33).

3.3.2.2 Steady-State Performance

Exact analysis of steady-state error is complicated due to the presence of switching element. However, in this section it is tried to evaluate mathematically the performance of proposed control law in terms of steady-state performance. It is reasonable to assume V as the uniform neighborhood of S_r which is a set of all the numbers in S those are very small in magnitude such that,

$$S_r = \bigcup_{p \in S} B_r(p),$$

$$B_r(p) = \{x \in S | d(x, p) < r\}.$$

For $p = 0$ and r is the center and radius of an open ball, from the above equations one can immediately notice that for any point $\delta \in S_r$ from Eqs. (3.1), (3.2), and (3.7), one can write,

$$\delta = \alpha x_1 + \dot{x_1}. \tag{3.34}$$

Taking the Laplace transformation and rearranging the terms, one can write the expression of $x_1(s)$ which is the x_1 in so-called s-domain, and s is the Laplace operator as per the following equation.

$$x_1(s) = \frac{\delta}{s(s+\alpha)} + \frac{x_1(0)}{s+\alpha}, \tag{3.35}$$

where $x_1(0)$ is the initial condition of the state. It is now obvious that the final value of the state $x_1(t)$ can be obtained by the final value theorem as,

$$\lim_{t \to \infty} x_1(t) = \lim_{s \to 0} s(x_1(s)) = \frac{\delta}{\alpha} \tag{3.36}$$

It is very clear from Eq. (3.36) that the state $x_1(t)$ is not forced to zero; instead, the higher values of alpha can help to achieve the goal of minimizing the steady-state error. But it is not feasible to achieve zero steady-state error.

Now, repeating the same procedure as above and assuming the value of T to be δ and one can rewrite Eq. (3.14) as,

$$\delta = S + \gamma \int_0^t S dt, \tag{3.37}$$

$$\delta = \alpha x_1 + \dot{x_1} + \gamma \int_0^t (\alpha x_1 + \dot{x_1}) dt. \tag{3.38}$$

Rearranging the terms and finding out the expression for $x_1(s)$, it can be written,

$$x_1(s) = \frac{\delta + x_1(0)s}{s^2 + (\alpha + \gamma)s + \gamma\alpha}. \tag{3.39}$$

Hence, in case of Eq. (3.40),

$$\lim_{t \to \infty} x_1(t) = \lim_{s \to 0} s(x_1(s)) = 0. \tag{3.40}$$

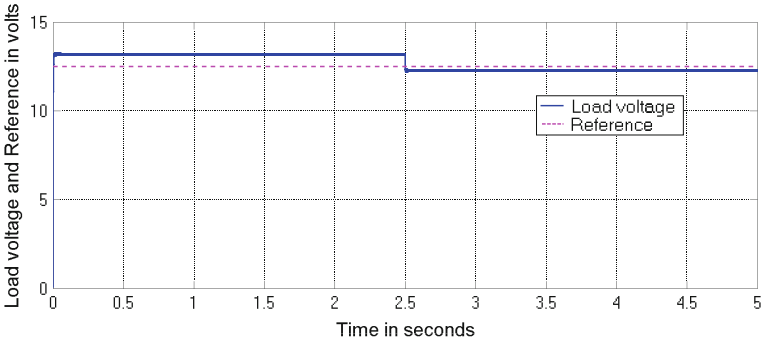

(a) Conventional SMC

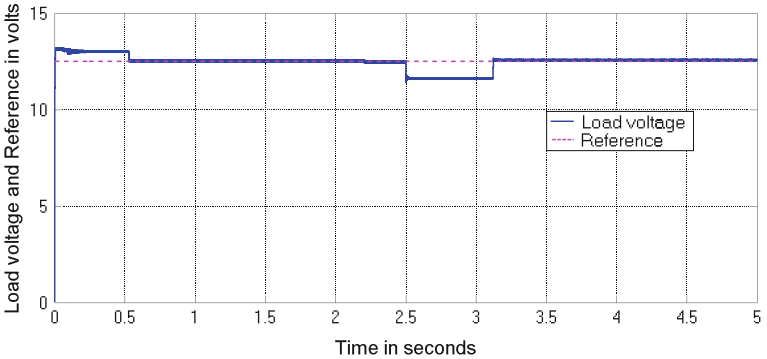

(b) Proposed SMC

Fig. 3.3 Simulation results for $\alpha = 600$ in **a** and $\alpha = 600$, $\gamma = 3.3$ in **b**. Load disturbance from 100 to 32 Ω at 2.5 s and reference voltage = 12.5 V

Table 3.1 Parameter settings for the system in Fig. 3.1

Symbol	Description	Value
L	Inductance	0.6 mH
C	Capacitance	100 μF
β	Voltage divider ratio	0.128
V	Supply voltage	24 V
V_{ref}	Reference voltage	19.5 or 12 V
r_L	Load resistance	100 Ω
	Initial capacitor voltage	0 V
ε	Dead zone in switching element	0.001

It is now clear that the proposed sliding function based SMC technique leads to zero steady-state error. But the conventional sliding function based SMC technique failed to eliminate the steady state error. This fact can be observed in the Fig. 3.3.

3.4 Simulation Results

To show the efficacy of the proposed algorithm, a MATLAB simulation is carried out with the system parameters shown in Table 3.1.

It can be observed from Fig. 3.3 that for the tuning parameter settings, $\alpha = 600$ and $\gamma = 3.3$, and the load voltage tracks well the reference voltage 12.5 V (dashed line). However, the load disturbance occurs at time 2.5 s; i.e., the load resistance suddenly drops from 100 to 32 Ω, and the proposed SMC tracks the reference very accurately (Fig. 3.3b). With the conventional SMC, load voltage fails to track the reference and exhibits a small amount of steady-state error that is apparent before and after the load disturbance (Fig.3.3a).

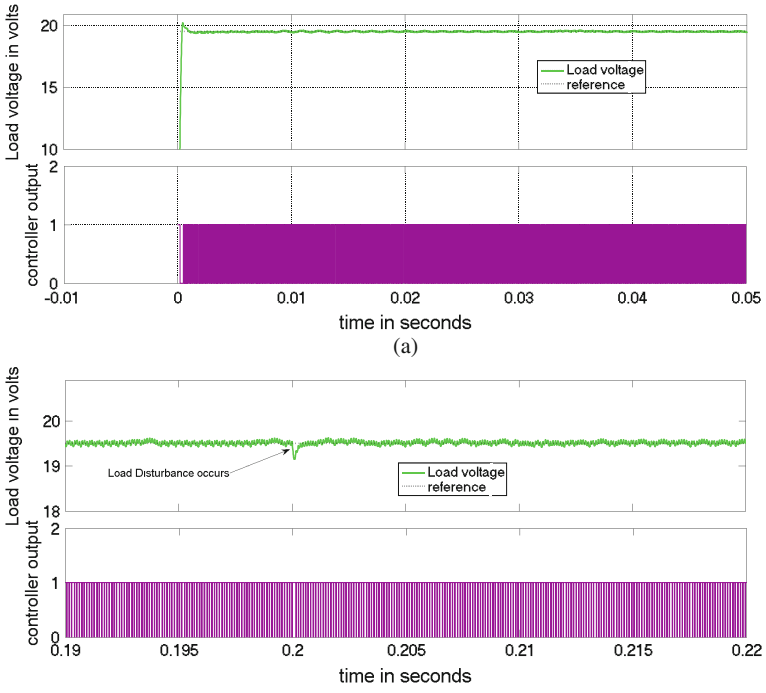

Fig. 3.4 **a** Load voltage and controller output for $\alpha = 6000$, $\gamma = 0.0020$. Load disturbance from 100 to 32 Ω introduced at 0.2 s and reference voltage = 19.5 V. **b** Scaled view of **a**

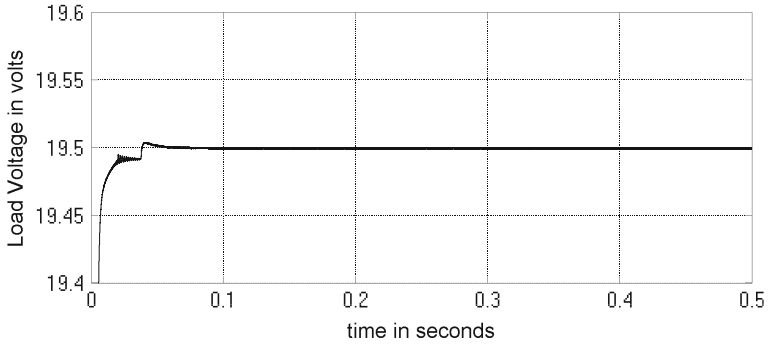

Fig. 3.5 Load voltage for $\alpha = 1000$, $\gamma = 100$

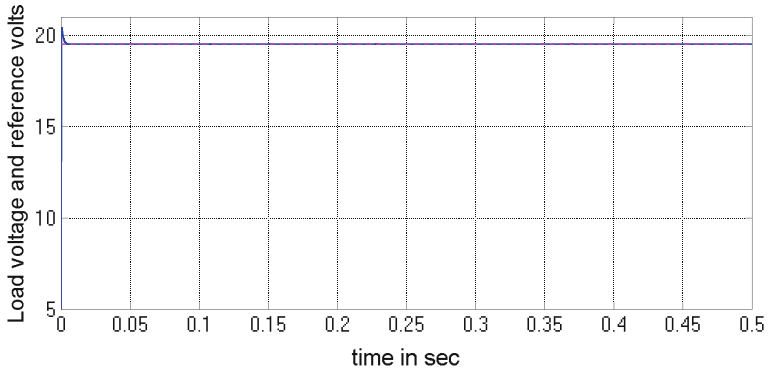

Fig. 3.6 Supply variations 50 Hz 2 V peak-to-peak AC sine wave

For the reference voltage of 19.5 V, the step response of load voltage is studied. The load resistance is suddenly varied from 100 to 32 Ω. The parameters for Fig. 3.4 are $\alpha = 6000$ and $\gamma = 0.0020$. Figure 3.4a shows the load voltage, reference, and controller output. The better view is presented in Fig. 3.5b to study the effects of the load disturbance.

Figure 3.5 shows the load voltage with tuning parameter set to $\alpha = 1000$ and $\gamma = 100$ and for the reference of 19.5 V. For the same parameter setting as in Fig. 3.5, the 2 V peak-to-peak, 50 Hz sine wave disturbance is introduced in the supply to explore its effects on load voltage. The load voltage is observed as shown in Fig. 3.6. To observe the effects, a scale-adjusted version of Fig. 3.6 is shown in Fig. 3.7. The effects of the power line disturbance are quite negligible as the chattering amplitude is less than 4 mV.

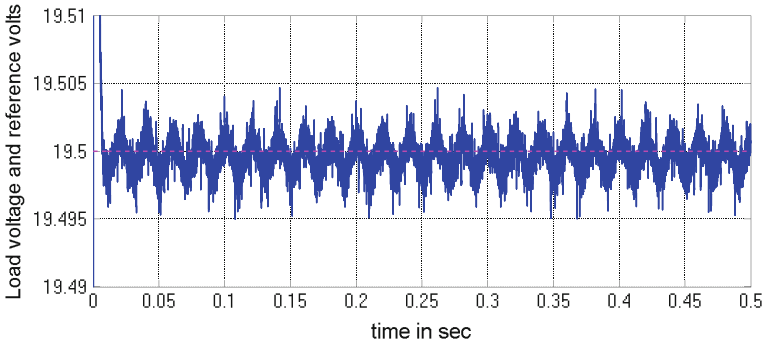

Fig. 3.7 Supply variations 50 Hz 2 V peak-to-peak AC sine wave scale magnified view

3.5 Experimental Results

To validate the proposed strategy, the implementation is carried out on an experimental setup. The setup includes STM32F407VG digital signal controller (DSC) from ST Microelectronics. It is a 32-bit DSC with ARM CORTEX M4 architecture operated with 168 MHz. The analog-to-digital converter (ADC) clock is set to 84 MHz, and the states are measured every 10 ms for the feedback control. The Buck converter with the parameters as mentioned in Table 3.1 is used for the experimentation. The current sensor CTSR 0.6 P from LEM is used for sensing the current. Figure 3.8 shows the load voltage response under (a) conventional SMC and (b) proposed SMC. It can be observed that the load voltage in Fig. 3.8a is 13.3 V for a given reference voltage of 12.5 V while with the proposed SMC the load voltage is quite near around 12.47 V as observed in Fig. 3.8b. The parameters are set as $\alpha = 600$ and $\alpha = 600$, $\gamma = 3.3$ for conventional and proposed SMC, respectively. Notice that the load resistance is 100 Ω.

Figure 3.9 shows the experimental result for load voltage for the same tuning parameters set in Fig. 3.8 but with the load 32 Ω. However, it can be noticed that with the proposed SMC, load voltage remains unchanged while the same drops just below the reference 12.5 V in the presence of load disturbance. The proposed control strategy as mentioned earlier results in better steady-state performance by reducing steady-state error. It can be observed from Figs. 3.10, 3.11, and 3.12 that for the mentioned values for tuning parameters and load disturbance the load voltage response confirms the simulation results except the conventional SMC causes the load voltage to drop down upon any reduction in load resistance. The proposed SMC results in better load voltage response even in the presence of load disturbances. Figures 3.13, 3.14, and 3.15 show the load voltage responses with mentioned conditions and tuning parameters.

It can be noticed from Fig. 3.16 that the higher value of the tuning parameter α, which is set 10000, results in overshoot. The DC–DC Buck converter used for the experiment is shown in Fig. 3.17. More understanding of the practical setup can be

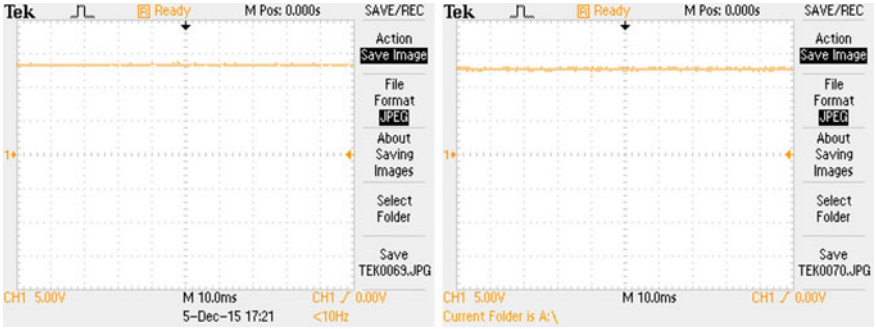

(a) Conventional SMC (b) Proposed SMC

Fig. 3.8 Experimental results for $\alpha = 600$ in **a** and $\alpha = 600$, $\gamma = 3.3$ in **b**. Reference voltage = 12.5 V

(a) Conventional SMC (b) Proposed SMC

Fig. 3.9 Experimental results for $\alpha = 600$ in **a** and $\alpha = 600$, $\gamma = 3.3$ in **b**. Load disturbance from 100 to 32 Ω. Reference voltage = 12.5 V

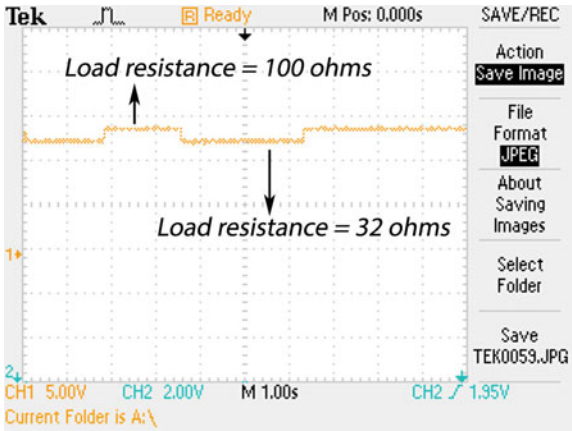

Fig. 3.10 Load voltage with conventional SMC when load varied from 100 to 32 Ω, $\alpha = 6000$

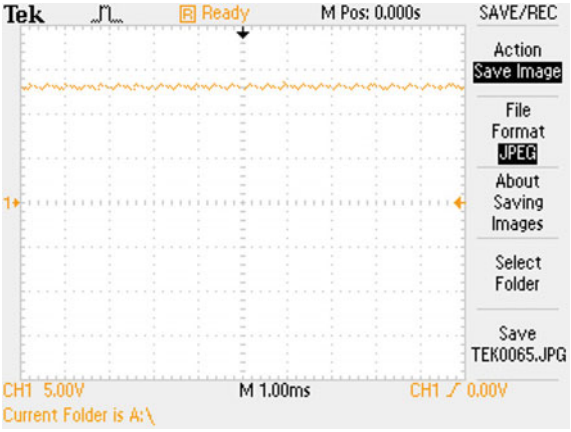

Fig. 3.11 Load voltage with proposed SMC with fixed load of 100 Ω, $\alpha = 6000$, $\gamma = 0.0020$

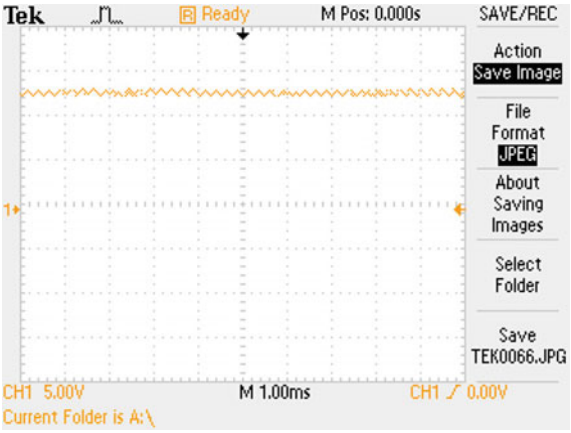

Fig. 3.12 Load voltage with proposed SMC with load 32 Ω, $\alpha = 6000$, $\gamma = 0.0020$

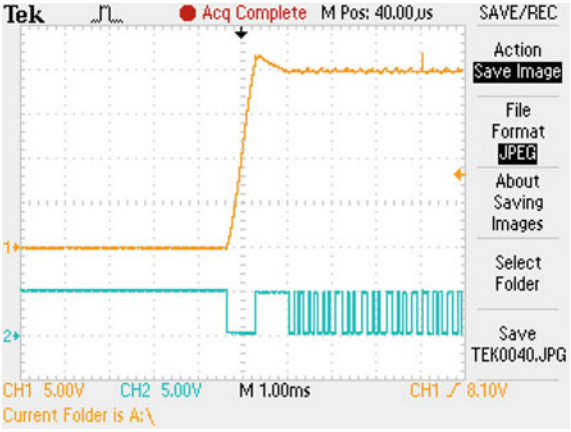

Fig. 3.13 Load voltage, pulses with load 100 Ω, $\alpha = 6000$, $\gamma = 0.0020$

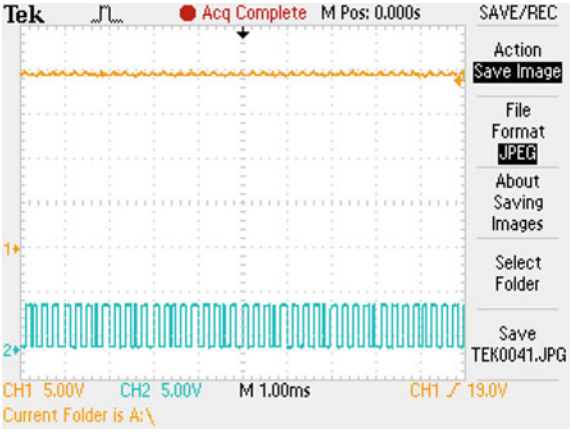

Fig. 3.14 Load voltage, pulses, with fixed load $100\,\Omega$, $\alpha = 6000$, $\gamma = 0.0020$

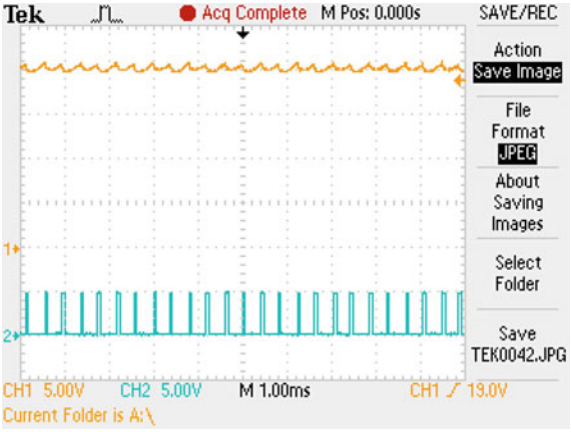

Fig. 3.15 Load voltage, pulses, with load varied from 100 to $32\,\Omega$, $\alpha = 6000$, $\gamma = 0.0020$

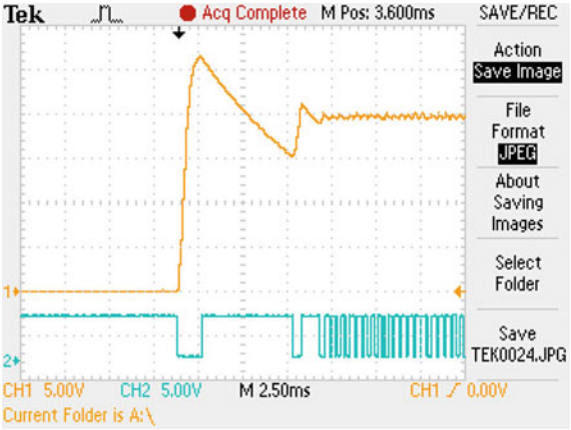

Fig. 3.16 Load voltage, pulses with load $100\,\Omega$, $\alpha = 10000$, $\gamma = 0.4$

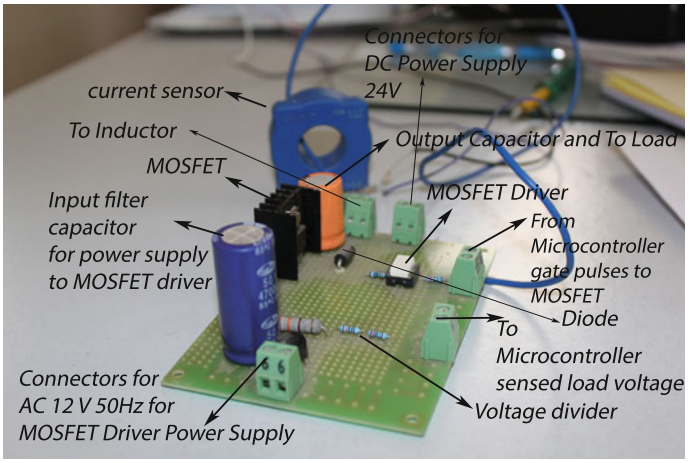

Fig. 3.17 Diagram for the DC–DC Buck converter circuit

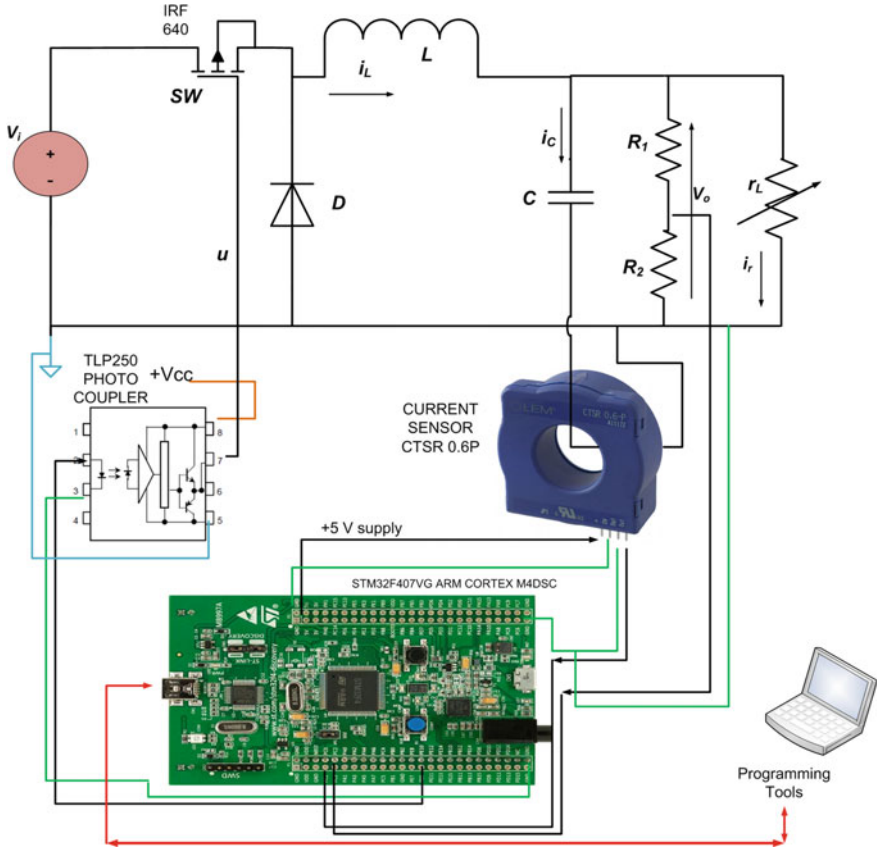

Fig. 3.18 DC–DC Buck converter practical circuit

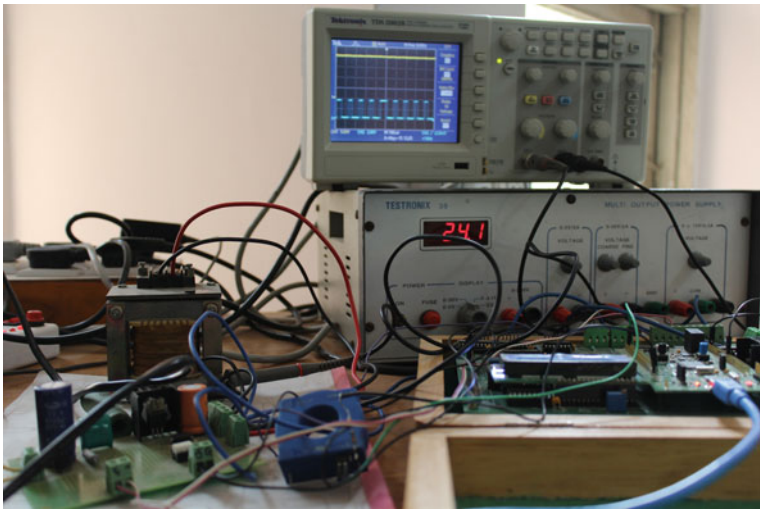

Fig. 3.19 Experimental setup

acquired with Fig. 3.18. The green lines are ground lines of DSC. We have shown the connections of the current sensor powered by DSC board itself. The connections of the photocoupler/MOSFET Driver TLP250 from TOSHIBA are shown. The general-purpose input–output (GPIO) port C pin 1 and 2 are used for sensing the analog values of the states for feedback control. The GPIO port E in 9 is selected as controller output. Figure 3.19 shows the experimental setup facilitated to obtain the experimental results.

3.6 Drawback of the Proposed Sliding Mode Control and Its Remedy

The problem with proposed modified SMC law is the poor control on settling time. Moreover, the proposed SMC law does not facilitate phase trajectory to hit the sliding hyperplane in finite time. Hence, the Integral SMC with Finite Time Reaching (ISMCFTR) is proposed. For that, let the sliding manifold be

$$T = S + \gamma \int_0^t |S|^{0.5} dt. \tag{3.41}$$

Setting $T = 0$, Eq. (3.41) can be written as,

$$S = -\gamma \int_0^t |S|^{0.5} dt. \tag{3.42}$$

Differentiating w.r.t. time both the sides of Eq. (3.42) and exchanging the terms for integration,

$$\frac{ds}{|S|^{0.5}} = -\gamma dt. \tag{3.43}$$

Setting the upper and lower limits for S as 0 and $S(0)$ and considering upper and lower limits for time as t_f and t_0, respectively, and integrating both the sides of Eq. (3.43) one can express Δt as,

$$\Delta t = t_f - t_0 = \frac{2\sqrt{S(0)}}{\gamma}. \tag{3.44}$$

It can be observed that the sliding mode occurs if the condition $T\dot{T} < 0$ is satisfied. Hence if $T > 0$, $u = 1$, from Eqs. (3.1) to (3.6),

$$\begin{aligned} &\dot{T} < 0 \\ &\quad \Longrightarrow \dot{S} + \gamma |S|^{0.5} < 0 \\ &\quad \Longrightarrow \dot{S} < -\gamma |S|^{0.5} \\ &\quad \Longrightarrow \alpha \dot{x_1} + \dot{x_2} < -\gamma |S|^{0.5} \\ &\quad \Longrightarrow \left(\alpha - \frac{1}{r_L C}\right) x_2 - \frac{1}{LC} x_1 < -\gamma |S|^{0.5} + \frac{\beta V_i}{LC} - \frac{V_\mu}{LC}. \end{aligned} \tag{3.45}$$

Similarly if $T < 0$, $u = 0$, from Eqs. (3.1) to (3.6),

$$\begin{aligned} &\dot{T} > 0 \\ \Longrightarrow &\left(\alpha - \frac{1}{r_L C}\right) x_2 - \frac{1}{LC} x_1 < -\gamma |S|^{0.5} - \frac{V_\mu}{LC}. \end{aligned} \tag{3.46}$$

If the above inequalities are satisfied, the SM exists. Note that in the vicinity of hyperplane, i.e., $S \approx 0$, the fractional power term in Eqs. (3.45) and (3.46) can be negligible.

The control law is given by,

$$u = \frac{1}{2}[1 + sgn(T)]. \tag{3.47}$$

To avoid abrupt changes in the ROE, the parameter $\alpha >> \frac{1}{r_L C}$ is preferred, while parameter γ can be set with the help of Eq. (3.41). The following section presents some simulation results for the Buck converter in Fig. 3.1.

3.7 Simulation Results for Integral Sliding Mode Control with Finite-Time Reaching

Note that the different parameter values are same as mentioned in Table 3.1 except the values of α and γ. Reference voltage is set to 12 V and $\alpha = 4000$. Effects of varying γ can be observed from the following figures.

Figure 3.20 shows the effects of varying parameter γ on load voltage in case of proposed SMC law. Note that there is an exponential convergence of error. It can be observed easily from Fig. 3.22 that the load voltage is quite controllable in the sense of time it takes to approach reference. The higher the values of γ, the faster the

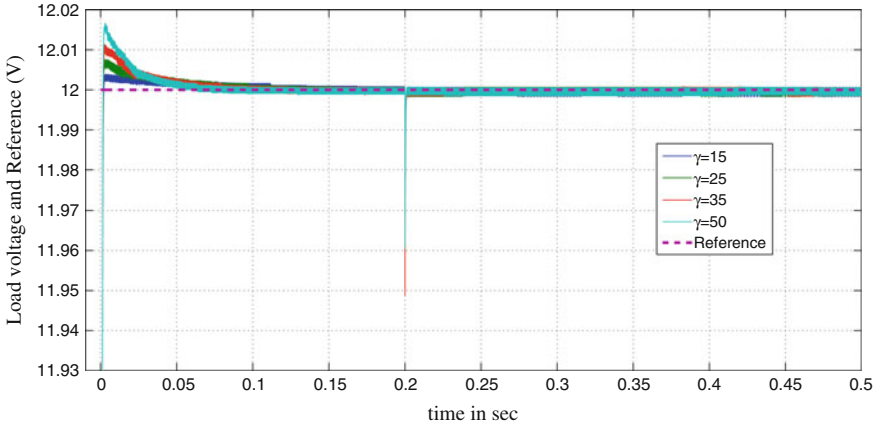

Fig. 3.20 Effects of varying parameter γ on load voltage in case of proposed SMC. Load disturbance occurs at 0.2 s. The load changes from 100 to 32 Ω

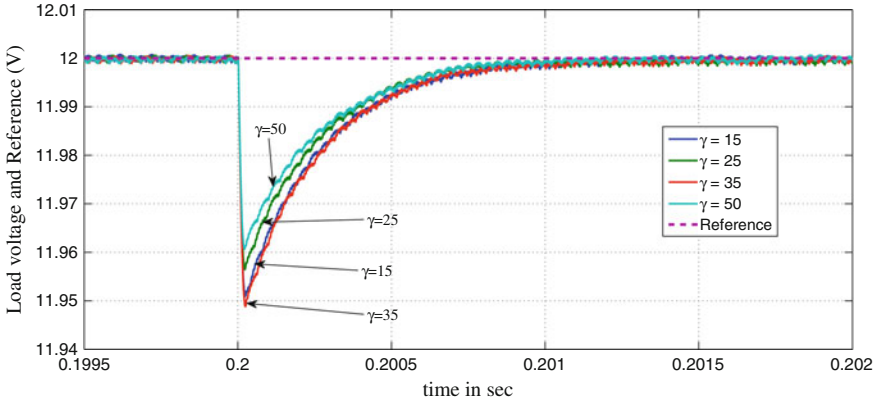

Fig. 3.21 Recovery of load voltage after the load disturbance in case of proposed SMC

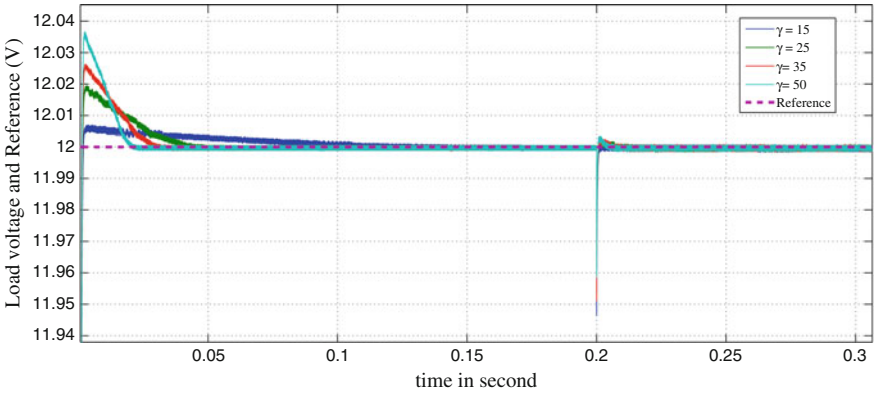

Fig. 3.22 Effects of varying parameter γ on load voltage in case of ISMFTR. Load disturbance occurs at 0.2 s. The load changes from 100 to 32 Ω

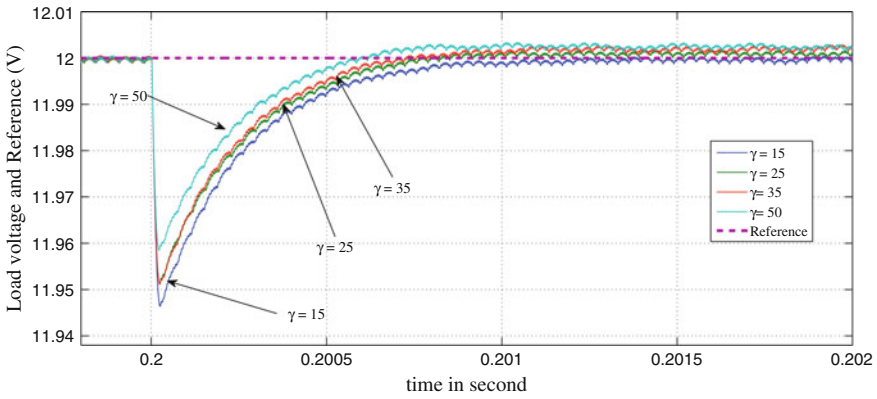

Fig. 3.23 Recovery of load voltage after the load disturbance in case of ISMFTR

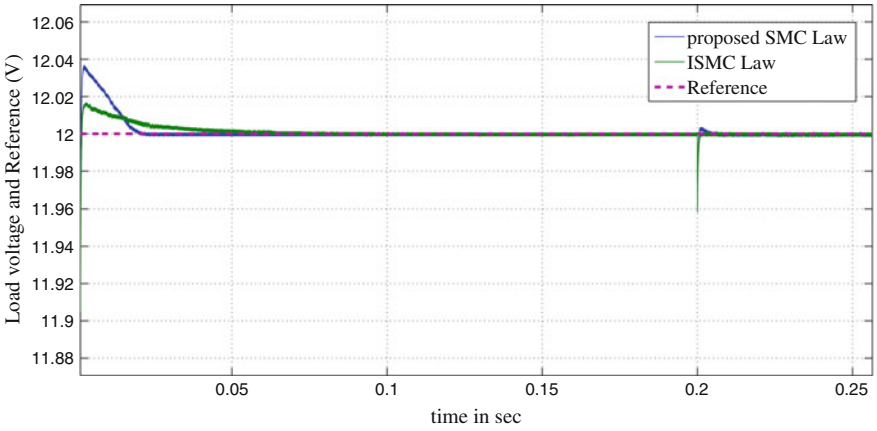

Fig. 3.24 Load voltage responses in case of proposed SMC law and proposed ISMFTR

response. The higher values of γ cause peak overshoot. The load voltage recovers after load disturbance under proposed SMC and proposed ISMCFTR as it can be observed from Figs. 3.21 and 3.23. Figure 3.24 shows the load voltage under proposed SMC and proposed ISMFTR for $\gamma = 50$ and $\alpha = 4000$ for reference of 12 V.

3.8 Conclusion

The proposed strategy is verified by simulation and experimentation results. The steady-state and dynamic behavior of the system with SMC laws was studied. The influence of tuning parameters on system performance is examined. The proposed strategy is able to improve overshoot and undershoots in the load voltage. The Region of Existence and the stability analysis are carried out for the proposed control algorithm. The simulation and experimental results show that the proposed control strategy proved to be satisfactorily in cases of sudden load disturbances. It is observed that the proposed SMC improves steady-state error in load voltage. To achieve better control on settling time and overshoot and to facilitate finite-time reaching the ISMCFTR is proposed. The simulation results are presented.

Now as the Buck converters are quite straightforward and inherently stable system, control design is usually straightforward. On the other hand, many applications require step-up or Boost converters, e.g., computer disk drive systems, electric vehicles, and some solar power systems. The step-up or Boost converters are having complex dynamics as they contain right-half s-plane zero. Such systems can cause inverse response or delayed responses. The complete treatment for designing SMC for DC–DC Boost converters is presented.

References

1. Ang, S., Oliva, A.: Power Switching Converters. CRC Press, Taylor & Francis Group, Boca Raton (2005)
2. Edwards, C., Spurgeon, S.: Sliding Mode Control Theory and Applications. Taylor & Francis, London (1998)
3. Li, H., Ye, X.: Sliding-mode PID control of DC-DC converter. In: 5th IEEE Conference on Industrial Electronics and Applications (2010)
4. Mohan, N., Undeland, T., Robbins, W.: Power Electronics. Wiley, Hoboken (2003)
5. Naik, B., Mehta, A.: Sliding mode controller with modified sliding function for buck type converters. In: 22nd IEEE International Symposium on Industrial Electronics. Taipei (2013)
6. Tan, S.C., Lai, Y.M., Tse, C.K.: Sliding Mode Control of Switching Power Converters. CRC Press, Boca Raton (2012)
7. Utkin, V., Guldner, J., Shi, J.: Sliding Mode Control in Electromechanical Systems. Taylor & Francis, London (1999)

Chapter 4
Sliding Mode Controller with PI-Type Sliding Function for DC–DC Boost Converter

4.1 Introduction

Recently, the battery-operated equipment is becoming popular among researchers. One example is battery-operated hybrid electric vehicle which uses the DC–DC Boost Converter. As stated earlier, the converter is used in computers and even in solar power systems. Hence, the control of such converters plays very important role in the overall performance of the systems. This chapter presents adaptive sliding mode controller with modified sliding function for DC–DC Boost Converter. The modification in the sliding function not only overcomes the limitations of the conventional sliding mode but also improves the performance of the converter with an additional tuning parameter. The simulation results show the efficacy of proposed adaptive sliding mode controller for DC–DC Boost Converter. The control of power electronic devices demands the better tracking performance and quick rejection of load disturbances. The sliding mode control (SMC) is inherently robust for matched uncertainty, and being a switched control strategy, it has become good control strategy for the power electronic converters.

4.2 Modeling of the Boost Converter

It is well known that sliding mode control requires model of the system. Researchers [2, 7, 8] have discussed various approaches for modeling of PEC. Due to the presence of the switching elements in the power electronic systems, the modeling [6] is not straightforward. Mathematical models of the power converters provide the pathway to various control methodologies discussed in the wide variety of literature.

Figure 4.1 shows the DC–DC Boost Converter [1, 3] in closed loop. The state-space model of the converter can be derived [7].

A. Mehta and B. Naik, *Sliding Mode Controllers for Power Electronic Converters*, Lecture Notes in Electrical Engineering 534,
https://doi.org/10.1007/978-981-13-3152-7_4

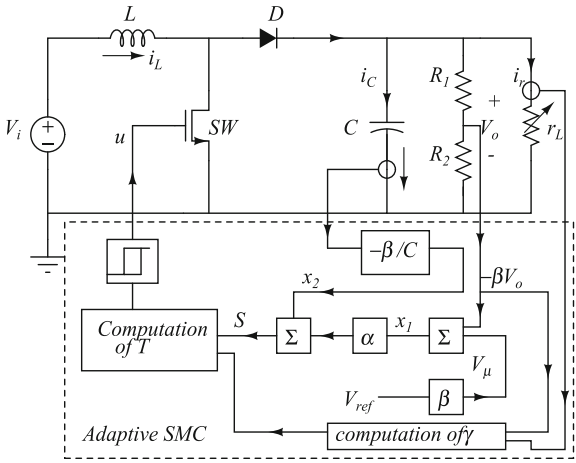

Fig. 4.1 DC–DC Boost Converter with adaptive SMC

Let us define states x_1 and x_2 as,

$$x_1 = V_\mu - \beta V_o, \tag{4.1}$$

$$x_2 = \dot{x}_1, \tag{4.2}$$

where $V_\mu = \beta V_d$ is the reference voltage corresponding to the desired load voltage V_d, $\beta = \frac{R_2}{R_1+R_2}$ is the voltage divider ratio. The SW is a MOSFET switch turned ON or OFF with the output of SM controller which is in the form of pulses. Please note that $u = 1$ means SW is closed and $u = 0$ means SW is open. L is an inductor, C is a capacitor, D is the free-wheeling diode, V_o is the output or load voltage, V_i is the input voltage, and r_L is the load resistance. Let us define $\bar{u} = 1 - u$.

From Eq. (4.2),

$$x_2 = -\beta \frac{dV_o}{dt},$$

$$x_2 = -\frac{\beta}{C} i_C,$$

where i_C is the capacitor current which can be measured as shown in Fig. 4.1.

Let i_L and i_r be the inductor current (that contributes to capacitor current) and load current, respectively. The above equation can be rewritten as,

$$x_2 = -\frac{\beta}{C}[i_L - i_r]. \tag{4.3}$$

Let the voltage drop across inductor be v_L then,

$$v_L = \bar{u}(V_i - V_o) = L\frac{di_L}{dt}.$$

$$\implies i_L = \int \frac{\bar{u}(V_i - V_o)}{L} dt.$$

The Eq. (4.3) can be written as,

$$x_2 = -\frac{\beta}{C}\left[\int \frac{\bar{u}(V_i - V_o)}{L} dt - \frac{V_o}{r_L}\right]. \tag{4.4}$$

Differentiating above equation with respect to time, $\dot{x_2}$ is obtained as follows:

$$\dot{x_2} = -\frac{\beta}{C}\left[\frac{\bar{u}(V_i - V_o)}{L} - \frac{dV_o}{dt}\frac{1}{r_L}\right]$$
$$\dot{x_2} = \frac{dV_o}{dt}\frac{\beta}{r_L C} + \frac{\beta\bar{u}(V_o - V_i)}{LC}. \tag{4.5}$$

Since $x_2 = -\beta\frac{dV_o}{dt}$, $\dot{x_2}$ is given by,

$$\dot{x_2} = -\frac{1}{r_L C}x_2 + \frac{\beta\bar{u}(V_o - V_i)}{LC}. \tag{4.6}$$

From Eqs. (4.2) and (4.6), the state-space model of the Boost Converter may be obtained as,

$$\begin{pmatrix}\dot{x}_1 \\ \dot{x}_2\end{pmatrix} = \begin{pmatrix}0 & 1 \\ 0 & -\frac{1}{r_L C}\end{pmatrix}\begin{pmatrix}x_1 \\ x_2\end{pmatrix} + \begin{pmatrix}0 \\ \frac{\beta(V_o - V_i)}{LC}\end{pmatrix}\bar{u}. \tag{4.7}$$

4.3 Conventional Sliding Mode Control

Let us define a sliding function [5] S which establishes linear relationship among states in Eqs. (4.1) and (4.2) such that,

$$S = \alpha x_1 + x_2, \tag{4.8}$$

where α is a scalar and it is tuned to achieve desired performance.

To ensure the finite-time convergence, reaching condition,

$$S\dot{S} < 0, \tag{4.9}$$

must be assured. This imposes the limitations over the existence regions of sliding modes [7] as discussed in [4]. In fact, the region of existence (ROE) is the region on the phase plane in which if the phase trajectory lies, the sliding modes can exist. The sliding mode control law can be defined as per the following rule:

$$\bar{u} = \begin{cases} 0 = OFF, & S > 0 \\ 1 = ON, & S < 0 \end{cases} \tag{4.10}$$

The above control law will trigger the switching across the sliding manifold S. The switching device has frequency limitation, and hence, for practical implementation the following control law is used:

$$\bar{u} = \begin{cases} 0 = OFF, & S > \varepsilon \\ 1 = ON, & S < -\varepsilon \end{cases} \tag{4.11}$$

where ε is a small positive number. The above control law Eq. (4.11) can reduce the severity of chattering by limiting chattering frequency, and hence, it is feasible for practical implementation.

4.3.1 Limitations of Conventional Sliding Mode Control

The behavior of the states on sliding surface $S = 0$ is given by,

$$x_1(t) = x_1(t_0)e^{-\alpha(t-t_0)}, \tag{4.12}$$

where t_0 is any point in time. It can be noted that increasing α makes the system faster. It is required to satisfy the reaching law, $\dot{S} < 0$ if $S > 0$ and vice versa. As discussed above for $S > 0$,

$$\begin{aligned} &\dot{S} < 0 \\ &\quad \Longrightarrow \alpha\dot{x_1} + \dot{x_2} < 0 \\ &\quad \Longrightarrow x_2\left(\alpha - \frac{1}{r_L C}\right) < 0. \end{aligned} \tag{4.13}$$

Similarly for $S < 0$

$$\begin{aligned} &\dot{S} > 0 \\ &\quad \Longrightarrow \alpha\dot{x_1} + \dot{x_2} + \frac{\beta(V_o - V_i)}{LC} > 0 \\ &\quad \Longrightarrow x_2\left(\alpha - \frac{1}{r_L C}\right) + \frac{\beta(V_o - V_i)}{LC} > 0 \end{aligned} \tag{4.14}$$

It is noted from inequalities Eqs. (4.13) and (4.14) that the parameter α should be chosen carefully. If there are major variations in the load, it is required to select $\alpha > \frac{1}{r_L C}$ to force the phase trajectory lie in the region of existence (ROE), on the phase plane. The inequalities involve α which affects the ROE on the phase plane. Thus, the choice of α is restricted as it affects the states' responses too as mentioned earlier. Moreover, the ROE varies with the load variations.

If the phase trajectory lies beyond the ROE on the phase plane, sliding modes may not be guaranteed. By modifying the sliding function, we can add one more tuning parameter which can compensate for the load variations. In fact, it makes the ROE independent of load variations. The α can be chosen as per the slower or faster dynamics requirements. The modification in sliding function leads to better steady-state and dynamic performances.

4.4 Adaptive SMC with Modified Sliding Function

Let a proportional–integral (PI)-type function of sliding function [4] be defined as,

$$T = S + \gamma sgn(S) \int_0^t |S| dt, \tag{4.15}$$

where T is the function of sliding function, 'sgn' represents the 'signum' function, and $\gamma > 0$ is a scalar. Note that T and S change their polarity simultaneously, and hence, the existence regions may be defined easily on the phase plane as in the case of conventional sliding function.

Let us define the control law such that,

$$\bar{u} = \begin{cases} 0 = OFF, & T > \varepsilon \\ 1 = ON, & T < -\varepsilon \end{cases}. \tag{4.16}$$

The existence of sliding modes is possible on the phase plane if the following teachability conditions are satisfied.

$$\lim_{T \to 0^+} \dot{T} < 0 \tag{4.17}$$

$$\lim_{T \to 0^-} \dot{T} > 0 \tag{4.18}$$

4.4.1 Existence of Sliding Modes

The existence of sliding modes is possible if the inequalities Eqs. (4.17), (4.18) are satisfied.

Case I:
If $T > 0, \dot{T} < 0$. So,

$$\begin{aligned} \dot{S} + \gamma S &< 0 \\ \implies \alpha \dot{x_1} + \dot{x_2} + \gamma \alpha x_1 + \gamma x_2 &< 0. \end{aligned} \tag{4.19}$$

Using Eq. (4.7) and considering $u = 0$ for $T > 0$ we may get,

$$\gamma \alpha x_1 + \left(\alpha - \frac{1}{r_L C} + \gamma \right) x_2 < 0 \tag{4.20}$$

Case II:
For $T < 0$, considering Eq. (4.7) and $u = 1$,

$$\gamma \alpha x_1 + \left(\alpha - \frac{1}{r_L C} + \gamma \right) x_2 + \frac{\rho (V_o - V_i)}{LC} > 0 \tag{4.21}$$

The equivalent control law u_{eq} can be derived as follows:

$$\begin{aligned} \gamma \alpha x_1 + \left(\alpha - \frac{1}{r_L C} + \gamma \right) x_2 + \left(\frac{\beta (V_o - V_i)}{LC} \right) u_{eq} &= 0 \\ \implies u_{eq} = - \frac{LC}{\beta (V_o - V_i)} \left[\gamma \alpha x_1 + \left(\alpha - \frac{1}{r_L C} + \gamma \right) x_2 \right] \end{aligned} \tag{4.22}$$

It can be noted that sliding modes exist along with switching action and u_{eq} is zero in case of ideal sliding mode. However, it is not practically possible, and switching action is inevitable.

The inequalities Eqs. (4.20), (4.21) show that the region in the phase plane which is bounded by two parallel lines and manifold $T, S = 0$. Also ROE is not affected by load variance with $\gamma = \frac{1}{r_L C}$; hence, the control is robust for load variations. The tuning parameter ψ can be tuned for faster or slower responses requirements. Which was possible with the modified SMC. Now, load can be estimated as $r_L = \frac{V_o}{i_r}$ and the parameter γ can be tuned as per the load.

$$\gamma = \frac{i_r}{V_o C} \tag{4.23}$$

Thus, the proposed SMC becomes adaptive the load variations unlike conventional sliding mode control.

Figure 4.1 shows the system with proposed control strategy where the load voltage and current are continuously monitored for in-line computation of γ.

Figure 4.2 shows the ROE and phase trajectory under the effluence of the proposed control strategy. The ROE is obtained by considering the case I and case II with

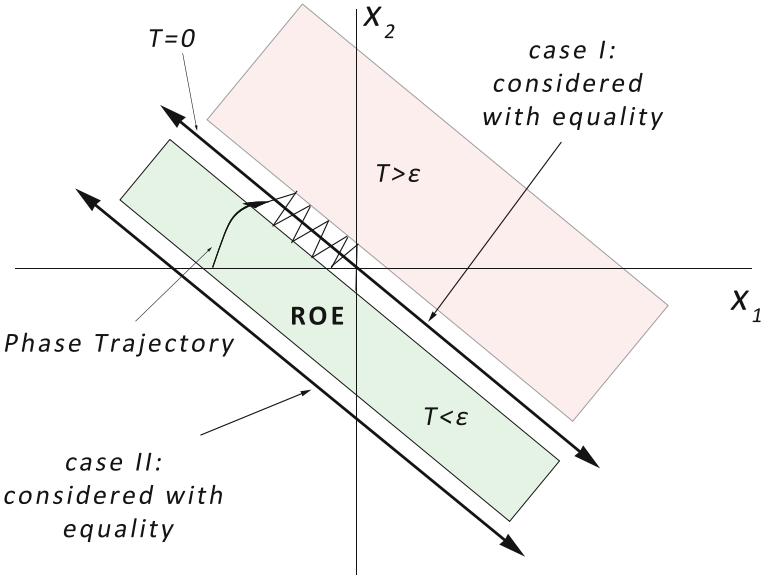

Fig. 4.2 Dynamics of states and region of existence (ROE) on phase plane

equality. The ROE on the phase plane is independent of load variation due to adaptive mechanism. Initial voltage of the capacitor can be set so as the phase trajectory can originate within the ROE.

4.5 Simulation Results and Discussion

The Boost Converter specifications with proposed control strategies for simulation are mentioned in Table 4.1.

The simulation results with conventional SMC and proposed SMC are presented in Figs. 4.3, 4.4, 4.5, and 4.6 for tracking control where the reference voltage is changed from 12 V to 20 V at time $t = 1$ s. Figures 4.3 and 4.5 show that the performance of the converter is satisfactory and tracks the reference voltage under both the strategies.

Figures. 4.4 and 4.6 show the variations in the load current corresponding to load changes.

To check the dynamic performance and robustness, the load disturbance is given by suddenly changing the load from 24 Ω to 10 Ω at $t = 2$ s. The performance of both the conventional and proposed techniques is shown in the magnified windows in Figs. 4.3 and 4.5. It is observed that the proposed SMC technique is faster than conventional SMC as it takes 10 ms to recover the reference voltage compared to 30 ms after the load disturbance is introduced.

Table 4.1 Parameters set for the Boost converter in Fig. 4.1

Symbol	Quantity	Value
L	Inductance	300 μH
C	Capacitance	250 μF
α	Tuning parameter	5000
β	Voltage divider ratio	0.0909
V_i	Supply voltage	12 V
V_d	Desired voltage	12–20 V
r_L	Load resistance	24–10 Ω
γ	Tuning parameter	166.6 $(=\frac{1}{r_L C})$
	Initial capacitor voltage	22 V
ε	Dead zone in switching system	0.1

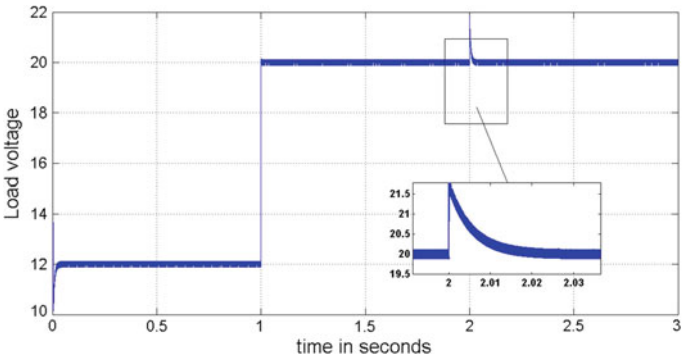

Fig. 4.3 Load voltage response with conventional SMC

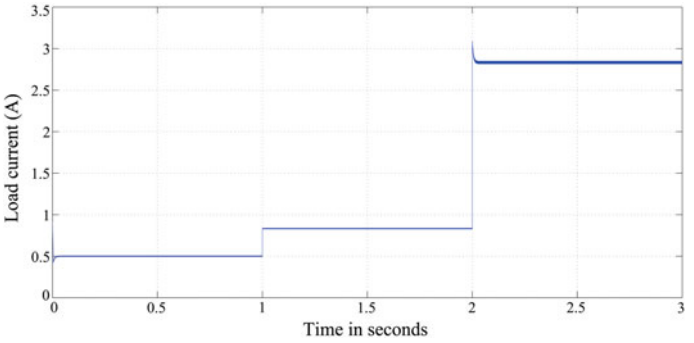

Fig. 4.4 Load current with conventional SMC

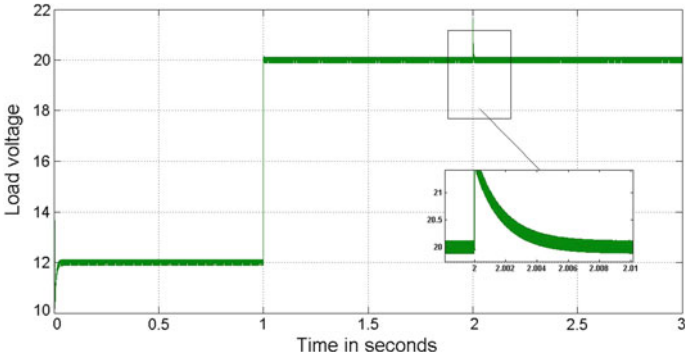

Fig. 4.5 Load voltage with proposed adaptive SMC with modified sliding function

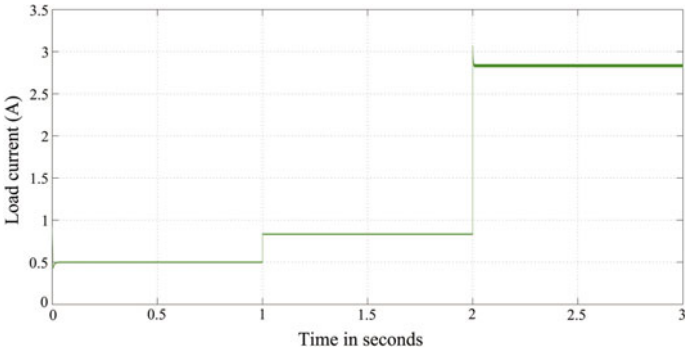

Fig. 4.6 Load current with proposed adaptive SMC with modified sliding function

4.6 Conclusion

The proposed adaptive sliding mode control with modified sliding function is applied to DC–DC Boost Converter. It is found that the proposed control strategy is better in terms of dynamic performance. The tuning parameter is adaptively tuned to meet the requirements for load changes, and the overall system response becomes faster. Simulation results show the efficacy of the control strategy.

There are many applications, however, such as battery-powered systems, where the input voltage can vary widely, starting at full charge and gradually decreasing as the battery charge is used up. At full charge, where the battery voltage may be higher than actually needed by the circuit being powered, a Buck regulator would be ideal to keep the supply voltage steady. However, as the charge diminishes, the input voltage falls below the level required by the circuit, and either the battery must be discarded or recharged; at this point the ideal alternative would be the boost regulator (source: http://www.learnabout-electronics.org/PSU/psu33.php). In such cases where battery is the source of energy or solar cells-based systems, the Buck–Boost converter can

be the choice. However, the Buck–Boost converters may be used for some electric motor drives and control systems. The conventional Buck–Boost converters give the inverted output voltage, i.e., polarity of the output voltage is opposite to that of supply voltage. However, many noninverting Buck–Boost converters like Zeta converters, Cuk converters are in existence. The next chapter deals with the modeling and SMC control and application of the Zeta converter as a part of DC–AC inverter system.

References

1. Ang, S., Oliva, A.: Power Switching Converters. CRC Press, Taylor & Francis Group, Boca Raton (2005)
2. Edwards, C., Spurgeon, S.: Sliding Mode Control Theory and Applications. Taylor & Francis, London (1998)
3. Mohan, N., Undeland, T., Robbins, W.: Power Electronics. Wiley, Hoboken (2003)
4. Naik, B., Mehta, A.: Adaptive sliding mode controller with modified sliding function for DC DC boost converters. In: IEEE International Conference on Power Electronics Drives and Energy Systems. Mumbai (2014)
5. Sabanovic, A., Fridman, L., Spurgeon, S.: Variable Structure Systems from Principles to Implementation. IET, London (2004)
6. Sira-Remirez, H., Silva-Ortigoza, R.: Control Design Techniques in Power Electronics Devices. Springer, London (2006)
7. Tan, S.C., Lai, Y.M., Tse, C.K.: Sliding Mode Control of Switching Power Converters. CRC Press, Boca Raton (2012)
8. Utkin, V., Guldner, J., Shi, J.: Sliding Mode Control in Electromechanical Systems. Taylor & Francis, London (1999)

Chapter 5
Sliding Mode Controller with PI-Type Sliding Function for Zeta Converter

5.1 Introduction to the Modeling of Zeta Converter

The circuit of zeta converter is shown in Fig. 5.1a. The modeling is done with normalization technique discussed in [8].

Operation of the Circuit in Continuous Conduction Mode

The zeta converter has two modes of operation named as charging mode and discharging mode. The charging mode occurs when the switch is ON, and hence, the diode is in reverse biased. The current through the inductors L_1 and L_2 is drawn from the source [8]. The discharging mode starts when switch is off. The diode is forward biased. In the discharging mode of operation, all the energy stored in L_2 is transferred to load R. Figure 5.1b, c helps understand the charging and discharging mode of operation of the zeta converter.

Modeling Approach

Normalization

The normalized system model is obtained by making changes in the scales measuring magnitudes of state variables and the time variable. A network containing R, L, and C, the normalized states x_1, x_2 and time τ can be obtained from current i, voltage v, and time t, respectively, as,

$$\begin{pmatrix} x_1 \\ x_2 \end{pmatrix} = \begin{pmatrix} \frac{1}{E}\sqrt{\frac{L}{C}} & 0 \\ 0 & \frac{1}{E} \end{pmatrix} \begin{pmatrix} i \\ v \end{pmatrix} \tag{5.1}$$

$$\dot{x_1} = \frac{dx_1}{d\tau} \tag{5.2}$$

$$\tau = \frac{t}{\sqrt{LC}} \tag{5.3}$$

A. Mehta and B. Naik, *Sliding Mode Controllers for Power Electronic Converters*, Lecture Notes in Electrical Engineering 534,
https://doi.org/10.1007/978-981-13-3152-7_5

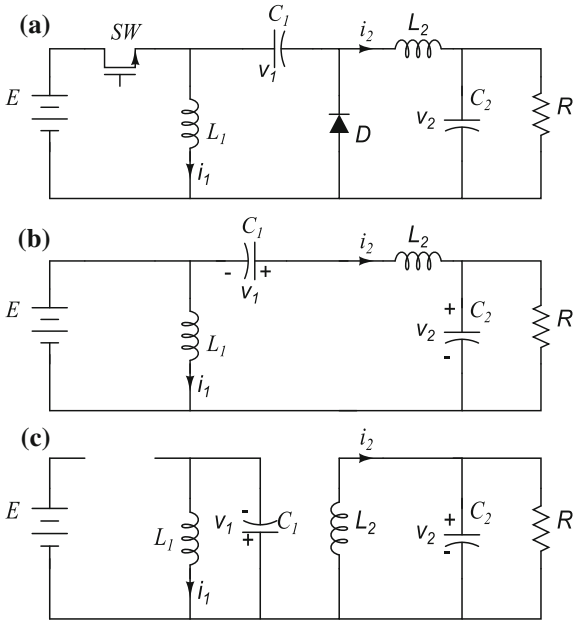

Fig. 5.1 **a** Diagram for Zeta converter circuit. **b** The equivalent circuit when switch is closed. **c** The equivalent circuit when switch is open

$$Q = R\sqrt{\frac{C}{L}}. \tag{5.4}$$

Model of the Zeta Converter

With the well-known notations and u as the switching control either ON or OFF, i.e., 1 or 0, respectively, the governing dynamical equations for the circuit in Fig. 5.1 can be given as,

$$L_1\frac{di_1}{dt} = -(1-u)v_1 + uE \tag{5.5}$$

$$C_1\frac{dv_1}{dt} = (1-u)i_1 - ui_2 \tag{5.6}$$

$$L_2\frac{di_2}{dt} = uv_1 - v_2 + uE \tag{5.7}$$

$$C_2\frac{dv_2}{dt} = i_2 - \frac{v_2}{R} \tag{5.8}$$

Please note that in Fig. 5.1, i and v denote current and voltage, respectively.

With these variable transformations in Eq. (5.1) and time transformation from Eq. (5.3) and from Eq. (5.5), the following two equations can be written.

$$\frac{dx_1}{dt} = \frac{1}{E}\sqrt{\frac{L_1}{C_1}}\frac{di_1}{dt} \tag{5.9}$$

$$\frac{dx_1}{dt} = \frac{1}{E}\sqrt{\frac{L_1}{C_1}}[-(1-u)v_1 + uE]/L_1 \tag{5.10}$$

Considering Eqs. (5.5), (5.9), and (5.10) and from Eqs. (5.2), (5.3) noting $\dot{x_1} = \frac{dx_1}{d\tau}$, one can derive the following equation.

$$\dot{x_1} = -(1-u)x_2 + u \tag{5.11}$$

Similarly, the remaining three equations can be derived from Eqs. (5.6), (5.7), and (5.8) as,

$$\dot{x_2} = (1-u)x_1 - ux_3 \tag{5.12}$$

$$\theta_1\dot{x_3} = ux_2 - x_4 + u \tag{5.13}$$

$$\theta_2\dot{x_4} = x_3 - \frac{x_4}{Q}, \tag{5.14}$$

where x_1, x_2, x_3, and x_4 are i_1, v_1, i_2, and v_2, respectively. Also note that $\theta_1 = \frac{L_2}{L_1}$ and $\theta_2 = \frac{C_2}{C_1}$, $Q = R\sqrt{\frac{C_1}{L_1}}$.

5.1.1 Study of Equilibrium Point Dynamics

From Eqs. (5.11) to (5.14), one can write the equilibrium point state equations with U as the input signal which is averaged u.

$$\begin{pmatrix} 0 & -(1-U) & 0 & 0 \\ 1-U & 0 & -U & 0 \\ 0 & U & 0 & -1 \\ 0 & 0 & 1 & \frac{-1}{Q} \end{pmatrix} \begin{pmatrix} x_{1e} \\ x_{2e} \\ x_{3e} \\ x_{4e} \end{pmatrix} = \begin{pmatrix} -U \\ 0 \\ -U \\ 0 \end{pmatrix} \tag{5.15}$$

Here x_{ie}, where i = 1 to 4 denotes the equilibrium states. From Eq. (5.15), one can derive the following set of equations.

$$x_{1e} = \frac{1}{Q}\frac{U^2}{(1-U)^2} \tag{5.16}$$

$$x_{2e} = \frac{U}{(1-U)} \tag{5.17}$$

$$x_{3e} = \frac{1}{Q}\frac{U}{(1-U)} \tag{5.18}$$

$$x_{4e} = \frac{U}{(1-U)} \tag{5.19}$$

Equation 5.19 shows that the converter can be operated in either step-up or step-down mode. Now the above equations can be written in a different way as,

$$x_{1e} = \frac{{x_{4e}}^2}{Q} \tag{5.20}$$

$$x_{2e} = x_{4e} \tag{5.21}$$

$$x_{3e} = \frac{x_{4e}}{Q} \tag{5.22}$$

$$U = \frac{x_{4e}}{(x_{4e} + 1)} \tag{5.23}$$

If we define the state vector as $x = [x_1, x_2, x_3, x_4]^T$, where T denotes the transpose then the model of the Zeta converter can be written from Eqs. (5.11) to (5.14) as,

$$\dot{x} = f(x) + g(x)u, \tag{5.24}$$

where

$$f(x) = \begin{pmatrix} -x_2 \\ x_1 \\ -\frac{1}{\theta_1}x_4 \\ \frac{1}{\theta_2}(x_3 - \frac{x_4}{Q}) \end{pmatrix} \tag{5.25}$$

$$g(x) = \begin{pmatrix} 1 + x_2 \\ -x_1 - x_3 \\ \frac{1}{\theta_1}(1 + x_2) \\ 0 \end{pmatrix}. \tag{5.26}$$

5.2 Selection of Sliding Surface

Selection of sliding surface [1, 9] in a random way is not preferable as it may result in an unstable behavior. To demonstrate, let us define a sliding surface S which can be expressed as,

$$S = \dot{x_4} + \alpha(x_4 - V_d), \tag{5.27}$$

where V_d is the desired output voltage of the Zeta converter circuit. This leads to the equivalent control law to be, $u_{eq} = \frac{V_d}{1+x_2}$. With this u_{eq}, Eqs. (5.11) and (5.12) can be rewritten as,

$$\frac{dx_1}{dt} = -x_2 + V_d, \tag{5.28}$$

$$\frac{dx_2}{dt} = x_1 - \frac{V_d}{1+x_2}(x_1 + x_{3e}). \tag{5.29}$$

The linearized zero dynamics at the equilibrium point $(x_{1e}, x_{2e}) = (\frac{{V_d}^2}{Q}, V_d)$ can be obtained by linearization technique. The first and second elements of the first row in the system matrix of Eq. (5.30) can be obtained by partial differentiation of Eq. (5.28) with respect to x_1 and x_2, respectively. Similarly, the first and second elements in the second row of system matrix of Eq. (5.30) can be obtained by partial differentiation of Eq. (5.29) with respect to x_1 and x_2, respectively, with considering $x_{1e} = \frac{{V_d}^2}{Q}$ and $x_{3e} = \frac{V_d}{Q}$ from Eqs. (5.20) and (5.22). Thus, the equilibrium point dynamics can be expressed as,

$$\begin{pmatrix} \delta\dot{x}_{1e} \\ \delta\dot{x}_{2e} \end{pmatrix} = \begin{pmatrix} 0 & -1 \\ \frac{1}{1+V_d} & \frac{V_d^2}{Q(1+V_d)} \end{pmatrix} \begin{pmatrix} \delta x_{1e} \\ \delta x_{2e} \end{pmatrix}, \tag{5.30}$$

where δ represents the deviation from the equilibrium point. By observing the matrix in the above equation, it can be noticed that the characteristic equation for the linearized zero dynamics of Eq. (5.30) can be given by,

$$det\left[(sI) - \begin{pmatrix} 0 & -1 \\ \frac{1}{1+V_d} & \frac{V_d}{Q(1+V_d)} \end{pmatrix}\right] = 0, \tag{5.31}$$

where s is the Laplace operator and I is the identity matrix. However, the characteristic equation becomes $s^2 - \frac{V_d}{Q(1+V_d)} + \frac{1}{1+V_d} = 0$ which has at least one root on the *s-plane* on the right half. This means that the equilibrium point dynamics exhibit the unstable dynamics. Hence, the sliding surface of Eq. (5.27) is not viable.

Let us select the sliding surface to be

$$S = x_1 - x_{1e} = x_1 - \frac{{V_d}^2}{Q}. \tag{5.32}$$

It can be proved that for some positive-definite function [7] of the states representing the linearized dynamics at equilibrium point $x_1 = \frac{V_d}{Q}$, $V = v(\delta x_2, \delta x_{3e}, \delta x_{4e}, \Theta)$, where v denotes a function of variables and Θ is sufficiently large to make V as positive definite. And if one can prove $\dot{V} < 0$, then stability is guaranteed. However, it can be shown that such a positive-definite function exists, and hence, Eq. (5.32) can be the choice [8]. The following conventional SMC control law is chosen

$$u = 0.5 * [1 - sign(x_1 - x_{1e})] \tag{5.33}$$

The SMC law with modified sliding function [4–6] for the Zeta converter for this case is

$$u = 0.5 * \left[1 - sign\left(S + \gamma \int Sdt\right)\right]. \tag{5.34}$$

The integral term is added for reducing the steady-state reference tracking error. The simulation results are presented in the following section.

Justification for the Choice of Sliding Function

With the sliding function or sliding surface given in Eq. (5.32), the equilibrium point dynamics are stable [8]. From Eq. (5.24), the equivalent control law u_{eq} can be obtained as,

$$u_{eq} = -\left[\frac{\partial S}{\partial x^T} f(x)\right]\left[\frac{\partial S}{\partial x^T} g(x)\right]^{-1} \tag{5.35}$$

Hence, u_{eq} is given by,

$$u_{eq} = \frac{x_2}{1 + x_2} \tag{5.36}$$

Also, u_{eq} can be obtained from Eq. (5.11) by setting $\dot{x_1} = 0$. The ideal sliding mode dynamics corresponding to $S = 0$, i.e., $x_1 = \frac{V_d{}^2}{Q}$ can be given as,

$$\frac{dx_2}{d\tau} = \frac{1}{1 + x_2}(x_{1e} - x_2 x_3) \tag{5.37}$$

$$\theta_1 \frac{dx_3}{d\tau} = x_2 - x_4 \tag{5.38}$$

$$\theta_2 \frac{dx_4}{d\tau} = x_3 - \frac{1}{Q} x_4 \tag{5.39}$$

For the stability assessment for equilibrium point dynamics, the following positive-definite function may be chosen [8].

$$V = \frac{1}{2}\left[(x_2 - x_{2e})^2 + \theta_1 (x_3 - x_{3e})^2 + \theta_2 (x_4 - x_{4e})^2\right] + \Theta - \int_0^\tau \frac{[x_2(\sigma) - x_{2e}][x_3(\sigma) - x_{3e}]}{1 + x_2(\sigma)} d\sigma \tag{5.40}$$

Here, $\Theta > 0$ is such that V is positive definite with $x_2 > 0$. With some mathematical arguments, it can be shown that,

$$\dot{V} = -\frac{1}{Q}(x_4 - x_{4e})^2 - x_{3e}\frac{(x_2 - x_{2e})^2}{(1 + x_2)} \leq 0. \tag{5.41}$$

Thus, the sliding surface S in Eq. (5.32) can be the choice. Now, switching across S results in stable equilibrium point dynamics. So does the switching across $\left(S + \gamma \int Sdt\right)$. The reason for the same can be very clear from the following arguments. Equating $\left(S + \gamma \int Sdt\right)$ to zero results in $S = -\gamma \int Sdt$. And for $\gamma > 0$, this condition leads to minimization of S.

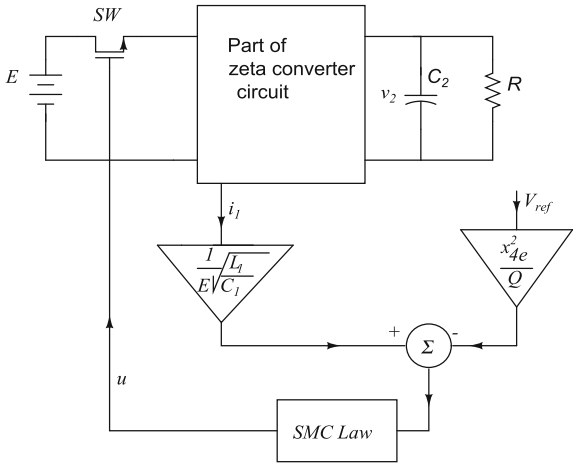

Fig. 5.2 Zeta converter circuit with SMC

5.3 Simulation Results with Concluding Remarks

In Fig. 5.2, the outlines of the implementation of the control strategies are given. Note that the normalized values of the i_1 are used. Moreover, the x_{4e} is given by the normalized equilibrium state and $x_{4e} = \frac{V_{ref}}{E}$. In Fig. 5.2, the block *SMC law* is a sliding mode controller using the control law mentioned in either Eq. (5.33) or in Eq. (5.34).

The simulation parameters are set as per Table 5.1. The figures are self-explanatory. In Fig. 5.2, the simulation model is shown. Figure 5.3 shows the load voltage and responses for the converter with the conventional and proposed SMC. The reference voltage is set to 60 V and undergoes step change to 150 V at 0.2 s. The dotted lines represent reference voltage. Figures 5.4 and 5.5 show the inductor currents through L_1 and L_2, respectively, with the conventional and proposed SMC. The graphs look almost same except a spike which is observed in Fig. 5.4b. The capacitor voltage across C_1 can be observed in Fig. 5.6 for the said control strategies. By observing Figs. 5.7 and 5.8, one can immediately observe that the steady-state error in reference tracking is reduced by using the proposed SMC in both the *step-down* and *step-up* mode of operation. For the *step-down* mode, i.e., for reference 60 V, the tracking error is 0.15 V for conventional SMC, and it is 0.02 V for proposed SMC as can be observed from Fig. 5.7a, b. Similarly from Fig. 5.8 the steady-state error can be observed for the *step-up* mode of operation, i.e., for reference voltage 150 V. For the conventional SMC, the steady-state error in reference tracking is 0.4 V while it is 0.35 V for the proposed SMC.

Table 5.1 Simulation parameters for Zeta converter under SMC

Symbol	Description	Value
L_1	Inductance	600 μH
L_2	Inductance	1.3 mH
C_1	Capacitance	15 μF
C_2	Capacitance	12 μF
V_i	Supply voltage	120 V
V_{ref}	Reference voltage	60 or 150 V
r_L	Load resistance	25 Ω
	Initial capacitor voltage	0 V
ε	Dead zone in switching element	0.001

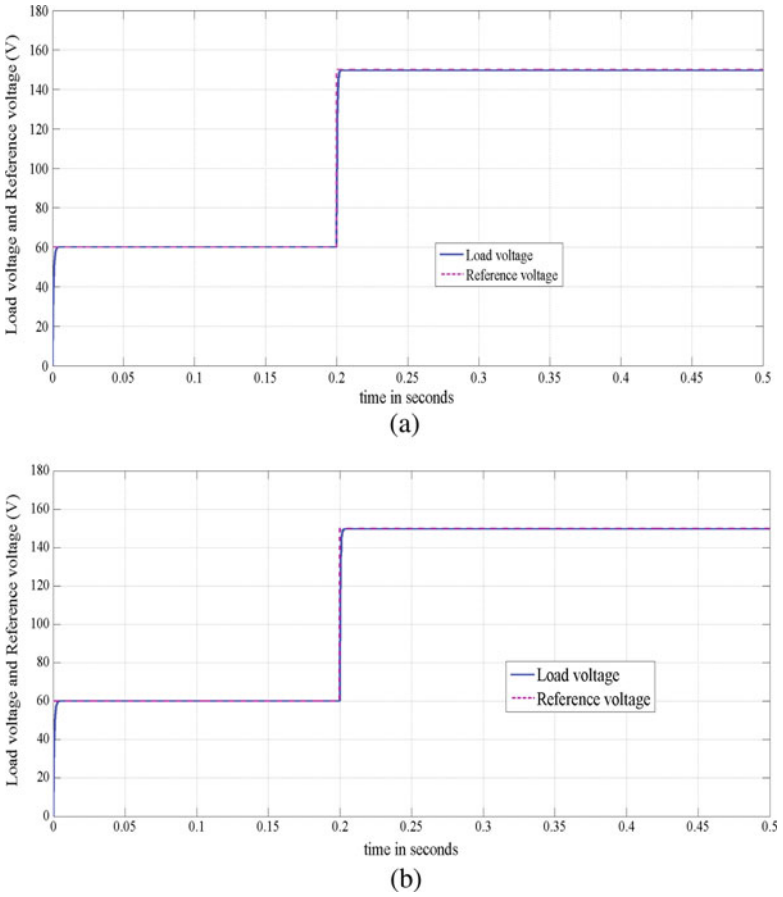

Fig. 5.3 Load voltage responses for step change in reference voltage from 60 V to 150 V, **a** conventional SMC, **b** proposed SMC

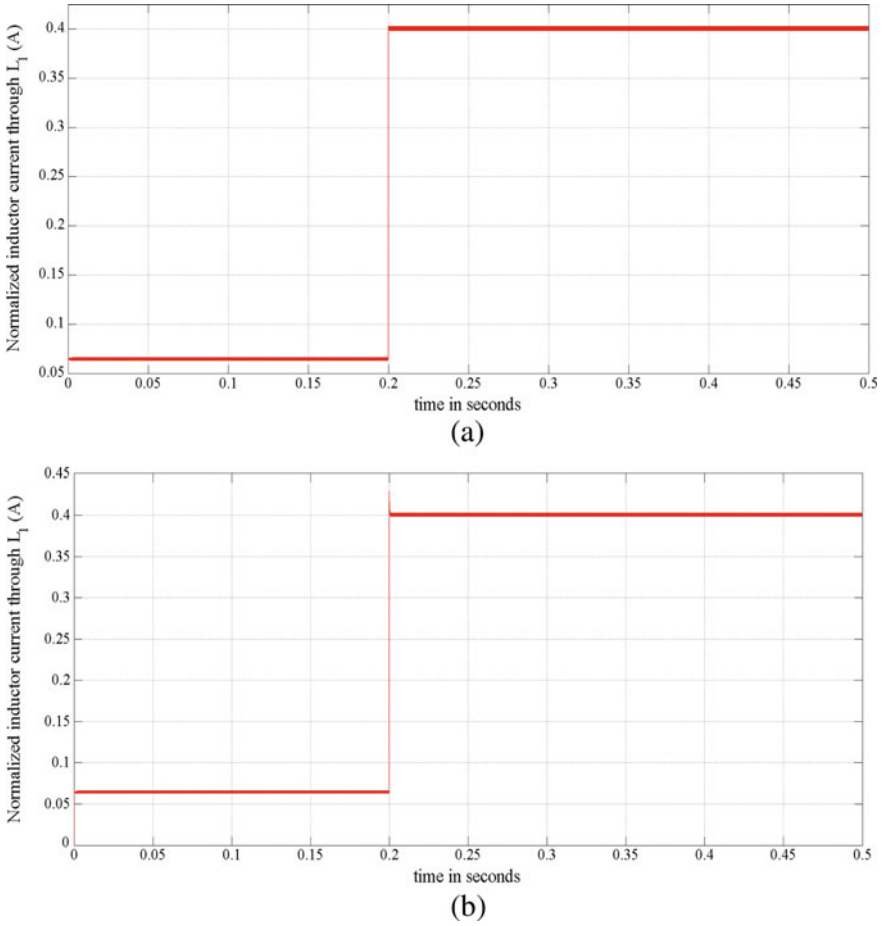

Fig. 5.4 Current through inductor L_1, **a** conventional SMC **b** proposed SMC

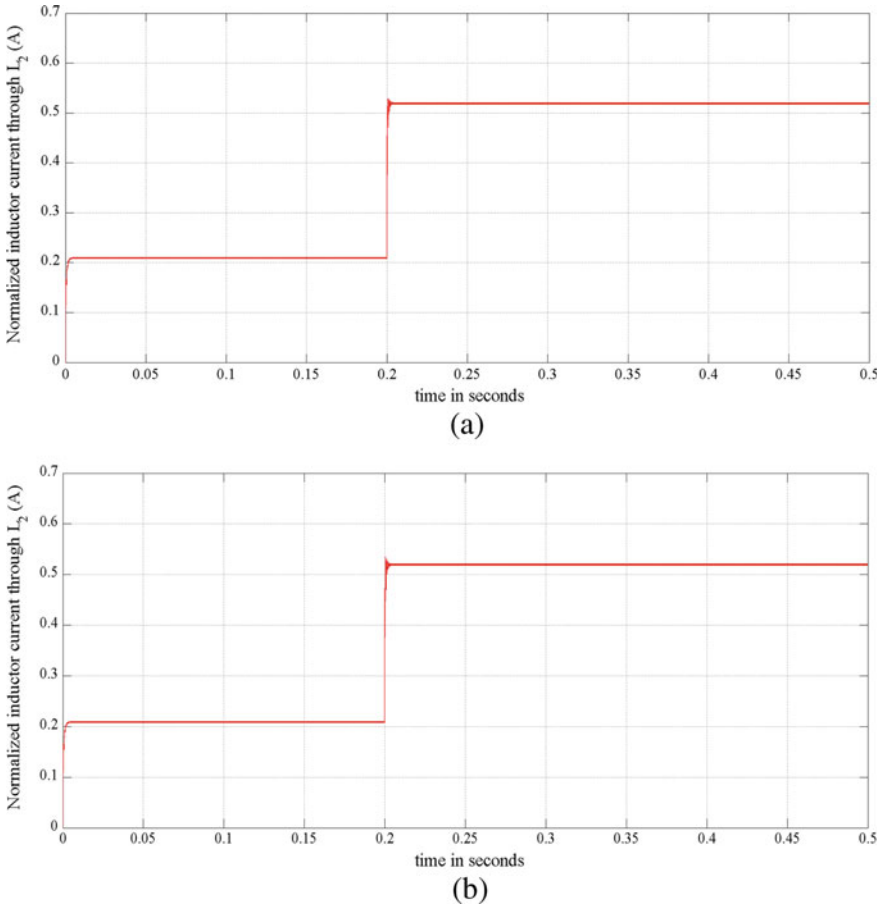

Fig. 5.5 Current through inductor L_2, **a** conventional SMC **b** proposed SMC

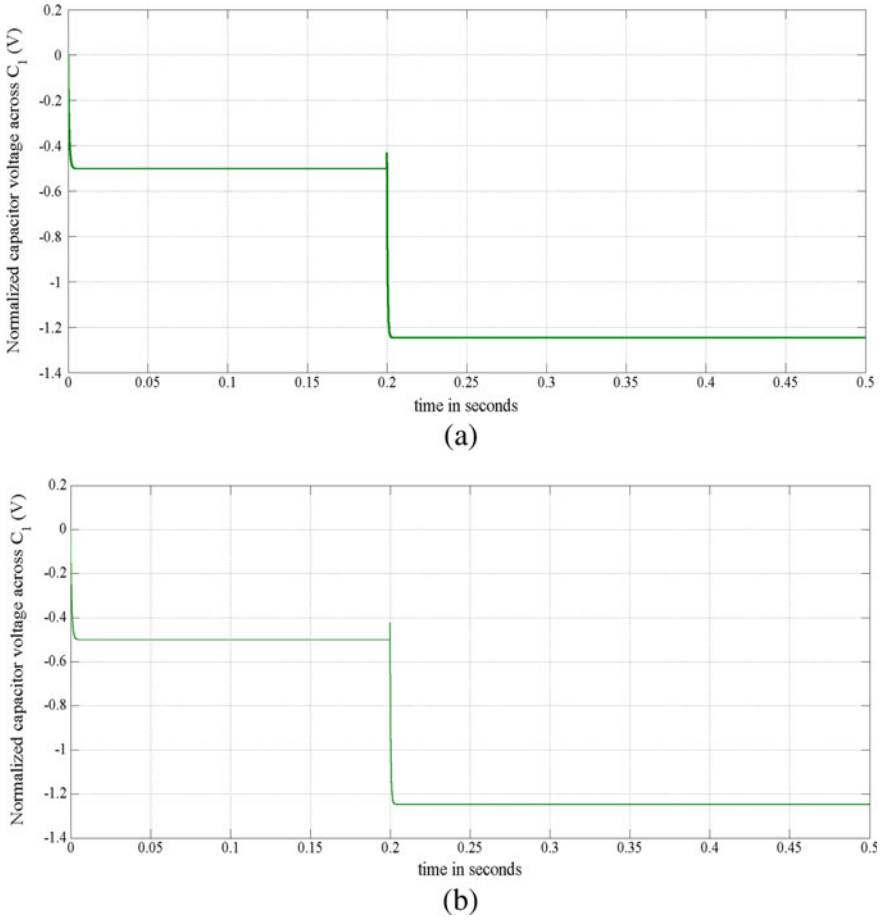

Fig. 5.6 Voltage across capacitor C_1, **a** conventional SMC **b** proposed SMC

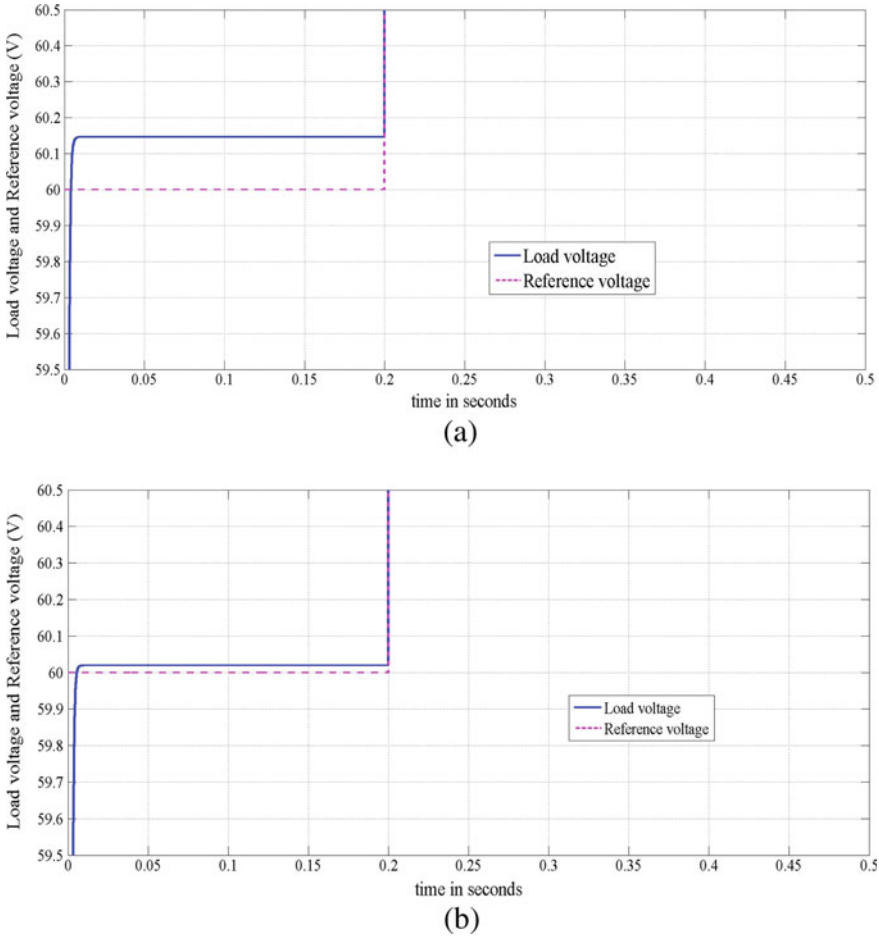

Fig. 5.7 Load voltage in step-down mode of operation, **a** conventional SMC, **b** proposed SMC

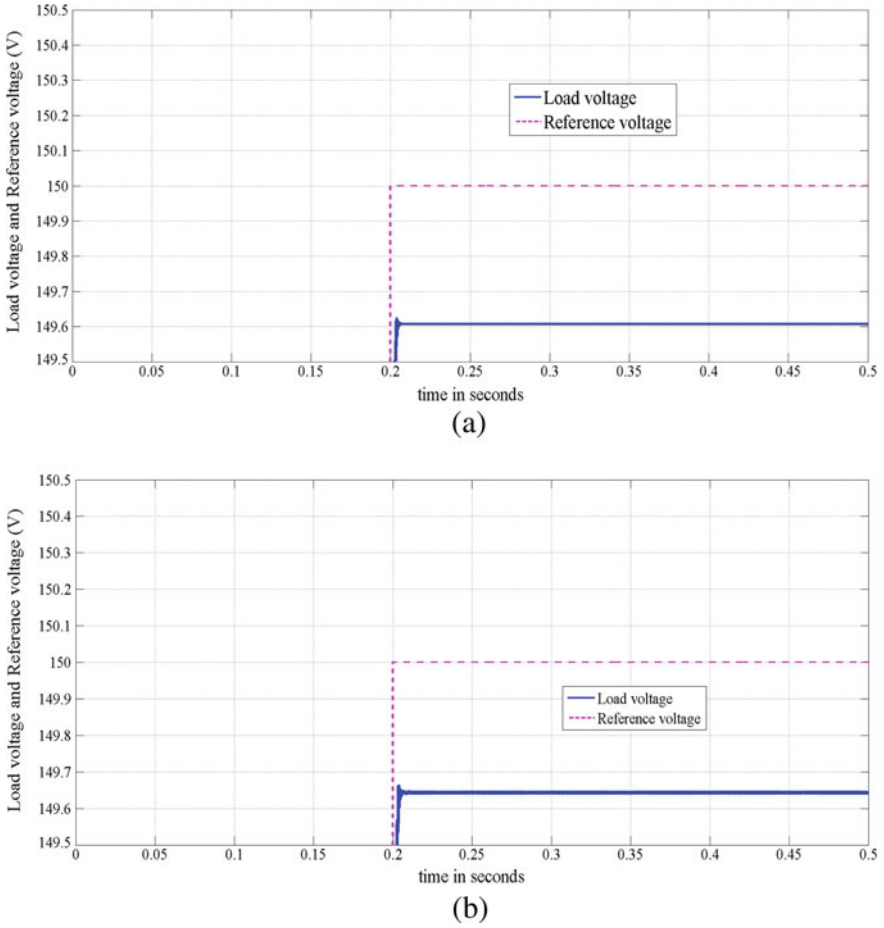

Fig. 5.8 Load voltage in step-up mode of operation, **a** conventional SMC, **b** proposed SMC

5.4 Conclusion

In this chapter, the modeling of the Zeta converter is presented with the normalization technique. The importance of selection of proper sliding surface is also explained. The detailed analysis of the converter is presented under the SMC. The Zeta converter is controlled with both conventional and proposed sliding mode controller. The simulation results show that the proposed SMC outperforms the conventional SMC as far as steady-state error is concerned.

Up till now, only the DC–DC converters with SMC are discussed. However, many AC applications such as inverters, UPS, and variable voltage variable frequency (VVVF) inverters are used widely in the various industrial applications. The idea of implementing sine wave inverter is presented in the next chapter. Moreover, the outlines of power factor controllers are given.

References

1. Edwards, C., Spurgeon, S.: Sliding Mode Control Theory and Applications. Taylor & Francis, London (1998)
2. Falin, J.: Designing DC/DC converters based on zeta topology. Analog. Appl. J. Tex. Instrum. **02**, 16–21 (2010)
3. Fan, H.: Design tips for an efficient non-inverting buck-boost converter. Analog. Appl. J. Tex. Instrum. 20–25 (2014)
4. Naik, B., Mehta, A.: Adaptive sliding mode controller with modified sliding function for DC-DC boost converters. In: IEEE International Conference on Power Electronics Drives and Energy Systems. Mumbai (2014)
5. Naik, B., Mehta, A.: Sliding mode controller with modified sliding function for buck type converters. In: 22nd IEEE International Symposium on Industrial Electronics. Taipei (2013)
6. Naik, B., Mehta, A.: Sliding mode controller with modified sliding function for DC-DC buck converter. ISA Trans. **70**, 279–287 (2017). Elsevier
7. Ogata, K.: Modern Control Engineering. Prentice Hall, New Jersey (1997)
8. Sira-Remirez, H., Silva-Ortigoza, R.: Control Design Techniques in Power Electronics Devices. Springer, London (2006)
9. Utkin, V., Guldner, J., Shi, J.: Sliding Mode Control in Electromechanical Systems. Taylor & Francis, London (1999)
10. Vuthchhay, E., Bunlaksananusorn, C.: Modeling and control of zeta converter. In: International Power Electronics Conference. Sapporo, Japan (2010)

Chapter 6
Application of Sliding Mode Controller with PI-Type Sliding Function for Inverter and Power Factor Controller

6.1 The Inverter System with Zeta Converter

The Buck–Boost converter like the Zeta converter can be a suitable converter for designing an inverter [2]. The detailed discussion on Zeta Buck–Boost converter is discussed in the previous chapter. Here the reference/desired voltage V_d for the Zeta converter output is the full wave rectified sine wave,

$$V_d = abs(160 * sin(2\pi ft), \tag{6.1}$$

(where *abs* denotes the absolute positive value). The output of the Zeta converter is then fed to the H-Bridge circuit using MOSFET or IGBT as switching devices shown in Fig. 6.1 [4, 5].

The switching logic in the figure is to switch opposite pair of IGBT/MOSFET with the sign or polarity of $V_{sine} = sin(2\pi ft)$. Figure 6.2 shows the load voltage and reference sine wave of Eq. (6.1) with 50.2 Hz frequency. It seems that the perfect tracking is not done, but for most of the practical applications, it is quite satisfactory. Figure 6.3 shows the FFT analysis for the voltage wave. The THD in percentage is about 4.63, and it may be quite acceptable.

6.2 Power Factor Controllers with Sliding Mode Controller with PI-Type Sliding Function

Power factor is the main aspect for any AC–DC power conversion. It directly reflects the efficiency and quality of such power electronic converters. The power factor controllers are generally designed with Boost converters for obvious reasons. The controller as its name suggests, keeps the supply voltage and current in phase and hence improves the supply-side power factor. The power factor controller (PFC) acts

A. Mehta and B. Naik, *Sliding Mode Controllers for Power Electronic Converters*, Lecture Notes in Electrical Engineering 534,
https://doi.org/10.1007/978-981-13-3152-7_6

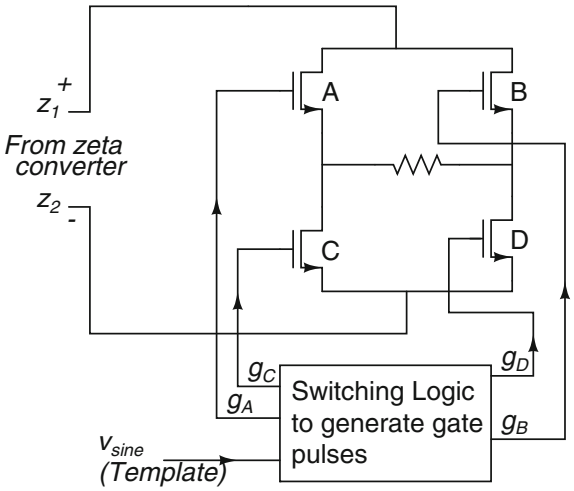

Fig. 6.1 Inverter circuit excited by the Zeta converter output

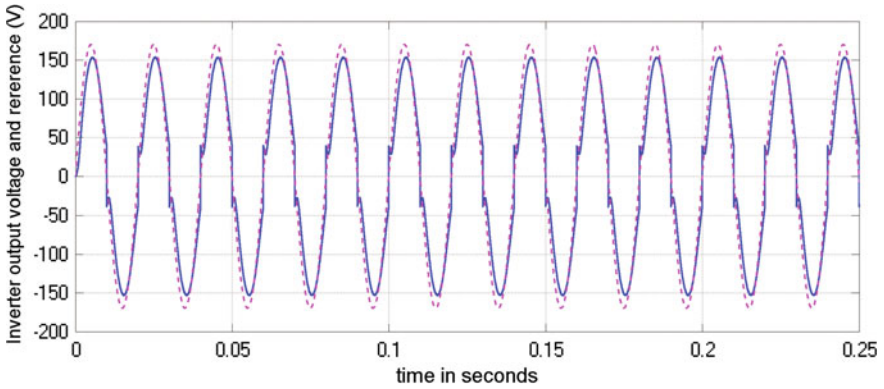

Fig. 6.2 Load voltage of the inverter circuit and reference sine wave (dotted line) 50.25 Hz

as a resistor on supply side. A sinusoidal reference is required. The application of SMC for PFC is available in [3, 6]. In this section, we directly present simulation results for PFC Boost controllers without discussing much about the theory. For the simulation study, the parameters are set as per the Table 6.1.

In Fig. 6.4, the supply current is amplified by factor 5 for better visualization in graph. The set point for the load–capacitor voltage V_{ref} is 400 V. The PID controller settings are as mentioned. It can be seen from Fig. 6.6 that he load voltage with little oscillations around the reference (400 V). While the supply voltage and current (V_s) and (I_s) are in phase. Thus, the goal is achieved. Figure 6.5 shows the same system with SMC and not using PWM for the inner control loop, i.e., current loop. The reference is 450 V. Note that V_{dc}, i_{dc} represent the load voltage and current,

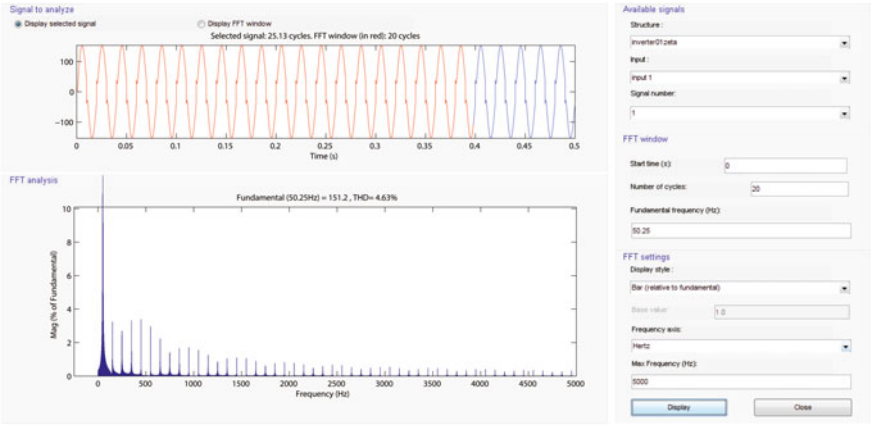

Fig. 6.3 FFT spectrum of the load voltage of the inverter

Table 6.1 Simulation parameters for Zeta converter and Inverter system under control

Symbol	Description	Value
L_1	Inductance	2 mH
C_1	Capacitance	940 μF
R	Load resistance	160 Ω
V_{ref}	Reference voltage	400 or 450 V
f	Supply frequency	50 Hz
f_s	PWM switching frequency	80 kHz

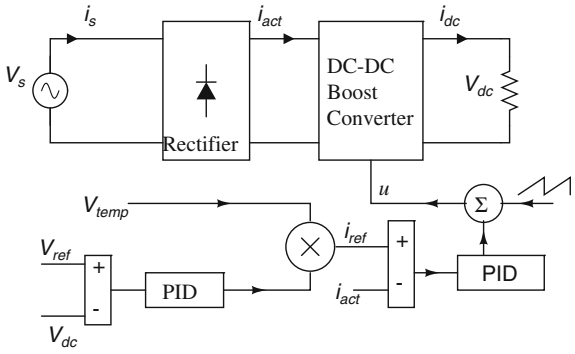

Fig. 6.4 Boost PFC with voltage and current references and with PWM/PI controller

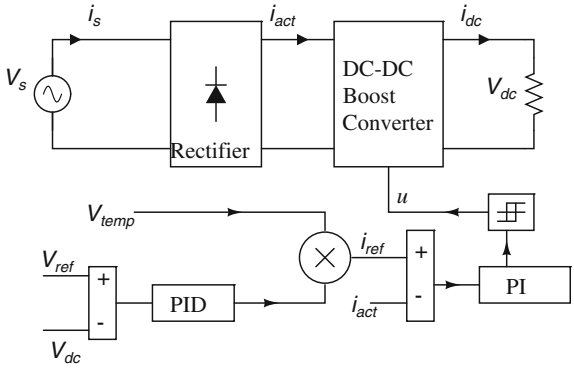

Fig. 6.5 Boost PFC with voltage and current references and with SMC controller

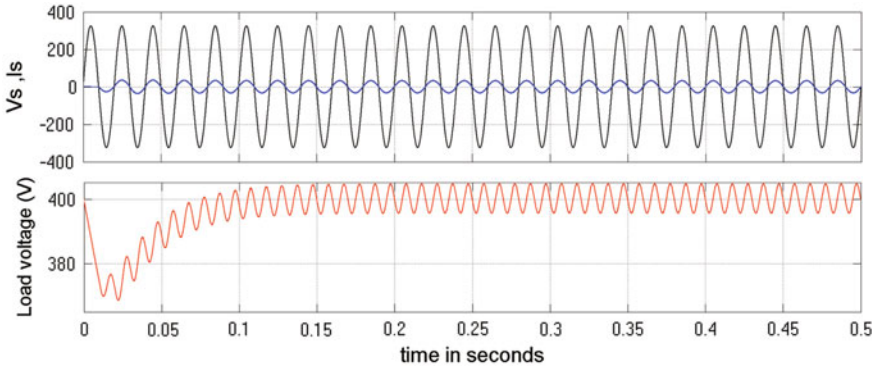

Fig. 6.6 Supply voltage, current and load voltage waveforms for PFC Boost controller with PWM/PI control

respectively. Also, i_{ref}, i_{act} represent the reference and actual inductor current for the DC–DC Boost converter. Moreover the $V_{temp} = |sin(2\pi ft)|$, where f is supply frequency. The results are shown in Fig. 6.7.

6.2.1 *Sliding Mode Control for Current Loop of Power Factor Controller*

The SMC for the inner loop which is current control loop can be given by the equation,

$$u = sgn\left(k_1 e + k_2 \int edt\right). \tag{6.2}$$

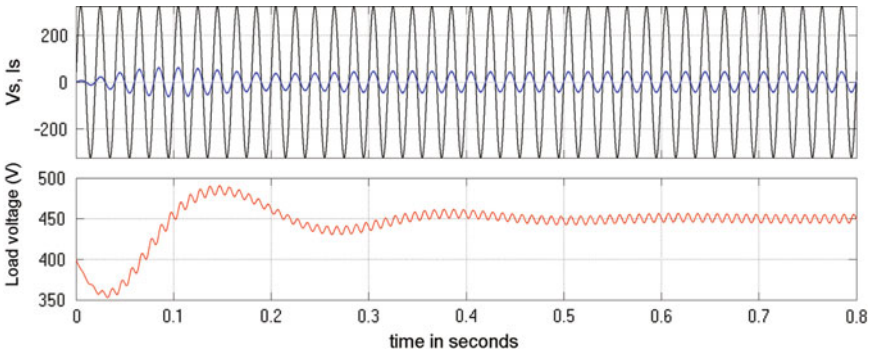

Fig. 6.7 Supply voltage, current and load voltage waveforms for PFC Boost controller with SMC control

Here, k_1, k_2 represent the proportional and integral gain, respectively, in the inner loop PI controller in Fig. 6.5. The error input to the PI controller,

$$e = i_{ref} - i_{act}. \tag{6.3}$$

The first-order dynamics of the error,

$$\frac{de}{dt} = \frac{di_{ref}}{dt} - \frac{di_{act}}{dt} = \dot{i_{ref}} - \frac{V_i}{L} + \frac{V_{dc}}{L}\bar{u}. \tag{6.4}$$

Here, V_i is the full wave rectified line voltage input to the Boost converter [1]. Also note that the $\bar{u}$ denotes the complement of u, i.e., $\bar{u} = 1 - u$ and needless to state that the $u = 1$ and $u = 0$ symbolizes the *ON* and *OFF* states of the switching device of the Boost converter.

From Eqs. (6.4) and (6.2), one can immediately notice that

$$\dot{e} = \dot{i_{ref}} - \frac{V_i}{L} + \frac{V_{dc}}{L}\left(1 - sgn\left(k_1 e + k_2 \int edt\right)\right). \tag{6.5}$$

Here, it is observed that for $e > 0$, the condition $i_{ref} < \frac{V_i}{L}$ must be satisfied for stability. Similarly, the condition $|\frac{2V_{dc}}{L}| > \left(i_{ref} - \frac{V_i}{L}\right)$ must be satisfied for $e < 0$. Hence, convergence of error is assured for $k_1, k_2 > 0$.

6.2.2 Simulation Results

The study of PFC boost circuit for current reference tracking is also carried out for PWM/PI and SMC controller actions. However, the sliding surface is chosen to be PI type in case of SMC. The open-loop response of PFC boost circuit is shown in

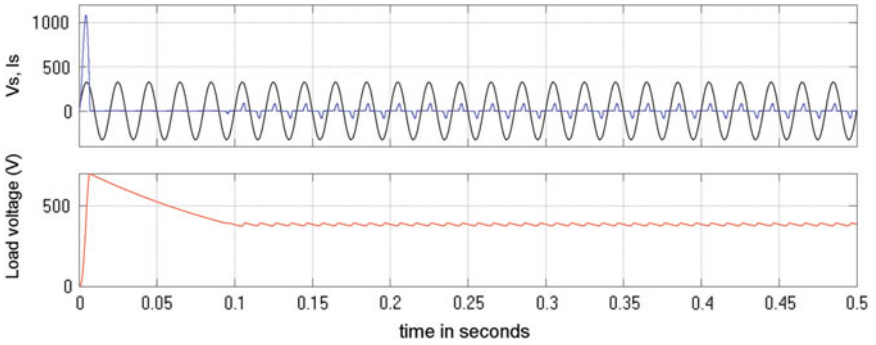

Fig. 6.8 Open-loop response of PFC boost system for duty cycle of 20%

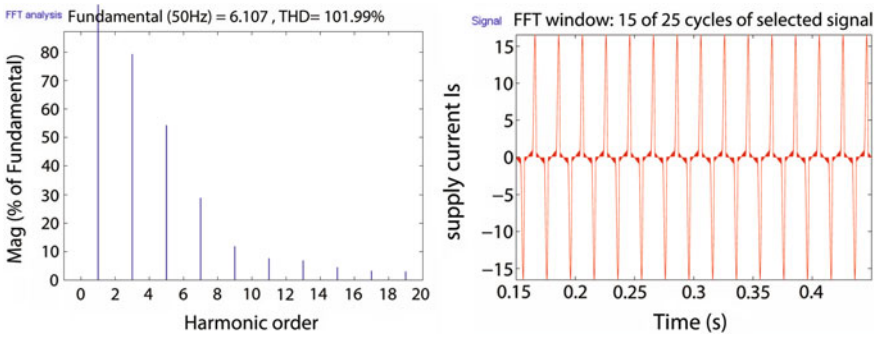

Fig. 6.9 FFT spectrum for PFC Boost controller in open loop

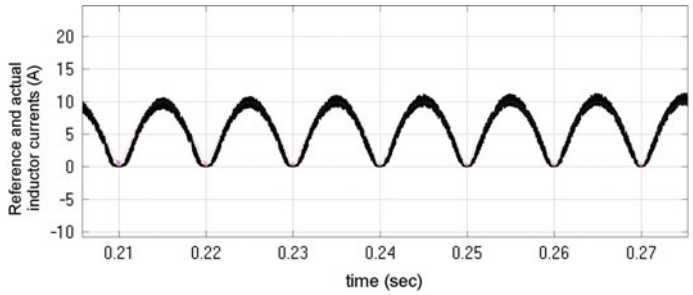

Fig. 6.10 PFC boost reference current tracking of 10 A with pwm/PI controller with proportional gain 2 and integral gain 50

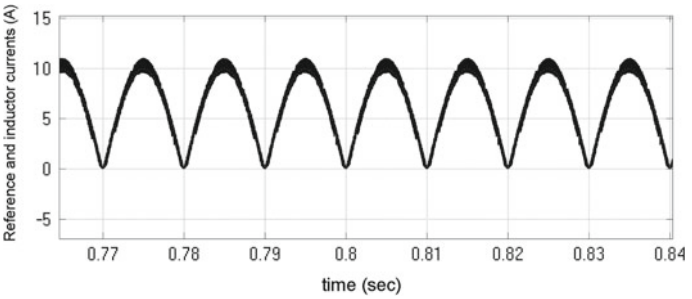

Fig. 6.11 PFC boost reference current tracking of 10 A with SMC controller with PI-type sliding surface proportional gain 2 and integral gain 0.01

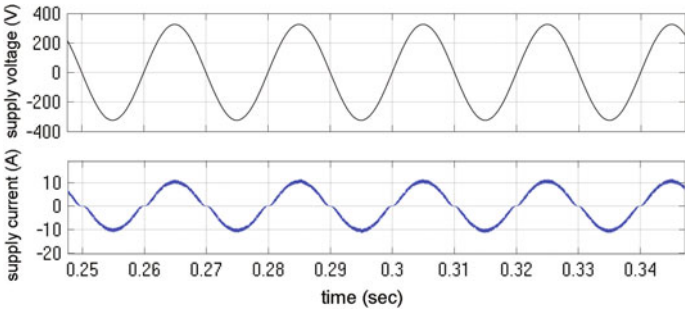

Fig. 6.12 Supply voltage and supply current for PFC boost circuit with pwm/PI control

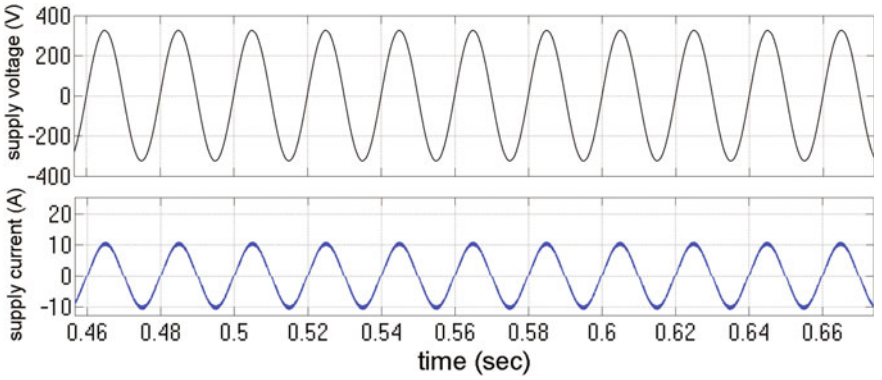

Fig. 6.13 Supply voltage and supply current for PFC boost circuit under SMC control

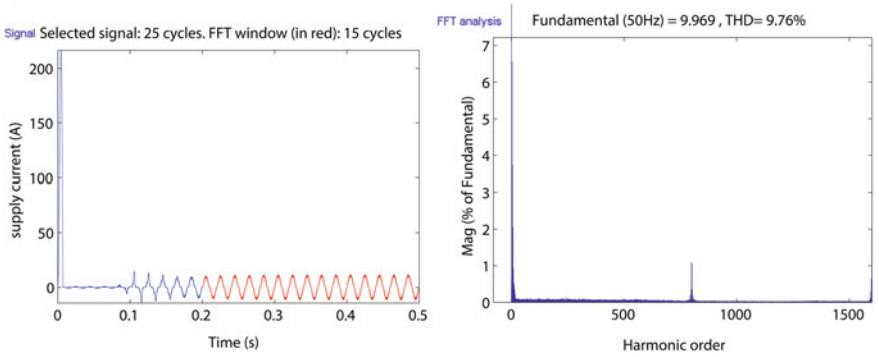

Fig. 6.14 FFT spectrum of supply current for PFC Boost controller with PWM/PI

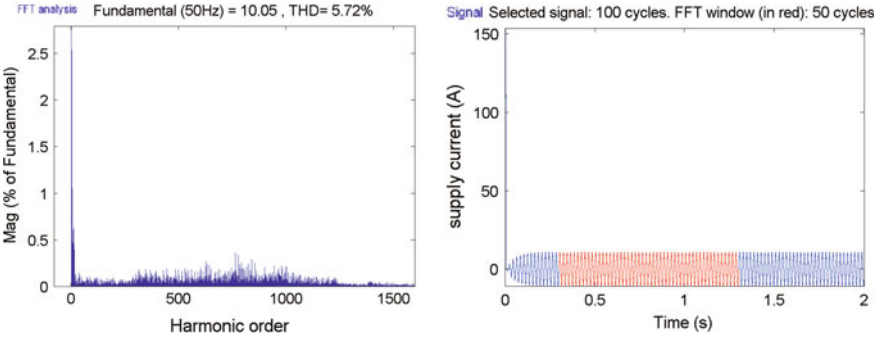

Fig. 6.15 FFT spectrum of supply current for PFC Boost controller with SMC

Fig. 6.8. The THD in percentage is shown for this open-loop case in Fig. 6.9 which are quite unacceptable. However, the reference current is tracked (reference current amplitude 10 A) in both the cases of PWM/PI and SMC controllers (Figs. 6.10, 6.11, 6.12 and 6.13). However, the FFT spectrum analysis and THD values can be observed in Figs. 6.14 and 6.15 for pwm/PI and SMC control actions, respectively, for PFC boost circuit. The THD value observed for the case of SMC controller is obviously better which is 5.72.

6.3 Conclusion

The idea of implementing the Zeta converter-based sine wave inverter is presented. The steady-state error is reduced. The power factor controller based on Boost converter is also controlled with both conventional PWM-based technique and proportional–integral-type sliding function-based SMC. The performance of the later is quite satisfactory in terms of THD.

The issue of chattering is well known for SMC. There are some techniques which can be applied to make chattering less severe. The higher-order sliding mode control (HOSMC) can alleviate chattering. There are many algorithms such as second-order SMC, suboptimal, twisting and super twisting algorithm (STA). In the next chapter, the application of second-order SMC (SOSMC) for DC–DC Buck converter is discussed to alleviates chattering in the load voltage. Comparison of performance of the converter under conventional or classical SMC and SOSMC is also presented with simulation and experimental results.

References

1. Ang, S., Oliva, A.: Power Switching Converters. CRC Press, Taylor & Francis Group, Boca Raton (2005)
2. Caceres, R., Barbi, I.: A Boost DC-AC converter analysis, design and experimentation. IEEE Trans. Power Electron. **14**(1), 134–141 (1999)
3. Chu, G., Tse, C., Chung, S., Tan, S.C.: A unified approach for the derivation of robust control for Boost PFC converters. IEEE Trans. Power Electron. **24**(11), 2531–2544 (2009)
4. Fridman, L., Moreno, J., Iriarte, R.: Sliding Mode After the First Decade of the 21st Century. Springer, Berlin (2011)
5. Mohan, N., Undeland, T., Robbins, W.: Power Electronics. Wiley, Hoboken (2003)
6. Shtessel, Y., Baev, S., Biglari, H.: Unity power factor control in three phase AC/DC Boost converter using sliding modes. IEEE Trans. Ind. Electron. **55**(11), 3874–3882 (2008)

Chapter 7
Output Feedback Second-Order Sliding Mode Controller for DC–DC Buck Converter

7.1 Introduction and Literature Survey

The DC–DC Buck converters need careful design as far as load disturbances, interference, and peak-to-peak ripple content are concerned. The quality of the output signal, i.e., load voltage, must be maintained at optimum level. Whether the power converters or more precisely power electronic converters (PECs) [13] are DC–DC Buck (step down), Boost (step up), or DC–AC Boost converters [3], they all are likely to involve the use of a good control system for one or other reasons. The reasons for using the control systems may be reference tracking requirements, load disturbance rejections, or stability improvement. There are many control strategies discussed in the wide variety of literature.

As it is stated earlier, the basic principles of SMC can be found in [4, 23]. The recent trends in SMC for PEC are well presented in [17, 20–22]. The fundamentals of PEC and classical control with pulse-width modulation-based PID controllers and state-space modeling are discussed in detail in [1]. The modified sliding function-based SMC for DC–DC Buck and adaptive SMC for DC–DC Boost converters are discussed in [14, 15], respectively. In [11], they have presented frequency-based and observer-based SMC. The adaptive terminal sliding mode control for DC–DC Buck converter is presented in [6]. However, many classical methods for modeling and control can be found in [10, 12, 18, 19]. Apart from SMC, some other similar kinds of control strategies are discussed in [16, 24]. The fixed-frequency hysteretic current (FFHC) controller that uses both SMC technique and fixed-frequency current controller with a hysteresis band to achieve all properties of the variable structure controller is discussed in [9]. However, SMC technique suffers from chattering phenomena, i.e., switching in the controlled variable due to the discontinuous nature of control law. In past few years, the higher-order SMC (HOSMC) [7, 8] came into existence which can alleviate chattering. The complete treatment of higher-order SMC (HOSMC) can be found in [2, 5].

A. Mehta and B. Naik, *Sliding Mode Controllers for Power Electronic Converters*, Lecture Notes in Electrical Engineering 534,
https://doi.org/10.1007/978-981-13-3152-7_7

There are different types of HOSMC strategies are available like second-order SMC (SOSMC), twisting algorithm, super twisting algorithm, prescribed convergence law (PCL) and suboptimal algorithm. Compared to other HOSMC like second-order SMC or twisting algorithm, the super twisting algorithm (STA) does not require the measurement of derivative of sliding surface or sliding function. But if the derivative of sliding function is feasible, the other methods can be preferred. Moreover, STA is a continuous control law which may not be ideal for the systems with discontinuous inputs like many of the switching PEC unless PWM-based control is used. In this chapter, the implementation of the second-order sliding mode control (SOSMC) or two-sliding control with the so-called prescribed convergence law is discussed. Also, the converter performance is tested with both conventional/classical sliding mode control and the two-sliding control. Here, the performance of the Buck converter with SOSMC is compared with that of classical SMC in terms of chattering alleviation. The output feedback with state estimation is used for the ease of implementation. The systematic implementation guidelines are provided. Effects of controller parameters are explored with simulation and experimental results. Effects of the load disturbance are also studied. Moreover, the stability bounds of the controller parameters are also obtained. Also, the effects of varying controller parameters on the controlled variable, i.e., load voltage, are explored for reference tracking. Finally, the simulation and experimental results are presented.

The chapter is organized as followed: In Sect. 7.2, the model of DC–DC Buck converter is presented. In Sect. 7.3, the SMC and second-order SMC (two-sliding mode control) are discussed in brief. The implementation guidelines are presented in Sect. 7.4. In Sects. 7.5 and 7.6, the simulation results and experimental results are presented respectively.

7.2 Modeling of DC–DC Buck Converter

A sliding mode voltage controlled (SMVC) DC–DC Buck converter model is derived using state-space approach [22]. A mathematical model of DC–DC Buck converter as shown in Fig. 7.1 in open loop can be derived using basic circuit analysis laws. The converter is with the pure resistive load whose output voltage is to be controlled with SMC. The converter is assumed to be operated in continuous current conduction mode [13]. Let $\beta = \frac{R_2}{R_1+R_2}$ be the voltage divider ratio. The values or R_1 and R_2 are very high compared to the load resistor to avoid loading effect. If V_{ref} is a reference voltage, $V_\mu = \beta V_{ref}$ is the scaled down version of reference voltage. L is an inductor, C is a capacitor, D is the free-wheeling diode, V_o is the output or load voltage, V_i is the input voltage, and r_L is the load resistance. The SW is a n channel MOSFET switch turned ON or OFF with the output of SM controller which is in the form of pulses. Noting that $u = 1$ means SW is closed and $u = 0$ means SW is open, the state-space model of the electrical system can be derived by defining the states as follows:

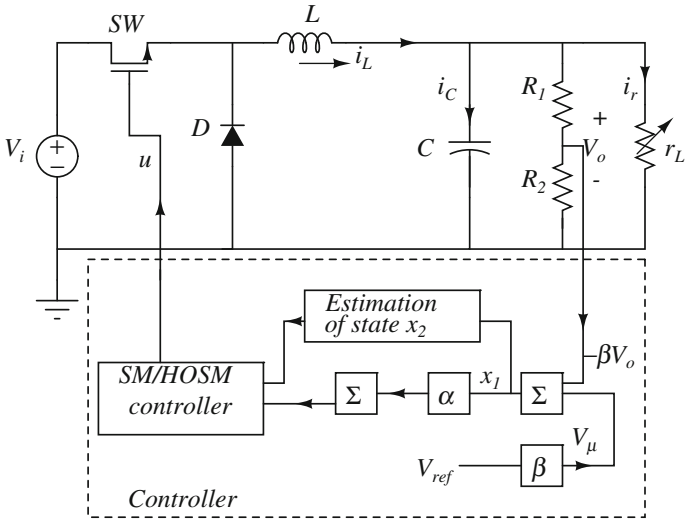

Fig. 7.1 DC–DC Buck converter with modified sliding function-based SMC

$$x_1 = V_\mu - \beta V_o, \tag{7.1}$$

$$x_2 = \dot{x}_1. \tag{7.2}$$

As stated earlier in Chap. 3, Sect. 3.2, the model of the DC–DC Buck converter can be given by,

$$\begin{bmatrix} \dot{x}_1 \\ \dot{x}_2 \end{bmatrix} = \begin{bmatrix} 0 & 1 \\ -\frac{1}{LC} & -\frac{1}{r_L C} \end{bmatrix} \begin{bmatrix} x_1 \\ x_2 \end{bmatrix} + \begin{bmatrix} 0 \\ -\frac{\beta V_i}{LC} \end{bmatrix} u + \begin{bmatrix} 0 \\ \frac{V_\mu}{LC} \end{bmatrix}. \tag{7.3}$$

7.3 The Control Techniques

Based on the valid state-space model of the converter circuit, the advance control technique may be suggested. Here, the SMC is the choice of interest. Moreover, the performance of the DC–DC Buck converter is evaluated with both the classical SMC and SOSMC. Following sections provide brief introduction to both the control techniques.

7.3.1 Classical Sliding Mode Control

The performance of the converter of interest is to be tested for both the classical SMC and SOSMC. Firstly, the brief outlines of classical SMC are presented. Let the sliding function S which establishes linear relationship among states be defined as

$$S = \alpha x_1 + x_2 = Jx, \tag{7.4}$$

where $J = [\alpha, 1]$, state vector $x = \begin{bmatrix} x_1 \\ x_2 \end{bmatrix}$, α is a scalar, $\alpha > 0$, and it controls the first-order dynamics of Eq. (7.4). By reducing the value of α, one can slow down the reaching mode dynamics. It is known that sliding mode control occurs if the reaching condition

$$S\frac{dS}{dt} < 0 \Rightarrow Jx\dot{x}'J' < 0, \tag{7.5}$$

is satisfied [4, 23]. Here, $'$ represents transpose of the vectors. The classical sliding mode control law [15] can be defined as

$$u = \frac{[1 + sgn(Jx)]}{2}. \tag{7.6}$$

Here, $sgn(.)$ is the signum function [2]. As it is well known, classical SMC has some draw backs. One of them is chattering or high-frequency switching. The SOSMC reduces the chattering in a considerable way as it will be shown later. Introduction of SOSMC used is presented below.

7.3.2 Introduction to Two-Sliding Control

Let the dynamical system be represented as

$$\dot{x} = Ax + Bv \tag{7.7}$$

and the first derivative of sliding surface be defined as

$$\dot{\sigma} = f(x, v, t), \tag{7.8}$$

where f is function of state vector, controller effort v(2-sliding control law) and time. The sliding modes are nth order sliding modes or n-sliding mode if $\sigma = \dot{\sigma} = \ddot{\sigma} = \ldots\ldots \frac{d^{n-1}\sigma}{dt} = 0$. There are many alternatives to two-sliding control like suboptimal

algorithm, twisting controller, super twisting controller. One of them is prescribed convergence law [5]. The controller with the prescribed convergence law is given by

$$v = -\kappa sgn(\dot{\sigma} + \psi|\sigma|^{0.5}sgn(\sigma)). \tag{7.9}$$

Let σ is defined as x_1 in Eq. (7.1) and $\kappa, \psi > 0$. With this definition, one can immediately notice from Eq. (7.4) that

$$\ddot{\sigma} = h(t, x) + g(t, x)v. \tag{7.10}$$

The following inequalities hold globally for the smooth functions h and g for some $K_m, K_M, Z>0$.

$$0 < K_m \leq g \leq K_M, \ |h| \leq Z \tag{7.11}$$

$$\ddot{\sigma} \in [-Z, Z] + [K_m, K_M]v \tag{7.12}$$

Let Γ be defined as $\Gamma = \dot{\sigma} + \psi|\sigma|^{0.5}sgn(\sigma)$. Then, Eqs. (7.9), (7.10), (7.11), and (7.12) yield

$$\dot{\Gamma} \in [-Z, Z] - \kappa[K_m, K_M]sgn(\Gamma) + 0.5\psi\dot{\sigma}|\sigma|^{-0.5} \tag{7.13}$$

As far as the condition, $\alpha K_m - Z > \frac{\psi^2}{2}$, the condition $\Gamma\dot{\Gamma} < 0$ is satisfied in the vicinity of $\Gamma = 0$ where $\dot{\sigma} = -\psi\sigma^{0.5}sgn(\sigma)$ and hence 1-sliding mode exists at each point except the origin on the phase plane σ versus $\dot{\sigma}$. This is because

$$\dot{\Gamma} \in [-Z - \kappa K_M sgn(\Gamma), Z - \kappa K_m sgn(\Gamma)] - 0.5\psi^2 \tag{7.14}$$

So, as stated above, the condition for one-sliding mode to exist is $\kappa K_m - Z > \frac{\psi^2}{2}$.

Any trajectory starting with $\Gamma > 0$ will hit the lower portion of the phase plane and hence will definitely terminate on $\Gamma = 0$. Similarly, the trajectory started with $\Gamma < 0$ also terminates on $\Gamma = 0$ and then reaches toward the origin in finite time.

The two-sliding mode control law in Eq. (7.9) is a suitable choice for the switching power converters because of its discontinuous nature. The many of the other alternatives for the two-sliding mode control are continuous in nature. Hence, they are tricky to be used with the systems like power electronic switching converters which do not allow the continuous inputs except pulse-width modulation (PWM)-based control which is not discussed here. In the next sections, the guidelines for deciding the stability bounds on the controller parameter, the implementation of SOSMC law, and simulation results are presented followed by experimental results.

7.4 Estimating the Stability Bounds of Controller Parameters

In this section, the bounds of the SOSMC parameters are obtained to assure stability of the overall system. From Eq. (7.3), it can be noticed that

$$\ddot{x_1} = \frac{-1}{LC}x_1 + \frac{-1}{r_L C}x_2 + \frac{\beta V_i}{LC}v + \frac{V_\mu}{LC}. \tag{7.15}$$

Let $\sigma = x_1$ as stated in the previous section and by observing Eqs. (7.10)–(7.15),

$$h = \left[\frac{-1}{LC}x_1 + \frac{-1}{r_L C}x_2 + \frac{V_\mu}{LC}\right], \tag{7.16}$$

$$g = \frac{\beta V_i}{LC}. \tag{7.17}$$

If R_{eff} is the effective series resistance in the charging path of the capacitor, the maximum charging current is $\frac{V_i}{R_{eff}}$. With this fact and from the definitions of the states, the bounds of g and h can be defined.

$$0 < \frac{\beta V_\mu}{LC} \leq g \leq \frac{\beta V_i}{LC} \tag{7.18}$$

$$|h| = \left|\frac{-1}{LC}x_1 + \frac{-1}{r_L C}x_2 + \frac{V_\mu}{LC}\right| \tag{7.19}$$

$$|h| = \left|\frac{-1}{LC}(V_\mu - \beta V_o) + \frac{-1}{r_L C^2}i_C + \frac{V_\mu}{LC}\right| \tag{7.20}$$

$$|h| \leq \frac{\beta V_o}{LC} + \frac{\beta V_i}{C^2 r_L R_{eff}} \tag{7.21}$$

The constraints on the controller parameters exist with the inequality $\kappa K_m - Z > \frac{\psi^2}{2}$ to be manifested as

$$\kappa \frac{\beta V_\mu}{LC} - \frac{\beta V_o}{LC} - \frac{\beta V_i}{C^2 r_L R_{eff}} > 0.5\psi^2 \tag{7.22}$$

This puts the constraint on controller parameter ψ.

7.5 Implementation of the Second-Order Sliding Mode Controller

The major issue of implementation is that the control law of Eqs. (7.9) and (7.12) involves the measurement or estimation of first derivative of state. However, the derivative of state x_1 is directly available as the capacitor current which is bidirectional or AC. This requires the use of fast and accurate current sensor with isolation. This adds extra cost for hardware implementation. Moreover, such sensors are prone to noise, and hence, extra care should be taken. However, the estimation of state and its first derivative is possible with the use of accurate and fast-computing device such as a digital signal controller. The algorithm for estimation of derivative $\dot{\sigma}$ is based on trapezoidal rule or Tustin's method. Algorithm 1 is suggested to implement the control law of Eq. (7.9).

Algorithm 1 To implement control law Eq. (7.9)

Require: $\kappa, \psi > 0$, parameter initialization $\sigma(k-1) = 0$
  TI: Timer Interrupt Routine()
  $x_1(k) \leftarrow$ measure state at sampling instant kT
  $x_1(k) \leftarrow \sigma(k)$
  $\dot{\sigma} \leftarrow \frac{2}{T}(\sigma(k) - \sigma(k-1))$
  if $\sigma < 0$ **then**
    $sgn(\sigma) = -1$
  else
    $sgn(\sigma) = 1$
  end if
  $|\sigma| = \sigma * sgn(\sigma)$
  $|\sigma|^{0.5} \leftarrow squareRoot(\sigma)$
  compute Γ
  $v \leftarrow -\kappa sgn(\Gamma)$
  if $v < 0$ **then**
    $SW \leftarrow OFF$
  else
    $SW \leftarrow ON$
  end if
  while 1 **do**
    wait for Timer Flag $TF = 1$
    if $TF = 1$ **then**
      $TF = 0$
      Execute $TI()$
    end if
  end while

Please note that in Algorithm 1, T and SW denote the sampling time and status of MOSFET switch. The k denotes the sampling instant.

Table 7.1 Parameters set for simulation and experiment for the system in Fig. 7.1

Symbol	Description	Value
L	Inductance	0.6 mH
C	Capacitance	100 μF
α	Controller parameter	4000
κ	Controller parameter	−4000
V_i	Supply voltage	24 V
V_{ref}	Reference voltage	12 V
r_L	Load resistance	100 Ω or 32 Ω
	Initial capacitor voltage	0 V
ψ	Controller parameter	1056
β	Voltage divider ratio	0.128

7.6 Simulation Results for DC–DC Buck Converter

The parameters in Table 7.1 are set for hardware implementation and software simulation. Figure 7.2 shows the load voltage for reference 12 V. The magnified view shows the chattering amplitude is about 0.10 volt peak to peak under the conventional SMC law. However, by observing the Fig. 7.3, one can immediately notice that the chattering amplitude is reduced to about 0.05 volt peak to peak with two-sliding mode control in action, while it is about 0.09 volt peak to peak for classical SMC. The load disturbance occurs at 0.2 s where load resistance changes to 32 from 100 Ω. Apparently, the two-sliding mode controller works better as expected in terms of steady-state performance which can be immediately observed from Figs. 7.2 and 7.3. The chattering alleviation is apparent if phase plane trajectories for conventional and second-order SMC controlled Buck converter are observed as shown in Figs. 7.4

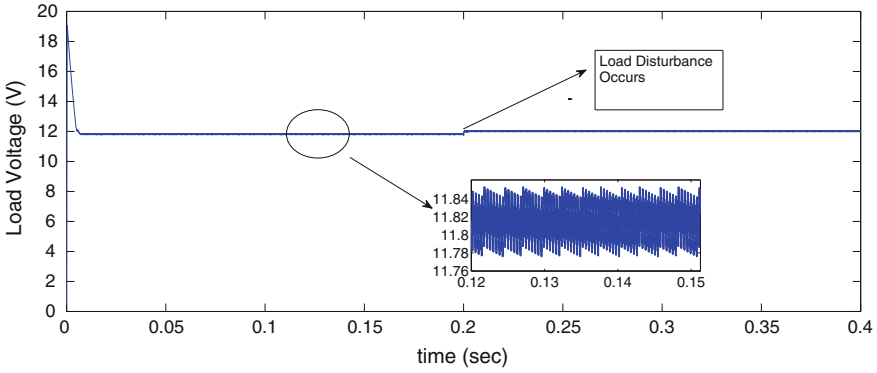

Fig. 7.2 Load voltage response of the DC–DC Buck converter with classical/conventional SMC

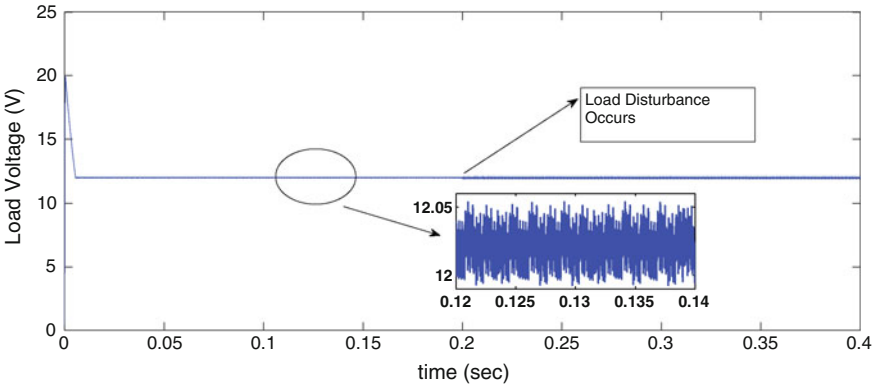

Fig. 7.3 Load voltage response of the DC–DC Buck converter with SOSMC

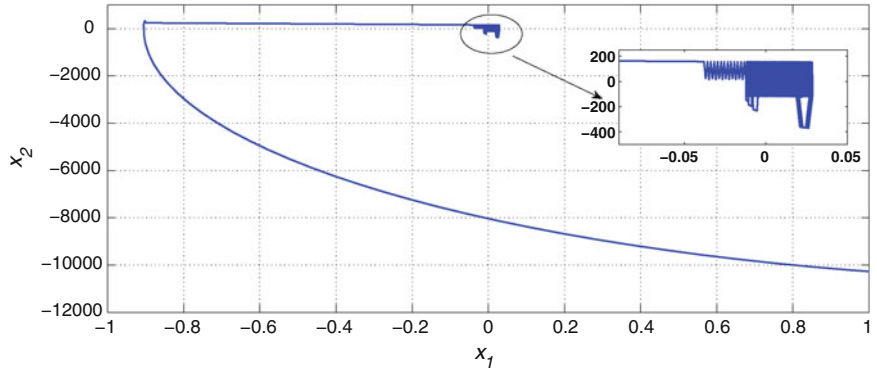

Fig. 7.4 Phase portrait of DC–DC Buck converter with classical SMC

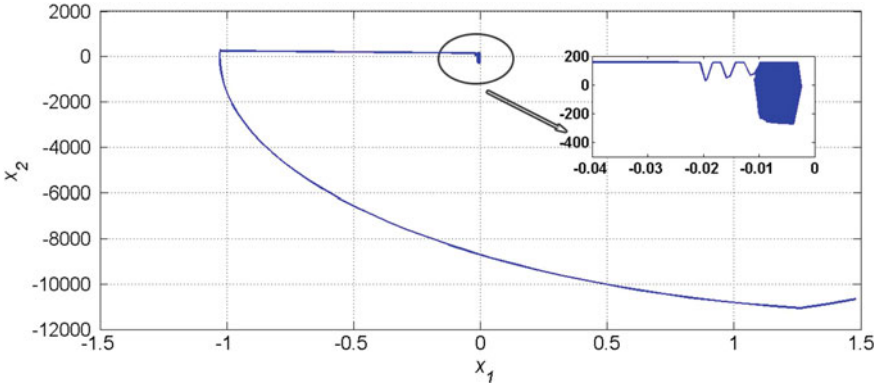

Fig. 7.5 Phase portrait of DC–DC Buck converter with SOSMC

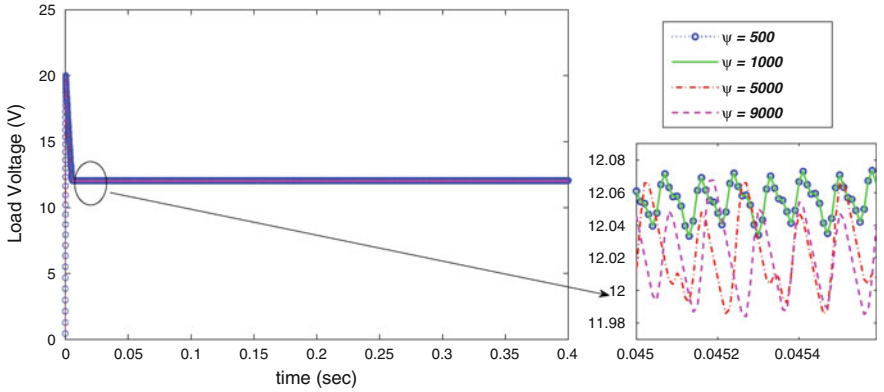

Fig. 7.6 Effects of the SOSMC controller parameters on load voltage

and 7.5. Minimization in state x_1 in Fig. 7.5 is more obvious compared to Fig. 7.4. It is clear from Fig. 7.6 that the higher values of ψ tend to increase the chattering amplitude in the load voltage.

7.7 Experimental Results

Figure 7.7 shows the load voltage and pulses to the switching device under the classical SMC law. The reference set is 12 V. The AC analysis for the same is presented in Fig. 7.8. Similarly, in Figs. 7.9 and 7.10, the response of load voltage with SOSMC controller output and AC analysis is presented, respectively. While comparing the Figs. 7.8 and 7.10, one can notice the chattering amplitude is reduced in Fig. 7.10 by

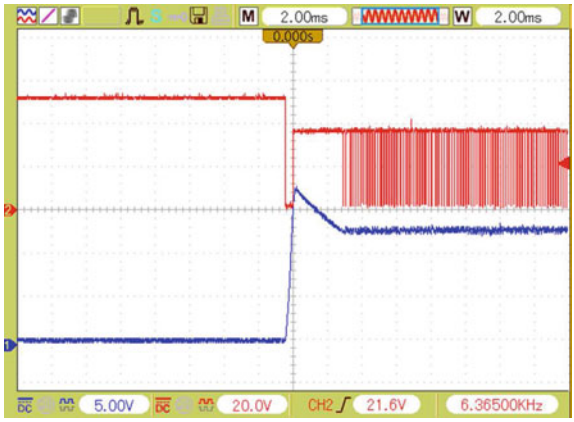

Fig. 7.7 Load voltage response of the DC–DC Buck converter with conventional SMC and controller output

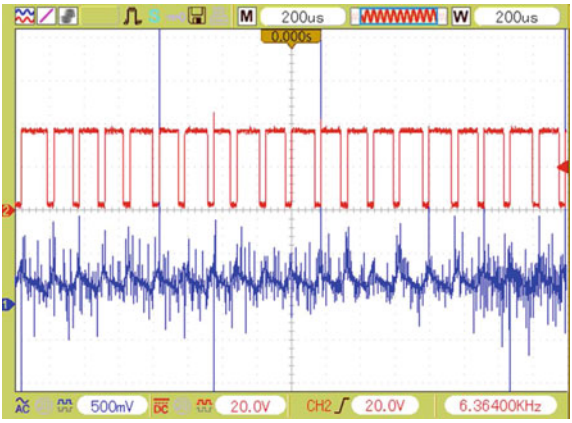

Fig. 7.8 AC analysis of load voltage response of the DC–DC Buck converter with conventional SMC and controller output with load disturbance of 100 to 30 Ω

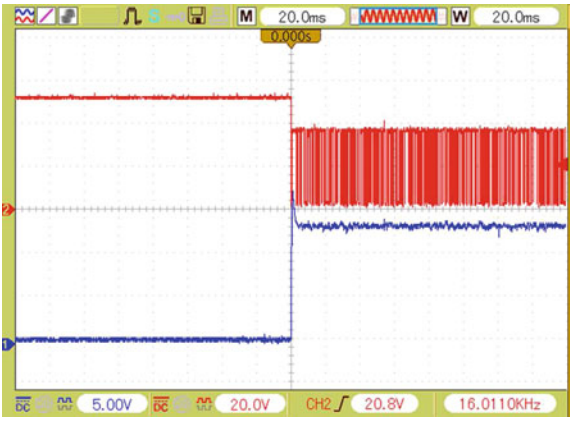

Fig. 7.9 Load voltage response of the DC–DC Buck converter with SOSMC and controller output

200 mV. The chattering frequency is 15.9 kHz in case of second-order SMC compared to 6.3 kHz that of conventional SMC. Practically, the load voltage response does not exhibit any significant change when load resistance is disturbed from 100 to 32 Ω. The chattering amplitude in the presence of load 32 Ω for conventional and second-order SMC laws is shown in the Figs. 7.11 and 7.12, respectively. One can observe that the chattering amplitude in Fig. 7.11 is approximately 1.5 times that of in Fig. 7.12. The circuit implementation guidelines can be obtained from the Fig. 7.13. The algorithm is implemented in software with digital signal controller STM32F407VG which is based on ARM Cortex M4 architecture.

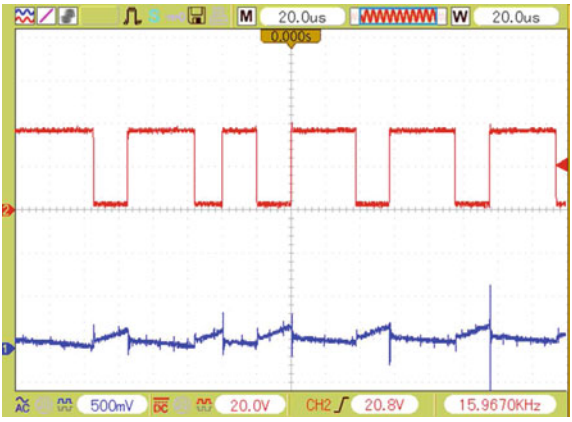

Fig. 7.10 AC analysis of load voltage response of the DC–DC Buck converter with SOSMC and controller output without load disturbance

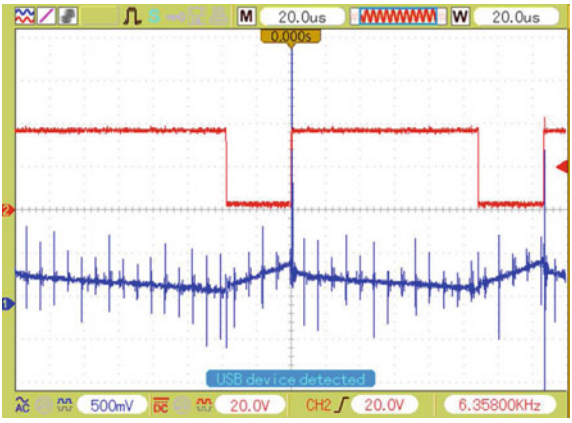

Fig. 7.11 AC analysis of load voltage response of the DC–DC Buck converter with conventional SMC and controller output without load disturbance

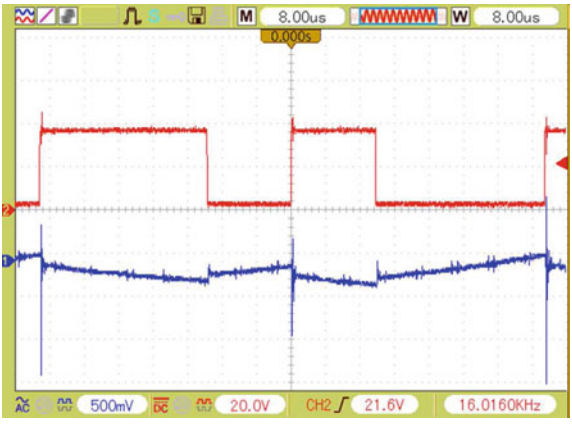

Fig. 7.12 AC analysis of load voltage response of the DC–DC Buck converter with SOSMC and controller output with load disturbance from 100 to 30 Ω

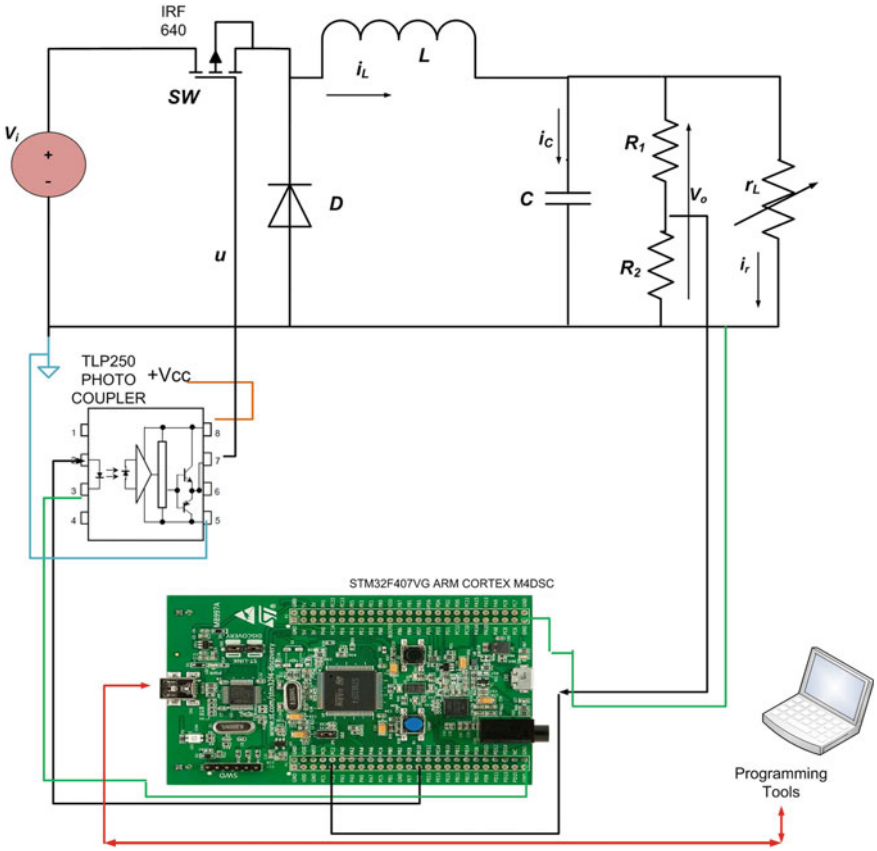

Fig. 7.13 DC–DC Buck converter with digital signal controller for circuit implementation

7.8 Conclusion

The load voltage reference tracking of the DC–DC Buck converter is tested with both the classical and PCL/SOSMC laws. The quality of the load voltage in terms of chattering is evaluated for both the control strategies. With the simulation and experimental results, it is very clear that the implementation of SOSMC with the proposed algorithm is quite effective to reduce the chattering effect. The performance with the load disturbance is also tested. The stability bounds of the controller (SOSMC) are also obtained with analysis. The proposed control methodology may be applicable for other switching PECs like DC–DC Boost converters, DC–AC inverters, and Buck–Boost converters.

References

1. Ang, S., Oliva, A.: Power Switching Converters. CRC Press, Taylor & Francis Group, Boca Raton (2005)
2. Barbot, J.P., Perruquetti, W.: Sliding Mode Control in Engineering. Marcel Dekker Inc., New York (2002)
3. Caceres, R., Barbi, I.: A boost DC-AC converter analysis, design and experimentation. IEEE Trans. Power Electron. **14**(1), 134–141 (1999)
4. Edwards, C., Spurgeon, S.: Sliding Mode Control Theory and Applications. Taylor & Francis, London (1998)
5. Fridman, L., Moreno, J., Iriarte, R.: Sliding Mode After the First Decade of the 21st Century. Springer, Berlin (2011)
6. Komurcugil, H.: Adaptive terminal sliding-mode control strategy for DC-DC buck converters. ISA Trans. **51**, 673–681 (2012). Elsevier
7. Levant, A.: Construction principles of output feedback 2-sliding mode design. In: 41st IEEE Conference on Decision and Control. Las Vegas (2002)
8. Levant, A.: Higher-order sliding modes, differentiation and output-feedback control. Int. J. Control **76**(9–10), 924–941 (2003)
9. Maity, S., Suraj, Y.: Analysis and modeling of an FFHC-controlled DC-DC buck converter suitable for wide range of operating conditions. IEEE Trans. Power Electron. **27**(12), 4914–4924 (2012)
10. Martinez-Salamero, L., Cid-Pastor, A., Aroudi, A.E., Giral, R., Calvente, J., Ruiz-Magaz, G.: Sliding-mode control of DC-DC switching converters. In: Preprints of the 18th IFAC World Congress, pp. 1910–1916. Milano, Italy (2011)
11. Mehta, A., Bandyopadhyay, B.: Frequency-Shaped and Observer-Based Discrete-time Sliding Mode Control. Springer, Berlin (2015)
12. Middlebrook, R., Cuk, S.: A general unified approach to modelling switching converter power stages. In: IEEE Power Electronics Specialists Conference, pp. 73–86 (1976)
13. Mohan, N., Undeland, T., Robbins, W.: Power Electronics. Wiley, Hoboken (2003)
14. Naik, B., Mehta, A.: Adaptive sliding mode controller with modified sliding function for DC-DC boost converters. In: IEEE International Conference on Power Electronics Drives and Energy Systems, Mumbai (2014)
15. Naik, B., Mehta, A.: Sliding mode controller with modified sliding function for buck type converters. In: 22nd IEEE International Symposium on Industrial Electronics. Taipei (2013)
16. Perry, A.G., Fen, G., Liu, Y.F., Sen, P.: A new sliding mode like control method for buck converter. In: 35th Annual IEEE Power Electronics Specialists Conference, pp. 3688–3693. Aachen, Germany (2004)
17. Sira-Remirez, H., Silva-Ortigoza, R.: Control Design Techniques in Power Electronics Devices. Springer, London (2006)
18. Smedley, K.M., Cuk, S.: One-cycle contol of switching converters. IEEE Trans. Power Electron. **10**(6), 625–633 (1995)
19. Spiazzi, G., Mattavelli, P., Rossetto, L.: Sliding Mode Control of DC-DC Converters. University of Padova, Italy (1997)
20. Tan, S.C., Lai, Y.M., Tse, C.K.: On the practical design of sliding mode voltage controlled buck converter. IEEE Trans. Power Electron. **20**(2), 425–436 (2005)
21. Tan, S.C., Lai, Y.M., Tse, C.K.: Indirect sliding mode control of power converters via double integral sliding surface. IEEE Trans. Power Electron. **23**(2), 600–611 (2008)
22. Tan, S.C., Lai, Y.M., Tse, C.K.: Sliding Mode Control of Switching Power Converters. CRC Press, Boca Raton (2012)
23. Utkin, V., Guldner, J., Shi, J.: Sliding Mode Control in Electromechanical Systems. Taylor & Francis, London (1999)
24. Wang, Q., Li, T., Feng, J.: Discrete time synergetic control for DC-DC converter. In: PIERS Proceedings, pp. 1086–1091. Xi'an, China (2010)

Chapter 8
Conclusions and Future Work

The monograph discussed the applications of conventional SMC and its limitations, especially for PEC. With the use of proposed SMC, the steady-state error is minimized. Moreover, the variations in ROE due to system parameters variations can also be counteracted in case of Buck and Boost converters. The proof of stability is given. The improvement in load disturbance rejection is demonstrated with simulation and experimental results. For Boost converter, the adaptive mechanism is incorporated to compensate load variations. Due to the proposed SMC for Boost converter, the load voltage settles quickly to reference compared to conventional SMC when load disturbance occurs. The Zeta converter is also controlled with conventional and proposed SMC. The idea of designing sine wave inverter with Zeta converter is also proposed. The results are presented and seem satisfactory. The power factor controller based on Boost topology is also tested for the performance with the use of SMC and PWM+PI control. The simulation results are quite better in case of SMC. The quality of load voltage is assessed in terms of THD.

Use of second-order sliding mode control (SOSMC) for DC–DC Buck or step-down converter is also proposed. The experimental and simulation results are presented. The experimental results confirm that the chattering alleviation is quite effective with the SOSMC. It is shown that the chattering amplitude is reduced 1.5 times compared to the conventional SMC case. The implementation guidelines are also presented. The use of digital signal controller (DSC) proved to be feasible while executing complex algorithms and state estimation.

Overall observations of simulation and experimental results depict that the proposed SMC is quite effective for various types of PEC. The proposed SMC is quite better for load disturbance rejection. It also improves the steady-state performance. The suitable choice of SOSMC for PEC can be the so-called prescribed convergence law (PCL). Because of the discontinuous nature of PCL, it is inherently suitable for the PEC. The conditions for application of PCL specifically for DC–DC Buck converter are derived. The output feedback is used for implementation. The bounds of controller parameters are obtained with analysis.

A. Mehta and B. Naik, *Sliding Mode Controllers for Power Electronic Converters*, Lecture Notes in Electrical Engineering 534,
https://doi.org/10.1007/978-981-13-3152-7_8

The digital implementation can be preferred over analog due to obvious reasons. The proposed SMC can be applied for multilevel converters. The practical aspects for application of SOSMC/HOSMC for higher-order and nonlinear converters like Buck–Boost, Zeta, and Cuk can be considered. The proposed SMC can be applied to more complex systems like three-phase converters and inverters. The feasibility of various available HOSMC techniques for PEC should be evaluated. The use of HOSMC with PWM technique can also be explored.

In future, the proposed control strategy shall be applied for a variety of DC–DC and DC–AC power electronic converters like Cuk converter, SEPIC, synchronous rectifiers, and three-phase controlled rectifiers. Moreover, the feasibility of the control strategy may be checked for low-power as well as high-power converters. The chattering alleviation may be considered for real-world applications.

Index

A. Mehta and B. Naik, *Sliding Mode Controllers for Power Electronic Converters*, Lecture Notes in Electrical Engineering 534,
https://doi.org/10.1007/978-981-13-3152-7